AFFDL-TR-76-36
VOLUME I

DEVELOPMENT OF RELIABILITY-BASED AIRCRAFT SAFETY CRITERIA: AN IMPACT ANALYSIS
VOLUME I
MODERN ANALYSIS, INCORPORATED

APRIL 1976

TECHNICAL REPORT AFFDL—TR-76-36, VOLUME I
FINAL REPORT FOR PERIOD APRIL 1975 - APRIL 1976

AIR FORCE FLIGHT DYNAMICS LABORATORY
AIR FORCE WRIGHT AERONAUTICAL LABORATORIES
AIR FORCE SYSTEMS COMMAND
WRIGHT-PATTERSON AIR FORCE BASE, OHIO 45433

NOTICE

When Government drawings, specifications, or other data are used for any purpose other than in connection with a definitely related Government procurement operation, the United States Government thereby incurs no responsibility nor any obligation whatsoever; and the fact that the Government may have formulated, furnished, or in any way supplied the said drawings, specifications, or other data, is not to be regarded by implication or otherwise as in any manner licensing the holder or any other person or corporation, or conveying any rights or permission to manufacture, use, or sell any patented invention that may in any way be related thereto.

This report has been reviewed by the Information Office (OI) and is releasable to the National Technical Information Service (NTIS). At NTIS, it will be available to the general public, including foreign nations.

This technical report has been reviewed and is approved for publication.

Robert L. Neulieb
ROBERT L. NEULIEB
Project Engineer

R.M. Bader
ROBERT M. BADER, Chief,
Structural Integrity Br
Structures Division

FOR THE COMMANDER

Howard L. Farmer
HOWARD L. FARMER, Colonel, USAF
Chief, Structural Mechanics Division

Copies of this report should not be returned unless return is required by security considerations, contractual obligations, or notice on a specific document.

AIR FORCE - 29 OCTOBER 76 - 300

UNCLASSIFIED

SECURITY CLASSIFICATION OF THIS PAGE *(When Data Entered)*

REPORT DOCUMENTATION PAGE		READ INSTRUCTIONS BEFORE COMPLETING FORM
1. REPORT NUMBER AFFDL-TR-76-36, Volume I	2. GOVT ACCESSION NO.	3. RECIPIENT'S CATALOG NUMBER
4. TITLE *(and Subtitle)* DEVELOPMENT OF RELIABILITY-BASED AIRCRAFT SAFETY CRITERIA: AN IMPACT ANALYSIS		5. TYPE OF REPORT & PERIOD COVERED Final Report April, '75-April, '76 6. PERFORMING ORG. REPORT NUMBER
7. AUTHOR(s) Masanobu Shinozuka		8. CONTRACT OR GRANT NUMBER(s) F33615-75-C-3066
9. PERFORMING ORGANIZATION NAME AND ADDRESS Modern Analysis Inc. 229 Oak Street Ridgewood, N. J. 07450		10. PROGRAM ELEMENT, PROJECT, TASK AREA & WORK UNIT NUMBERS 13670123
11. CONTROLLING OFFICE NAME AND ADDRESS Air Force Flight Dynamics Laboratory Air Force Systems Command Wright-Patterson Air Force Base, Ohio 45433		12. REPORT DATE April 1976 13. NUMBER OF PAGES 125
14. MONITORING AGENCY NAME & ADDRESS *(if different from Controlling Office)*		15. SECURITY CLASS. *(of this report)* Unclassified 15a. DECLASSIFICATION/DOWNGRADING SCHEDULE

16. DISTRIBUTION STATEMENT *(of this Report)*

Approved for public release; distribution unlimited

17. DISTRIBUTION STATEMENT *(of the abstract entered in Block 20, if different from Report)*

18. SUPPLEMENTARY NOTES

19. KEY WORDS *(Continue on reverse side if necessary and identify by block number)*

Safety, Reliability, Durability, Damage Tolerant Design, Fail Safe Design, Random Loading, Rise and Fall of Random Processes, Crack Propagation, Fracture Mechanics, Proof Load Testing, Full-Scale Testing, Inspections, NDI Techniques.

20. ABSTRACT *(Continue on reverse side if necessary and identify by block number)*

The random stress processes, composite Gaussian or single Gaussian, are constructed on the basis of exceedance curves for different aircraft under various flight conditions. The fatigue crack propagations under such stress processes are estimated with the aid of fracture mechanics method. The crack propagation rate under random loading is assumed to be proportional to the expected value of a power of the range of stress intensity factor which is in turn proportional to the expected value of the same power of the rise and fall of the stress

DD FORM 1 JAN 73 1473 EDITION OF 1 NOV 65 IS OBSOLETE

UNCLASSIFIED

SECURITY CLASSIFICATION OF THIS PAGE *(When Data Entered)*

process involved. The residual strength is evaluated as a function of crack size either under the assumption of slow crack growth design or under the assumption of fail safe design. Two different models as to the basic mechanical nature of the crack are used for the analysis and their interrelationships are discussed. One of these is the crack initiation model in which a crack of certain size is assumed to initiate at "randomly distributed time" t_o and then propagate in accordance with the propagation law of fracture machanics. The other is the pre-existing crack model which assumes the initial existence of "a crack of random size" that propagates immediately upon application of the stress process. With the aid of the random process theory, the failure rate is evaluated as the expected rate of upcrossing of the residual strength by the stress process. The probability of aircraft failure is obtained from the failure rate taking into consideration the effect of inspection procedures and proof loads. The latter, however, is considered only in conjunction with pre-existing crack model. The significance of full-scale testing is also reviewed from the view point of reliability implementation and demonstration. Numerical examples are worked out to illustrate the numerical significance of various analytical models and to indicate the sensitivity of the probability of failure to the parameters involved in the models.

FOREWORD

The research work reported herein was conducted at Modern Analysis Inc., Ridgewood, New Jersey, for Air Force Flight Dynamics Laboratory, Air Force Systems Command, Wright-Patterson Air Force Base, Ohio, under constract F33615-75-C-3066, project 1367, task number 01, with Dr. R. L. Neulieb (AFFDL/FBE) acting as project engineer.

The research was performed by Dr. M. Shinozuka of Modern Analysis Inc. as principal investigator with Drs. A. M. Freudenthal of George Washington University, R. Vaicaitis of Columbia University and J. T. P. Yao of Purdue University providing technical assistance. The computer programs were developed by Mr. T. Hisada and Mr. Peter Wai, both of Columbia University. Work began April 1975 and was completed April 1976. The final report in two volumes was submitted on April 30, 1976.

TABLE OF CONTENTS

LIST OF ILLUSTRATIONS

LIST OF ILLUSTRATIONS (CONTINUED)

LIST OF ILLUSTRATIONS (CONTINUED)

LIST OF TABLES

LIST OF SYMBOLS

A_{1b}, A_{2b}, A_{3b} = parameters to determine rise and fall of stress process corresponding to clear air turbulence, thunderstorms and maneuvers, respectively

$a(t)$ = total crack length at time t

a^* = crack size at $t = t_o$ or upper bound of pre-existing crack size in $G(a_o)$ method

a_o = pre-existing crack size in $G(a_o)$ method or crack size initiated at $t = t_o$ in $W(t_o)$ method

a_{ic} = initial critical crack size

a_s = fail-safe crack size

a_{TH} = threshold crack size

a_1 = smallest crack size detectable by inspection

a_2 = smallest crack size always detectable by inspection

a_1' = crack size detectable by cursory inspection

a_{op} = smallest initial crack size eliminated from population by proof load test

b = parameter in crack propagation model

c, c' = material constants

d = parameter in spectral density of maneuver loading

e = parameter in crack propagation model

$F(a)$ = probability of detecting a crack of size a

$F^*(a)$ = probability of not detecting a crack of size a

$F_c(a)$ = probability of detecting a crack of size a by cursory inspection

$F_c^*(a)$ = probability of not detecting a crack of size a by cursory inspection

$f_\sigma^{(k)}(x)$ = probability density function of random standard deviation σ

$f_R(x)$ = probability density function of residual strength R

$G(a_o)$ = probability density function of initial crack distribution

$G'(a_o)$ = probability density function of initial crack distribution after proof load test

g = gravitational acceleration

h_k = failure rate

h_o = failure rate corresponding to threshold R_o

i = imaginary unit or index

j = index

K_c = critical stress intensity factor

ΔK = range of stress intensity factor

$\overline{\Delta K^b}$ = average of the b-th power of range of stress intensity factor

k = index

m = parameter appearing in expression for $U_2(a)$ or index

$N^{(i)}$ = characteristic frequency

N_g = characteristic stress response frequency corresponding to gust

N_m = characteristic stress response frequency corresponding to maneuvers

N_z = characteristic stress response frequency corresponding to ground-air-ground loads

$P(j)$ = probability of first aircraft failure in $[0, jT_o]$

P_o = probability of first aircraft failure with no inspections

$P_M(j)$ = probability of first failure in $[0, jT_o]$ in a fleet of M airplanes

$\bar{P}$ = mean value of failure probability

p_1, p_2, p_3 = fractions of aircraft flight time spent in clear air turbulence, thunderstorm and maneuver, respectively

R_o = ultimate material strength

$R(t_m)$ = residual material strength at time t_m after crack size reaches a_{ic}

$S_b(t)$ = ground loads

$S_i(t)$ = individual Gaussian (patch) stress process

$S_g(t)$ = gust loads

$S_{gC}(t)$, $S_{gT}(t)$ = loads due to clear air and thunderstorm turbulence, respectively

$S_k(t)$ = single or composite Gaussian load processes; k = 1 for CAT, k = 2 for thunderstorm and k = 3 for maneuver

$S_m(t)$ = maneuver loads

$S_i^*(\omega)$ = stress response spectral density corresponding to $S_i(t)$

$S_g^*(\omega)$ = stress response spectral density corresponding to gust

$S_m^*(\omega)$ = stress response spectral density corresponding to maneuver

$\overline{S^b}$ = average of b-th power of rise and fall of stress process

$\overline{S_{gC}^b}$, $\overline{S_{gT}^b}$, $\overline{S_m^b}$, $\overline{S_z^b}$ = average of b-th power of rise and fall of stress process corresponding to clear air turbulence, thunderstorm, maneuver and ground-air-ground load, respectively

S_o = parameter appearing in expression of spectral density for maneuver loading

T = service life of aircraft or flight time between inspections

T_o = time intervals between inspections

T_o^* = minimum life in Weibull distribution

TH = subscript indicating threshold value

t = time

t_{ic} = time at which initial critical crack size a_{ic} is reached

t_{TH} = time at which crack size reaches a_{TH}

t_n = time after crack initiation

t_o = time to crack initiation treated as a random variable

U_1 = inspection probability

$U_2(a)$ = crack detection probability

V_o = coefficient of variation of ultimate strength

$W(t_o)$ = probability density function of time to crack initiation

X_o = stress associated with one g loading

$X_1, X_2, \ldots\ldots, X_n$ = system variables for sensitivity analysis

$\bar{X}_1, \bar{X}_2, \ldots\ldots, \bar{X}_n$ = average values of system variables

Z = ground-air-ground load

α = shape parameter in Weibull distribution

α^* = shape parameter in initial crack distribution

α_i = sensitivity index

β = scale parameter in Weibull distribution

β^* = scale parameter in initial crack distribution

β_c = measure of bandwidth of rectangular spectral density

λ, λ' = material constants

μ_o = mean of residual strength R

$\nu_k^+(R_o)$ = rate of upcrossing of threshold R_o by a compound Gaussian process

$\nu^+(R_o, \sigma)$ = rate of upcrossing of threshold R_o by a Gaussian process with mean X_o and standard deviation σ

ξ = factor indicating residual strength at fail-safe crack size a_s

ρ = number of cursory inspections in an interval between rigorous inspections

σ = standard deviation

σ_R = standard deviation of residual strength R

σ_{C1}, σ_{C2}, σ_{C3} = stress intensities due to clear air turbulence, thunderstorm and maneuver, respectively

σ_S = standard deviation of stress

τ = number of rigorous inspections

ω = frequency in rad/sec

ω_B = break frequency

ω_C = upper cut off frequency

I. Introduction

The probabilistic concepts were first introduced in the 1940's (e. g. Ref. 1) in dealing with the assessment and assurrance of structural safety, and have been developed over the last three decades into what is currently known as the structural reliability analysis (e. g. Ref. 2). Recently, attempts are being made in various disciplines of engineering to implement these concepts in design situations in the form of probabilistic structural design by devising reliability-based design criteria (e. g. Refs. 3 and 4).

The emphasis of the structural reliability analysis has been placed in the estimation of the structural safety in terms of the reliability which is defined as the probability that a structure subjected to loads and/or other adverse environments will perform its specified mission without failure. In the classical approach, this probability is estimated under the assumption that all possible failure mechanisms under the projected operational conditions and all pertinent parameters having significant effects on these failure mechanisms are known and at the same time, probabilistic characteristics (such as probability distributions) of all these parameters are also known. In some cases, the failure mechanism itself might exhibit intrinsic random characteristics (e. g., fatigue or crack initiation process). Every effort should be made to

improve the confidence of such an estimate making use of all available probabilistic and statistical techniques. The level of sophistication of these techniques should not only reflect the quality and quantity of the information available but also be consistent with the present state of the art of (a) structural or stress analysis, (b) failure analysis, particularly techniques of predicting various modes of structural failure, (c) environmental and load analysis including projection techniques of future operational conditions and (d) inspection techniques and repair capabilities. This clearly indicates that the confidence of the reliability estimate is simply a reflection of the accuracy of the information and the state of the art of the engineering science pertinent to the reliability and maintainability problem at hand.

The current general consensus seems to be such that the reliability analysis and the probabilistic design based on it are referred to as classical unless the following conditions are met: (1) An active recognition is given to the problem of the statistical confidence to the extent that an effort is made to estimate such a confidence with possible use of the Bayesian concept and (2) the problem of structural safety is considered in a wider perspective in relation to other significant factors, such as economic considerations. Hence, the reliability-based design criteria in modern context should be developed from the view point of systems analysis with an emphasis on a systematic

and consistent use of analytical tools as well as empirical data available at the present time for the ultimate purpose of making design and management decisions.

In spite of the difficulties often associated with the structural reliability analysis such as due to system complexity, insufficiency of data, limitation in the current technical knowledge, etc., the techniques typical of the reliability analysis play a central role in the development of the reliability-based design criteria: With the aid of these techniques, a definitely better understanding will be achieved on (a) the effect of increasing the value of significant design and management parameters (such as safety and load factors, stress allowables and inspection period) on the structural reliability, (b) the sensitivity of the structural reliability to other design and management parameters, (c) the additional information needed to improve accuracy of the reliability estimate and (d) from this understanding, a consistent and systematic way of making design and management decisions will emerge. Items (a) and (b) will indicate the impact of design and management decisions on the reliability level while Item(c) the cost of improving the confidence in the reliability estimate. Also, sensible and well disciplined use of subjective engineering judgement in the Bayesian framework is considered potentially beneficial in certain decision situations to bring about the compromise required and even desirable for reasonable blending

between the analytical rigor and the availability of pertinent information.

The purpose to be achieved by the design of aircraft structures in accordance with specified reliability-based criteria is to ensure a quantitatively specifiable, optimal level of reliability for a fleet of estimated order of magnitude of airplanes intended to be operated within the frame of an adequately defined spectrum of missions in the course of the anticipated service life. The level of reliability must be uniquely related to the expected performance of the aircraft structure in terms of the inspection and repair policy as well as in terms of the variability of the missions, of the material performance and of the environment. Any significant change in these features should clearly be reflected in the change of the associated reliability level so that, as the need arises, fleet management decisions can be based on the rational assessment of the consequences of such changes. Thus, it is clear that a computational routine should be developed which would permit the quantitative assessment of the effect on the reliability level at any time during the service life, of any significant change in the conditions under which the principal design and management decisions have been derived. In fact, the establishment of such a routine should be a part of the major effort in developing the reliability-based design criteria. Such a routine is also used to identify those design and management

parameters whose variations produce no significant changes on the reliability level.

In order to achieve the purpose outlined above, the procedures of probability-based structural design (for example, as summarized in Ref. 5) must be developed considering crack initiation and propagation processes, residual strength, inspection policy, crack detection capability, proof test, etc. so as to combine all significant aspects of aircraft design that reflect not only the selected specific structural scheme with its associated potential failure mechanism but also the anticipated inspection requirements.

To achieve the requirement for actual demonstration and compliance that the specified reliability-level has been attained, order-statistical procedures as well as fracture-mechanics considerations must be combined with the procedures referred to above into an effective operational demonstration of the fleet reliability level, for example, on the basis of the observation of the time to the initiation of a crack of critical or propagating size in the first and possibly second unit of the considered fleet.

The general framework for the development of reliability-based criteria for aircraft, however, will necessarily emerge as a compromise between the application of such basic theoretical procedures of probabilistic structural design and the requirements of ready implementation of such criteria. These

requirements should provide a format that makes it reasonably simple to translate design-procedures and design-decision processes currently used in the Air Force and in the airframe industry into formally not too dissimilar procedures and processes which reflect, however, the new probabilistic concept of the engineering reality. Thus, in order to assess the reliability of an existing fleet of airplanes as well as to set the criteria for the design of an airframe for a unit of a future fleet, the statistical distribution of each of the significant influencing factors, such as service loading, structural performance parameters of the material as well as of the fabricated structure, environmental conditions, inspection and repair procedures must be adequately characterized.

In this regard, the present circumstances are much more favorable, although far from being perfect yet, because the immediate availability of relevant data on these factors has, in recent year, systematically increased as exemplified by Refs. 6 - 15 on the gust and maneuver loading, Ref. 16 on the ultimate strength of aircraft structures and Ref. 17 on the fatigue crack initiation. Also, encouraging is the fact that the use of such information either for the purpose of reliability estimation or for the purpose of developing reliability-based design and management criteria has recently begun to appear in the literature; for example, Refs. 18 - 22 on inspection, crack detection and repair of fatigue sensitive structures,

Refs. 24 and 25 describing a possible statistical approach useful for reliability demonstration, Refs. 25 and 26 on the damage tolerant requirements and Ref. 27 on the overall reliability study involving crack initiation and propagation processes under random loading conditions as well as optimum inspection policy.

The analytical reliability analysis of aircraft structures developed in this study combines the material selection procedures and the material allowables, statistical nature of loads, fatigue crack initiation and initial crack distribution models, crack propagation and strength degradation, full-scale testing proof load testing, and various crack inspection techniques.

The material selection is made on the primary requirement that the aircraft design result in a light-weight and cost-effective yet durable structure with low structural maintenance needs. Recent studies, quite often, indicate that high static strength metals tend to exhibit relatively inferior fatigue performance (not only the average trend but also the statistical scatter) compared with medium static strength metals. This should be reflected in the scatter factor in the durability analysis (Ref. 28). A similar trend appears to exist in the fracture performance of metals as exemplified by a diagram showing the relationship between the crack length parameter and the structural efficiency parameter (Ref. 25). The material allowables are currently based on relevant MIL-HDBKs as well as on the experiments performed to augment the data base particularly

on fatigue and fracture characteristics. The allowables are basically responsible both for the size of major structural components and for the durability and damage tolerant performance of the elements thus having a direct impact on the risk of failure.

The random loading on aircraft structures considered herein is a flight-by-flight loading consisting of ground loads, gust loads due to clear air turbulence (including operational gust) and thunderstorms, ground-air-ground loads and maneuver loads. These loads are modeled either as composite Gaussian random processes consisting of a sequence of Gaussian patches, or as single Gaussian processes. Experimental information tends to indicate that most of the gust loading and the maneuver loading for cargo or transport type airplanes can be modeled by composite Gaussian processes while the maneuver loading for fighter type airplanes can be approximated more closely by single Gaussian processes (Refs. 6, 8 - 12).

The random characteristics of crack initiation and growth are treated in two different ways. In one approach, the time to crack initiation is considered as a random variable having a two-parameter Weibull distribution. In an alternative and newly proposed approach, the initial crack size in the structure is considered as a random variable. The analysis method used in this approach does not depend on the particular form of the distribution of initial crack size. For useful comparison of these approaches, however, physically compatible

distributions of time to crack initiation and of initial crack size must be provided. For this reason, the probability density function of the initial crack size is determined by a compatible transformation of the probability density function of the time to crack initiation. Then, aircraft reliability study is performed using both of these approaches.

Both approaches use fracture mechanics method to estimate propagated crack size and corresponding residual strength under random service loading conditions. For this purpose, the statistics of rise and fall of the random stress process need to be evaluated. This is achieved by utilizing the approximate analytical methods given in Refs. 29 and 30 or digital simulation techniques (Refs. 31 - 33). The residual strength is assumed to be related either to the existing crack size and fracture toughness by the Griffith-Irwin equation in case of slow crack growth design while it is obtained as a function of crack size and other parameters of redundancy in case of redundant design. Once the residual strength is established, the failure rate is evaluated as the rate of upcrossing of the residual strength by the random stress process. The probability of aircraft failure is then computed on the basis of this failure rate taking the inspection procedures into consideration.

Because only one full-scale model can usually be used for static (to verify the design ultimate), fatigue, and damage

tolerance test, the statistical significance of such tests should be carefully examined by the mathematical statistics method together with the aid of the test performed on laboratory specimens and structural components. Also, it is highly important to clarify the relations between variability of the fracture control and fatigue parameters observed in material tests on specimens of various sizes and thickness, and the expected scatter for full-scale structural parts or complete structures, as influenced by the material, the fabrication and assembly and the structural configuration itself.

In the present study, the effect of proof test is investigated by appropriately truncating the probability density of the initial crack distribution.

Investigation of the impact of inspection procedures on the aircraft reliability is one of the central themes of this study. The purpose of inspection is obviously to detect fatigue cracks in critical structural details so that the componer can be repaired or replaced thus increasing aircraft reliability. The probability of crack detection depends on the particular inspection technique used and it is usually an increasing function of the crack size. Two basic types of inspection techniques are included in this study: (1) Periodic base or depot (rigorous) inspections utilizing a particular NDI technique and (2) cursory inspections to detect relatively large crack sizes performed periodically between the rigorous

inspections. The important factors in this connection are the inspection interval and the magnification factor associated with it as specified in MIL-A-83444. Determination of the optimum inspection interval balancing the inspection cost and the resulting increase in aircraft reliability is also an important item to be considered.

Numerical results are presented to show the effect of inspection frequency, type of inspection, choice of crack propagation model, proof test, and the type of loading. Sensitivity studies are also performed to identify and examine those parameters to which the aircraft reliability is most sensitive.

II. Random Loading

The operational flight-by-flight service loads produce "component stress processes" such as $S_b(t)$, $S_{gC}(t)$, $S_{gT}(t)$, $S_m(t)$ and $Z(t)$ due respectively to ground load, clear air turbulence, thunderstorm turbulence, maneuver and ground-air-ground load in addition to the special loads due to refueling, terrain following, etc. (Figure 1). The component process $S_b(t)$ due to taxiing produces mainly stresses opposite in sign to those under flight conditions and therefore have an effect on the fatigue life. However, the effect is believed to be insignificant in comparison to that due to other loadings and is disregarded in this study.

The process $Z(t)$ due to ground-air-ground load can be considered as a random variable. The magnitude of this loading is large and it exerts a significant effect on the total fatigue life of the aircraft.

Flight data tend to indicate that the component process $S_g(t)$ - either $S_{gC}(t)$ or $S_{gT}(t)$ due to gust can successfully be modeled as "composite Gaussian random process" composed of individual Gaussian patches with different standard deviations, which are treated as random variables. A composite process model results in an exceedance of the type $\exp[-x]$. Figure 2 indicates that such composite model can also be applied in approximation to maneuver loads for transports and possibly for bombers, while the exceedance of a single Gaussian process is of the type $\exp[-x^2]$ (see Figure 3; note that the abscissa is in x^2) and fits well to fighter maneuver loads.

In this study, options are provided to treat the component processes $S_g(t)$ and $S_m(t)$ either as composite Gaussian processes or as single Gaussian processes.

1. The Expected Rate of Upcrossings

The expected rate of upcrossings by the k-th composite random stress process $S_k(t)$ can be defined as

$$\nu_k^+(R_o) = \int_0^\infty f_{\sigma_i}^{(k)}(x)\,\nu^+(R_o, x)\,dx \qquad (1)$$

where $f_\sigma^{(k)}(x)$ are the probability density functions of the random variable σ (standard deviation) and $\nu^+(R_o, x)$ is the expected upcrossing rate of the threshold R_o (ultimate strength) by an individual stress process $S_i(t)$ with standard deviation x. For a Gaussian process $S_i(t)$ with mean X_o and standard deviation σ_i, $\nu^+(R_o, \sigma_i)$ can be written (e. g., Ref. 34) as

$$\nu^+(R_o, \sigma_i) = N^{(i)} \exp\{-(R_o - X_o)^2/2\sigma_i^2\} \qquad (2)$$

where $N^{(i)}$ is the characteristic stress frequency (the expected rate of zero upcrossings) given by

$$N^{(i)} = \frac{1}{2\pi}\left(\int_{-\infty}^{\infty} \omega^2 S_i^*(\omega)\,d\omega \Big/ \int_{-\infty}^{\infty} S_i^*(\omega)\,d\omega\right)^{\frac{1}{2}} \qquad (3)$$

in which $S_i^*(\omega)$ is the spectral density of the stress history $S_i(t)$.

2. Gust and Maneuver Loads as Composite Gaussian Processes

Gust loads $S_g(t)$ are modeled as composite Gaussian processes and classified into $S_{gC}(t)$ and $S_{gT}(t)$ due respectively to clear air turbulence and thunderstorm. For a transport type airplane, the maneuver loading can also be approximated by a composite Gaussian process. The standard deviations of individual patches σ_i, i = 1, 2, ... (see Fig. 1) within the k-th composite stress process are taken to be statistically independent and identically distributed random variables with half normal densities (Refs. 8 and 9);

$$f_{\sigma_i}^{(1)}(x) = (2/\pi\sigma_{C1}^2)^{\frac{1}{2}}\exp\{-x^2/2\sigma_{C1}^2\} \quad x \geq 0 \qquad (4a)$$

$$f_{\sigma_i}^{(2)}(x) = (2/\pi\sigma_{C2}^2)^{\frac{1}{2}}\exp\{-x^2/2\sigma_{C2}^2\} \quad x \geq 0 \qquad (4b)$$

$$f_{\sigma_i}^{(3)}(x) = (2/\pi\sigma_{C3}^2)^{\frac{1}{2}}\exp\{-x^2/2\sigma_{C3}^2\} \quad x \geq 0 \qquad (4c)$$

in which σ_{C1}, σ_{C2} and σ_{C3} are the "intensities" of stress resulting from clear air turbulence, thunderstorm and maneuver, respectively. It is implied here that composite Gaussian processes associated with clear air turbulence, thunderstorm and maneuver are respectively identified by k = 1, 2 and 3. Using Eqs. 2 and 4, the expected upcrossing rates of these composite Gaussian processes are evaluated from Eq. 1 as

$$\nu_1^+(R_o) = N_g \exp\{-(R_o - X_o)/\sigma_{C1}\} \quad \text{CAT} \tag{5a}$$

$$\nu_2^+(R_o) = N_g \exp\{-(R_o - X_o)/\sigma_{C2}\} \quad \text{Thunderstorm} \tag{5b}$$

$$\nu_3^+(R_o) = N_m \exp\{-(R_o - X_o)/\sigma_{C3}\} \quad \text{Maneuver} \tag{5c}$$

where

$$N_g = \frac{1}{2\pi}\{\int_{-\infty}^{\infty} \omega^2 S_g^*(\omega)\,d\omega / \int_{-\infty}^{\infty} S_g^*(\omega)\,d\omega\}^{\frac{1}{2}} \tag{6}$$

$$N_m = \frac{1}{2\pi}\{\int_{-\infty}^{\infty} \omega^2 S_m^*(\omega)\,d\omega / \int_{-\infty}^{\infty} S_m^*(\omega)\,d\omega\}^{\frac{1}{2}} \tag{7}$$

in which $S_g^*(\omega)$ and $S_m^*(\omega)$ are the spectral densities of stress processes due to gust and maneuver, respectively. It is important to note that Eqs. 5a, 5b and 6 are derived under the assumption that the analytical forms of $S_i^*(\omega)$ are identical irrespective of index i and therefore they can be written as $S_g^*(\omega)$ multiplied by a constant depending on i. This assumption also implies that the spectral shapes of individual Gaussian processes $S_i(t)$ are identical whether due to clear air turbulence or thunderstorm. The same assumption is used for Eqs. 5c and 7.

The expected upcrossing rate under the combined loading is then determined as

$$\nu^+(R_o) = \sum_{k=1}^{3} p_k \nu_k^+(R_o) = p_1 N_g \exp\{-(R_o - X_o)/\sigma_{C1}\}$$

$$+ p_2 N_g \exp\{-(R_o - X_o)/\sigma_{C2}\} + p_3 N_m \exp\{-(R_o - X_o)/\sigma_{C3}\} \tag{8}$$

in which p_1, p_2 and p_3 represent the fraction of clear air turbulence, thunderstorm and maneuver, respectively. It should be noted that $p_1 + p_2 + p_3 = 1$.

3. Gust and Maneuver Loads as Single Gaussian Processes

When gust and/or maneuver loads are taken as single Gaussian processes $S_k(t)$, the probability density function in Eq. 1 can be replaced by a delta function

$$f_{\sigma_i}^{(k)}(x) = \delta(x - \sigma_{sk}) \tag{9}$$

in which σ_{sk} is the standard deviation of the stress corresponding to a single Gaussian process. Then, from Eqs. 1 and 9, the average upcrossings are

$$\nu_k^+(R_o) = N^{(k)} \exp\{-(R_o - X_o)^2/2\sigma_{sk}^2\} \tag{10}$$

where $N^{(k)}$ is obtained from Eq. 3 by replacing $S_i^*(\omega)$ by $S_k^*(\omega)$ the spectral density of $S_k(t)$.

4. Combination of Composite and Single Gaussian Processes

It should be noted that with this approach a segment of the random load can be treated as a composite process, while the remaining portion can be taken as single Gaussian processes. For example, if the gust is considered as composite processes

and the maneuvers as a single Gaussian process, the expected rate of upcrossing under the combined effect is

$$\nu^+(R_o) = p_1 N_g \exp\{-(R_o - X_o)/\sigma_{C1}\} + p_2 N_g \exp\{-(R_o - X_o)/\sigma_{C2}\}$$

$$+ p_3 N_m \exp\{-(R_o - X_o)^2/2\sigma_{S3}^2\} \quad . \qquad (11)$$

where $N_m = N^{(3)}$ is obtained from Eq. 7 with $S_m^*(\omega)$ replaced by $S_{\underline{3}}^*(\omega)$ (spectral density of maneuver load process $S_{\underline{3}}^*(t) = S_m(t)$ idealized as a single Gaussian process).

III. Fatigue Crack Propagation

1. Crack Propagation under Constant Amplitude Load

The fracture mechanics theory is applied to cracks of detectable size initiated at certain time or to preexisting cracks for the purpose of determining their propagating size under a stress history. Under a constant amplitude stress history, crack propagation can be represented by the well known power law formula (e. g. Refs. 35 - 39)

$$\frac{da}{dn} = c(\Delta K)^{b} \qquad \Delta K > \Delta K_{TH} \qquad (12)$$

where da/dn is the rate of crack propagation (per cycle), "a" is crack size, ΔK is range of stress intensity factor and c and e are material constants. These material constants exhibit statistical variations from specimen to specimen. However, within a specimen, it appears, they can be treated as deterministic quantities. The values of these constants are determined from the experimental results such as those shown in Figs. 4 and 5. The value of b equal to 4.0 has been used by many investigators. It is also pointed out that below the threshold value ΔK_{TH}, the rate of crack propagation is drastically reduced as observed in Figs. 4 and 5 and is so treated in the present analysis.

2. Crack Propagation under a Random Loading

The available experimental and empirical information on crack propagation under random loading suggests that a modified form of the power law given in Eq. 12 be constructed to represent the fatigue crack growth under such loading. In the present study, based on the experimental data given in Figs. 6 and 7, it is assumed that the crack propagation under random loading follows the law corresponding to the bilinear relationship as depicted in Fig. 8, which is expressed as

$$\frac{da}{dn} = c(\overline{\Delta K^b})^{\lambda/b} \qquad \text{for} \quad (\overline{\Delta K^b})^{1/b} \geq (\overline{\Delta K^b})^{1/b}_{TH} \tag{13a}$$

$$\frac{da}{dn} = c'(\overline{\Delta K^b})^{\lambda'/b} \qquad \text{for} \quad (\overline{\Delta K^b})^{1/b} < (\overline{\Delta K^b})^{1/b}_{TH} \tag{13b}$$

where c, c', λ and λ' are material parameters to be determined from Figs.6, 7 and 9. The expected value of the b-th power of the range of stress intensity factor, $\overline{\Delta K^b}$, can be related to the expected value of the b-th power of rise and fall of the stress, $\overline{S^b}$, and the crack length a as follows (Refs.29,37,38).

$$\overline{\Delta K^b} = \overline{S^b}(\pi a/2)^{b/2} \tag{14a}$$

$$(\overline{\Delta K^b})^{1/b}_{TH} = (\overline{S^b})^{1/b}(\pi a_{TH}/2)^{\frac{1}{2}} \tag{14b}$$

Eq. 14b provides the definition of a_{TH}. The last two equations are valid for a single through crack in an infinite plate with

stress intensity factor K given by $K = S(\pi a/2)^{1/2}$. It follows from Eqs. 13 and 14 that

$$\frac{da}{dn} = c(\overline{S^b})^{\lambda/b} (\pi/2)^{\lambda/2} a^{\lambda/2} \qquad (\overline{\Delta K^b})^{1/b} \geq (\overline{\Delta K^b})_{TH}^{1/b} \qquad (15a)$$

$$\frac{da}{dn} = c'(\overline{S^b})^{\lambda'/2} (\pi/2)^{\lambda'/2} a^{\lambda'/2} \qquad (\overline{\Delta K^b})^{1/b} < (\overline{\Delta K^b})_{TH}^{1/b} \qquad (15b)$$

The present formulation is based on the existing practice of data processing where the logarithm of the rate of crack propagation under random loading is plotted against $(\overline{\Delta K^b})^{1/b}$ with the same value of b as used in Eq. 12. As Fig. 9 illustrates, however, the experimental result indicate that the plot does not necessarily result in a straight line and that the slope of such a plot is generally different from b mentioned above. In fact, the present study uses the bilinear relationship with two distinct slope values λ and λ' and a threshold value $(\overline{\Delta K^b})_{TH}^{1/b}$.

Solving Eqs. 15a and 15b, fatigue crack length at time t_n can be obtained from

$$a(t_n) = \{a_o^{1-\lambda/2} + (1 - \lambda/2)c(\pi/2)^{\lambda/2} Q^{\lambda/b} N_o^{1-\lambda/b} t_n\}^{2/(2-\lambda)}$$

$$a_o \geq a_{TH} \qquad (16)$$

$$a(t_n) = \{a_o^{1-\lambda'/2} + (1 - \lambda'/2)c(\pi/2)^{\lambda'/2} Q^{\lambda'/b} N_o^{1-\lambda'/b} t_n\}^{2/(2-\lambda')}$$

$$a_o \leq a(t) \leq a_{TH} \qquad (17)$$

$$a(t_n) = \{a_{TH}^{1-\lambda/2} + (1-\lambda/2)c(\pi/2)^{\lambda/2} Q^{\lambda/b} N_o^{1-\lambda/b} (t_n - t_{TH})\}^{2/(2-\lambda)}$$

$$a_o \leq a_{TH} \leq a(t) \tag{18}$$

where a_o is the initial crack size, $t_n = t - t_o$, t_o is time to crack initiation (this is equal to zero if preexisting crack is considered), $Q = N_o \overline{S^b}$ with

$$\overline{S^b} = (p_1 N_g \overline{S^b_{gC}} + p_2 N_g \overline{S^b_{gT}} + p_3 N_m \overline{S^b_m} + N_z \overline{S^b_z})/N_o \tag{19}$$

$$N_o = p_1 N_g + p_2 N_g + p_3 N_m + N_z \tag{20}$$

$$t_{TH} = \frac{2}{2-\lambda'} \{a_{TH}^{1-\lambda'/2} - a_o^{1-\lambda'/2}\}/\{c' Q^{\lambda'/b} N_o^{1-\lambda'/b} (\pi/2)^{\lambda'/2}\} \tag{21}$$

In Eqs. 19 - 21, $\overline{S^b_{gc}}$, $\overline{S^b_{gT}}$, $\overline{S^b_m}$, $\overline{S^b_z}$ are the expected values of the b-th power of rise and fall of stress histories associated with clear air turbulence, thunderstorm, maneuver and ground-air-ground load, respectively.

IV. Statistics on Rise and Fall of a Random Process

As observed in Sec. III, the rate of crack propagation is directly proportional to the expected value of the b-th power of the rise and fall of the random stress process.

If the stress process $S_{\underline{k}}(t)$ associated with a particular loading (e. g. clear air turbulence, thunderstorm, etc.) is a single Gaussian with mean zero and standard deviation σ_{Sk} the expected value can be written in the form

$$\overline{S^b_{\underline{k}}} = A\ \sigma^b_{Sk} \tag{22}$$

where A is determined either by using the approximate analytical techniques proposed in Refs. 29 and 30 or by the method of random process simulation (Refs. 31 - 33). If the stress process $S_{\underline{k}}(t)$ is a composite process consisting of patches of single Gaussian processes $S_i(t)$ with mean zero and standard deviation σ_i, the expected value of the b-th power of the rise and fall of $S_i(t)$ is given, similarly to Eq. 22, by

$$\overline{S^b}(\sigma_i) = A\ \sigma^b_i \tag{23}$$

and the expected value of the b-th power of the rise and fall of the composite process $S_{\underline{k}}(t)$ is given by

$$\overline{S_k^b} = \int_0^\infty \overline{S^b}(x) f_\sigma^{(k)}(x)\,dx \qquad (24)$$

where $f_\sigma^{(k)}$ is the density function of σ_i as introduced in Sec. II.

From Eqs. 4a, 4b, 4c, 22, 23 and 24, $\overline{S_k^b}$ for clear air turbulence (k = 1), thunderstorm (k = 2) and maneuver (k = 3) are obtained as

$$\overline{S_{gC}^b} = A_{1b}\{(2n-1)!!\}\sigma_{C1}^{2n} \qquad (b = 2n)$$

$$= A_{1b}(2/\pi)^{\frac{1}{2}} n!\, 2^n \sigma_{C1}^{2n+1} \qquad (b = 2n+1) \qquad (25)$$

$$\overline{S_{gT}^b} = A_{2b}\{(2n-1)!!\}\sigma_{C2}^{2n} \qquad (b = 2n)$$

$$= A_{2b}(2/\pi)^{\frac{1}{2}} n!\, 2^n \sigma_{C2}^{2n+1} \qquad (b = 2n+1) \qquad (26)$$

$$\overline{S_m^b} = A_{3b}\{(2n-1)!!\}\sigma_{C3}^{2n} \qquad (b = 2n)$$

$$= A_{3b}(2/\pi)^{\frac{1}{2}} n!\, 2^n \sigma_{C3}^{2n+1} \qquad (b = 2n+1) \qquad (27)$$

with $(2n-1)!! = 1\cdot 3\cdot 5\cdots\cdots\cdots(2n-1)$.

In Eqs. 25 - 27, A_{1b}, A_{2b} and A_{3b} represent the coefficient A in Eq. 23 associated with the stress due to clear air

turbulence, thunderstorm turbulence and maneuver, respectively.

For the purpose of evaluating these coefficients by simulation method, sample time histories of S(t) are generated by means of the simulation technique given in Refs. 31 - 33 assuming the normalized spectral density function shown in Fig. 10 which can be expressed as

$$S(\omega) = \frac{1}{(1 - \beta_c)\omega_c} \qquad \text{for} \quad \beta_c\omega_c \leq \omega \leq \omega_c$$
$$= 0 \qquad \text{otherwise} \tag{28}$$

where β_c = measure of bandwidth of $S_i(t)$ and ω_c = upper cutoff frequency. Portions of these simulated time histories are shown in Figs. 11 - 16 for various values of parameter β_c. Then, the average of the b-th power of rise and fall of $S_i(t)$ is computed using the two counting methods indicated in Fig. 17. In the first method (case I), every one of rise and fall is computed, raised to the power b and averaged, while in the second method (Case II) the rise and fall are constructed by considering only those alternating peaks and troughs which are the maxima or the minima in the time intervals between successive zero crossings. The results are summarized in Figs. 18 - 21 for various values of b. The irregularity factors evaluated from the sample time histories compare extremely well with the theoretical result as shown in Table

1. Also, a comparison between the values of A obtained form simulation and the ones by the approximate theoretical methods (Refs. 29 and 30) is presented in Table 2. A good agreement is observed for those values of b considered in the theoretical methods under the conditions of Ref. 30 (narrow Band with $\beta_c \doteq 1.0$) and of Ref. 29 (wide band with $\beta_c \doteq 0$). The results for narrow band cases are particularly useful with respect to the stress response process to turbulence, since such response process is expected to be narrow band because of structural filtering effects.

A collection of many acceleration records during maneuver indicates that the (acceleration) load history exhibits the characteristics of a wide band random process. To represent the maneuver load in frequency domain, therefore, the following form of spectral density has been empirically suggested for a fighter type airplane (Ref. 12).

$$S_m(\omega) = \frac{S_o}{2\pi\{1 + (\omega/\omega_B)^d\}} \qquad \omega_D \leq \omega < \infty \qquad (29)$$

where $d = 2.6$, $\omega_B = 2\pi \times 0.031$(rad/sec) and $S_o \doteq 30$ (g^2·sec) with ω_D indicating the lower cut-off frequency. If the maneuver loading is assumed to be a (single) Gaussian random process, then the load exceedance curve (interpreted as indicating level crossing) is symmetric with respect to negative and positive loading. Experimental measurements tend to

indicate (as shown in Fig. 2) that such an assumption may be valid for an airplane of transport type. However, as observed experimentally and also as specified in Military standards (see Fig. 3), the positive and negative parts of the load exceedance curve for a fighter due to maneuvers are markedly different. To account for this fact, the following procedure is proposed: Consider two Gaussian processes $Y_p(t)$ and $Y_n(t)$ which are associated with the symmetric exceedance curves respectively constructed from positive and negative parts of the (specified) asymmetric exceedance curve. Let σ_p and σ_n denote the standard deviations of $Y_p(t)$ and $Y_n(t)$. These standard deviations can be evaluated from the positive and negative slopes of the specified asymmetric exceedance curve. Then, digitally generate $Y_p(t)$ in the same manner as above using the spectral density given in Eq. 29 (see Fig. 22 for sample time history) and construct Y(t) so that

$$\begin{aligned} Y(t) &= Y_p(t) && Y_p(t) \geq 0 \\ &= rY_p(t) && Y_p(t) < 0 \end{aligned} \qquad (30)$$

where $r = \sigma_n/\sigma_p$. The process Y(t) thus constructed produces the same exceedance curve as specified. A sample time history of Y(t) with $\omega_D = 2\pi \times 0.007$ rad/sec and $r = 0.3$ is shown in Fig.23.

From the time history $Y(t)$, the expected value of the b-th power of rise and fall, $\overline{S_m^b}$, is calculated using the counting procedures indicated in Fig. 17. It should be noted that the parameters d, ω_B, ω_D, S_o in Eq. 29 can be adjusted to represent maneuver loading for a variety of fighters under different flight conditions. The transformation between the maneuver loading in terms of acceleration, $Y(t)$, and stress, $S_m(t)$, can be performed in a quasi-static manner. This is due to the fact that maneuver loads are applied at a relatively slow rate in comparison to the structural dynamic sensitivity of a critical part in an aircraft. The energy in the maneuver spectral density $S_m(\omega)$ is concentrated at low frequencies while the peaks of the absolute frequency response function $|H(\omega)|$ appear at higher frequencies. Thus, the time history of the stress at a particular critical point in the aircraft due to maneuvers can be written as $S_m(t) = CY(t)$ where C is a proportionality constant. For example, from Ref. 13 (Fig. 24) it can be observed that $C \doteq 4 KGF/mm^2$ for wing-root bending stress for a fighter.

Because of this proportionality, the coefficient A in the equation $\overline{S_m^b} = A\sigma_{3S}^b$ (see Eq. 22) is identical with the coefficient A in the equation $\overline{Y^b} = A\sigma_p^b$ where $\overline{Y^b}$ is the expected value of the b-th power of rise and fall of $Y(t)$. Hence, the values of A are evaluated from time histories of $Y(t)$ (Fig. 23) and plotted in Fig. 25 as functions of b (dotted curves). The solid curves in Fig. 25 indicate the values of A appearing in the equation

$\overline{Y_p^b} = A\sigma_p^b$ and obtained from time histories of $Y_p(t)$ (Fig. 22). The dotted and solid curves in Fig. 25, therefore, show the difference between $\overline{S_m^b}$ based on the specified asymmetric exceedance curve and on the corresponding symmetric exceedance curve. It is pointed out that if $Y_p(t)$ is a narrow band, $\overline{S_m^b}$ evaluated from $Y(t)$ is equal to $\overline{S_m^b}$ evaluated from $Y_p(t)$ multiplied by $(1 + r)^b/2^b$. In the numerical example that follows, the solid curve for Case II is used for aircraft of transport type because they tend to have symmetric exceedance curves as previously mentioned while the dotted curve for Case II is used for fighter aircraft.

V. Residual Strength

1. Slow Crack Growth Model

When the crack is interpreted as initiating rather than pre-existing, a crack of size a_o is initiated at time t_o after the aircraft is placed into operation. Then, the initiated crack grows in its size in the manner as described in Sec. III, and under the slow crack growth design, the (initial) ultimate material strength R_o starts to decrease as crack reaches the initial critical crack size a_{ic} at time t_1 (= $t_o + t_{ic}$) where t_{ic} is the time required for the crack to increase its size from a_o to a_{ic}.

The relationship between the residual strength and the crack size can be expressed by the equation of Griffith-Irwin type

$$K_C = R_o\sqrt{\pi a_{ic}/2} \tag{31a}$$

$$K_C = R(t_m)\sqrt{\pi a(t_m)/2} \tag{31b}$$

where a_{ic} is usually larger than a_{TH} and K_C = critical stress intensity factor, $a(t_m)$ = crack size at time $t_1 + t_m$; i.e., at time t_m after the crack reaches a_{ic}. The interrelationship among R_o, $R(t_m)$, a_o, a_{ic}, $a(t_m)$, etc. is schematically illustrated in Fig.[26] while the relationships among t_o, t_1, t_m, t_{ic} and t_n (t_n will be defined later) are illustrated in Figure 27.

The time t_{ic} is evaluated from Eq. 16 or Eq. 17 as

$$t_{ic} = \frac{2}{2-\lambda}(a_{ic}^{1-\lambda/2} - a_o^{1-\lambda/2}) / cQ^{\lambda/b} N_o^{1-\lambda/b} (\pi/2)^{\lambda/2}$$

$$a_{ic} > a_o \geq a_{TH} \qquad (32a)$$

$$t_{ic} = \frac{2}{2-\lambda'}(a_{TH}^{1-\lambda'/2} - a_o^{1-\lambda'/2}) / c'Q^{\lambda'/b} N_o^{1-\lambda'/b} (\pi/2)^{\lambda'/2}$$

$$+ \frac{2}{2-\lambda}(a_{ic}^{1-\lambda/2} - a_{TH}^{1-\lambda/2}) / cQ^{\lambda/b} N_o^{1-\lambda/b} (\pi/2)^{\lambda/2}$$

$$a_o < a_{TH} \qquad (32b)$$

Then, the expression for the residual strength as a function of time t_m becomes

$$R(t_m) = R_o a_{ic}^{\frac{1}{2}} / \{a_{ic}^{1-\lambda/2} + (1 - \lambda/2)c(\pi/2)^{\lambda/2} Q^{\lambda/b} N_o^{1-\lambda/b} t_m\}^{1/(2-\lambda)}$$

(33)

It is important to note that all the equations and the definitions of parameters appearing in this subsection are valid even when the crack of size a_o is assumed to be pre-existing (rather than initiating at t_o) so long as t_o is taken to be zero.

2. The Fail-Safe Design

A design practice to prevent the reduction of the residual strength from reaching an excessive level is to introduce crack stoppers in the structure, thus making the design fail safe. In this case, Eqs. 31a and 31b are no longer valid to represent the strength of a cracked structure. The strength of the fail safe structures depends on a particular design and the residual strength should be determined by individual analysis and testing. Following Refs. 27, 40 and 41, the residual strength after t_n flight hours is assumed to be

$$R(t_n) = R_o\{1 - (1 - \xi)\left(\frac{a(t_n) - a_o}{a_s - a_o}\right)^{\frac{1}{2}}\} \qquad (34)$$

where a_s = fail-safe crack size, $R_o\xi$ = residual strength at the fail-safe crack size a_s, and $0 < \xi < 1$.

VI. Failure Rate

A failure of the structure occurs when the residual strength $R(t_n)$ is exceeded by the applied (random) stress. Then, the problem is essentially that of a first-passage probability with a variable one-sided threshold (Refs. 42 - 44). The expected upcrossing rate $\nu_k^+(R_o)$ of the stress process $S_k(t)$ with respect to the threshold value R_o (initial resisting strength) obtained in Sec. II can also be used in approximation for the expected rate with the variable threshold $R(t_n)$. The expected failure rate $h_k(t_n, R_n)$, or risk function, associated with this first passage problem can then be approximated by

$$h_k(t_n, R_n) = \nu_k^+(R_n)/M_c \tag{35}$$

where R_n is written for $R(t_n)$ and the clumpsize $M_c \geq 1$ (Refs. 43 and 44). For aircraft structures, the difference between the initial strength R_o and the stress X_o due to one g load is by design much larger than the standard deviation of the stress process, and also the restriction on the length of service life as well as the implementation of the inspection maintains the residual strength $R(t_n)$ at a higher level compared with X_o in terms of the standard deviation of the stress process. Therefore, the events of stress excursion beyond the threshold can be assumed to be statistically independent and hence

$M_c = 1$ is used for the present purposes.

In this investigation, the residual strength is also considered as a random variable and therefore, the failure rate given in Eq. 35 with $M_c = 1$ is modified as

$$h_k(t_n) = \int_{-\infty}^{X_o} f_R(x)dx + \int_{X_o}^{\infty} \nu_k^+(x) f_R(x)dx \qquad (36)$$

where $f_R(x)$ is the probability density function of the residual strength $R(t_n)$. In this equation, the value of unity is used for simplicity in place of $\nu_k^+(x)$ for the values of x less than X_o. Since this is the range of x where $f_R(x)$ is insignificantly small, the resulting value of the integration is rather insensitive to the assumption of $\nu_k^+(x)$ in this range of x.

A further modification is necessary when the loads on the aircraft can be controlled by pilots or by other means. For example, if the controlled maneuver results in a truncation of the load spectrum, the failure rate is obtained from

$$h_k = \int_{-\infty}^{X_o} f_R(x)dx + \int_{X_o}^{\infty} \nu_k^+(x) f_R(x)dx - \int_{m_T X_o}^{\infty} \nu_k^+(x) f_R(x)dx \qquad (37)$$

where $m_T X_o$ is the truncation level with $m_T (>1)$ being the truncation index. To determine the failure rate due to a combined effect of each component process k, one can use

$$h(t_n) = \sum_{k=1}^{3} p_k h_k(t_n) \tag{38}$$

For a Gaussian distribution of the residual strength $R(t_n)$ with mean value $\gamma_n \mu_o$ and standard deviation $\sigma_R = V_o \gamma_n \mu_o$, the probability density function is

$$f_R(x) = \frac{1}{\sqrt{2\pi}\sigma_R} \exp\{-\frac{(x - \gamma_n \mu_o)^2}{2\sigma_R^2}\} \tag{39}$$

where for the slow crack growth model, γ_n is obtained from Eq. 33 as

$$\gamma_n = a_{ic}^{\frac{2-\lambda}{2}} / \left(a_{ic}^{\frac{2-\lambda}{2}} + (1 - \lambda/2) c (\pi/2)^{\lambda/2} Q^{\lambda/2} N_o^{1-\lambda/b} (t_n - t_{ic})\right)^{\frac{1}{2-\lambda}} \tag{40}$$

and, for the fail-safe design model, from Eq. 34,

$$\gamma_n = 1 - (1 - \xi)\{\frac{a(t_n) - a_o}{a_s - a_o}\}^{\frac{1}{2}} . \tag{41}$$

When $t_n = t_{ic}$ in Eq. 40 and $t_n = 0$ in Eq. 41, γ_n becomes unity and the density function in Eq. 39 represents that of the initial resisting strength R_o.

Using Eq. 39 in Eqs. 36 and 38 with expression of $\nu_k^+(x)$ given in Eq. 5, one obtains the failure rate associated with a combined stress process with no load truncation as

$$h(t_n) = \sum_{i=1}^{3} \tfrac{1}{2} P_i N_i \{ [1 - \mathrm{erf}(\frac{\eta_i}{\sqrt{2} r_i})] + \exp[-(2\eta_i - r_i^2)/2] \times$$

$$[1 + \mathrm{erf}(\frac{\eta_i - r_i^2}{\sqrt{2} r_i})] \} \qquad (42)$$

in which $N_1 = N_2 = N_g$, $N_3 = N_m$, $\eta_i = (\gamma_n \mu_o / \sigma_{ci}) - (X_o / \sigma_{ci})$, $r_i = V_o \gamma_n \mu_o / \sigma_{ci}$, $V_o = \sigma_{R_o} / \mu_o$, $i = 1, 2, 3$.

When each of the component loading processes is assumed to be a single Gaussian with a truncated average upcrossing rate, the failure rate associated with the combined stress is obtained from Eqs. 10, 37, 38 and 39.

$$h(t_n) = \sum_{i=1}^{3} \tfrac{1}{2} P_i N_i \{ (1 - \mathrm{erf}(\frac{\eta_i}{\sqrt{2} r_i})) + (1 + r_i^2)^{-\frac{1}{2}} \exp[-\tfrac{1}{2}(\frac{1}{V_x^2} + \frac{1}{V_o^2})$$

$$+ \tfrac{1}{2}(\frac{r_i}{V_x} + \frac{1}{V_o})^2 (1 + r_i^2)^{-1}] [\mathrm{erf}(\frac{\eta_i}{\sqrt{2}\eta_i} (1 + r_i^2)^{-\frac{1}{2}})$$

$$+ \mathrm{erf}\{ \frac{1}{\sqrt{2}} \cdot \frac{1}{\sqrt{r_k^2 + 1}} [(m_T - 1) \frac{r_i}{V_x} + m_T \cdot \frac{1}{r_i V_x} - \frac{1}{V_o}] \}] \} \qquad (43)$$

where $V_x = \sigma_s / X_o$.

If the combined stress process consists of single and composite Gaussian processes, the failure rate can be expressed in an appropriate combination of terms appearing in Eqs. 42 and 43. The computer program is written so that an arbitrary combination of this nature can be accommodated.

VII. Periodic Inspections

The purpose of inspection is to detect the fatigue and pre-existing cracks in the structural components so that, before cracks become critical,they can be replaced by uncracked components to endure their designed initial strength at least at the time of replacement. In this study, two types of aircraft inspection at different levels of sophistication are considered: (1) "rigorous" periodic inspections which might correspond to the depot or base level inspection (Ref. 45) utilizing particular non-destructive inspection (NDI) techniques and (2) "cursory" inspections which might correspond to in-flight evident, ground evident, walk around and special visual inspections (Ref. 45).

The probability of detecting a fatigue crack at a structural detail during a rigorous inspection depends on the probability of inspecting this cracked detail and the resolution capability of the particular inspection technique. Typical NDI techniques presently used include delta scan, shear wave ultrasonic, magnetic particle, X-ray, and magnetic rubber inspection (MRI) methods.

Define U_1 as the probability of inspecting a cracked detail and $U_2(a)$ as the probability of detecting a crack of size a. Then, the probability of detecting a crack during a rigorous inspection can be obtained in general from

$$F(a) = U_1 U_2(a) \tag{44}$$

where it was assumed that U_1 and $U_2(a)$ are independent. The probability of not detecting a crack $F^*(a)$ is obviously equal to $1 - F(a)$.

Since at this time, the information on the probability U_1 is limited, it is assumed in this study that $U_1 = 1$, i. e., every critical detail will be inspected. Based on the experimental and empirical results, however, the detection probability $U_2(a)$ may be constructed in the following fashion (Refs. 21, 25 and 27).

$$\begin{aligned} U_2(a) &= 0 && a < a_1 \\ &= [(a - a_1)/(a_2 - a_1)]^m && a_1 \leq a \leq a_2 \\ &= 1 && a_2 < a \end{aligned} \tag{45}$$

where $1/8 < m < 1/5$ for accurate NDI techniques, $m > 1/5$ for more crude NDI techniques, a_1 = the minimum crack size below which the crack cannot be detected with the particular detection technique used, a_2 = the maximum crack size beyond which the crack can always be detected.

In Fig. 28 , a plot of $U_2(a)$ is shown for two different values of parameter m (=1/8 and 1) with a_1 = .02" and a_2 = .3". Detection probabilities experimentally obtained for X-ray,

ultrasonic and dye penetrant techniques are also indicated in this figure (Ref. 25).

A similar crack detection probability model can be constructed for the cursory inspections. However, since no definite experimental information is presently available, the following simple form is assumed for the probability;

$$\begin{aligned} F_c(a) &= 0 && a < a_1' \\ F_c(a) &= 1 && a \geq a_1' \end{aligned} \qquad (46)$$

where a_1' = the crack size below which the crack cannot be detected by cursory inspection and beyond which the crack is always detected. The probability of not detecting a crack by the cursory inspection is $F_c^*(a) = 1 - F_c(a)$.

VIII. Probability of Failure

1. Probability of Failure Based on Distribution of Time to Crack Initiation

Following Ref. 27 for the development of this subsection, let P_o be the probability of failure of the aircraft within the intended service life T with no inspection. Then, assuming the time t_o to crack initiation to be a random variable with a probability density function $W(t_o)$, the probability of failure can be expressed as

$$P_o = 1 - \exp\{-Th_o-(T/\beta)^{\alpha}\} - \int_0^T W(t)\exp\{-th_o-H(T-t)\}dt \quad (47)$$

where h_o is the expected failure rate corresponding to the threshold R_o or $h_o = h(t_o)$ in Eq. 38, and

$$H(t_n) = \int_0^{t_n} h(t)dt \quad (48)$$

In this study as in Ref. 27, a two-parameter Weibull distribution of the time to crack initiation is used for $W(t_o)$;

$$W(t_o) = \frac{\alpha}{\beta}\left(\frac{t_o}{\beta}\right)^{\alpha-1}\exp\{-\left(\frac{t_o}{\beta}\right)^{\alpha}\} \qquad t_o \geq 0 \quad (49)$$

However, when the minimum life T_o^* is reliably known, the following three parameter Weibull density can advantageously

be used (Ref. 46).

$$W(t_o) = \frac{\alpha}{\beta}\left(\frac{t_o - T_o^*}{\beta}\right)^{\alpha-1} \exp\{-[(t - T_o^*)/\beta]^{\alpha}\} \quad t_o \geq T_o \qquad (50)$$

in which α = shape parameter and β = scale parameter.

Assume now that the aircraft is subjected to a rigorous inspection at the end of each T_o flight hours as indicated in Fig. 29. The probability of failure P(j) within the $[o, jT_o]$ interval (j-1 inspections) can then be obtained from

$$P(j) = P_j^* + \sum_{i=1}^{j-1} \int_0^{T_o} q_{ij}(t) W[(i-1)T_o + t]dt \qquad (51)$$

$$j = 2, 3, \ldots$$
$$i = 1, 2, \ldots\ldots, j-1$$

where

$$q_{ij}(t) = F[a(T_o - t)]C_{ij}^{(1)}(t) + \{\prod_{k=1}^{j-i} F^*[a(kT_o - t)]\}V_{ij}(t)$$

$$+ \delta_{j-i-2} \sum_{k=2}^{j-i} \{\prod_{m=1}^{k-1} F^*[a(mT_o - t)]\} F[a(kT_o - t)]C_{ij}^{(k)}(t) \qquad (52)$$

$$P_j^* = \exp\{-[(j-1)T_o/\beta]^{\alpha}\} - \exp\{-[jT_o/\beta]^{\alpha} - jT_o h_o\}$$

$$- \int_0^{T_o} W[(j-1)T_o + t]\exp\{-h_o[(j-1)T_o + t] - H(T_o - t)\}dt \qquad (53)$$

$$j = 1, 2, \ldots.$$

$$V_{ij}(t) = 1 - \exp\{-h_o[(i-1)T_o + t] - H[(j-i+1)T_o - t]\} \qquad (54)$$

$$C_{ij}^{(k)}(t) = 1 - \exp\{-h_o[(i-1)T_o+t]-H(kT_o-t)-K_{j-i-k+1}\}$$
$$k = 1, 2, \ldots\ldots, (j-i) \quad (55)$$

$$K_k = -\ln [1 - P(k)] \quad (56)$$

where $\delta_{j-i-2} = 1$ if $j-i-2 \geq 0$, and $\delta_{j-i-2} = 0$ otherwise.

The probability of failure given in Eq. 51 is for a single aircraft. Assuming the event of failure of each aircraft to be statistically independent, the probability of first failure in a fleet of M aircraft in $[0, jT_o]$ interval is

$$P_M(j) = 1 - [1 - P(j)]^M \quad (57)$$

2. Probability of Failure Based on Distribution of Initial Crack Size with No Cursory Inspection

In this case, the (initial) crack of size a_o is assumed to be pre-existing in the structure with a probability density function $G(a_o)$. Although a number of alternative analytical forms appear to be possible (Ref. 47), this investigation uses a particular form of $G(a_o)$ in the analysis which is compatible with the two parameter Weibull density given in Eq. 49.

The significance of the compatibility is as follows: An initial crack of size a_o increases its size under loading history and attains a specified size a^* ($>a_o$) at time t_o.

If the crack propagation law given in Eq. 17 is used under the assumption that $a^* \leq a_{TH}$, then t_o and a_o are related by

$$t_o = \frac{a^{*1-\lambda'/2} - a_o^{1-\lambda'/2}}{(1 - \lambda'/2)c'(\pi/2)^{\lambda'/2}Q^{\lambda'/b}N_o^{1-\lambda'/b}} \tag{58}$$

Now interpret a* as the crack size initiated at time t_o in the crack initiation model considered in the preceding subsection, where symbol a_o is used for the initiated crack size rather than a*, however. Then, a density function $G(a_o)$ of initial crack size a_o can be derived from the density function $W(t_o)$ of t_o with the aid of the relationship given in Eq. 58;

$$G(a_o) = -\frac{dt_o}{da_o} W(t_o) \tag{59}$$

with

$$\frac{dt_o}{da_o} = \frac{-a_o^{-\lambda'/2}}{c'(\pi/2)^{\lambda'/2}Q^{\lambda'/b}N_o^{1-\lambda'/b}} \tag{60}$$

If Eq. 49 is used for $W(t_o)$ in Eq. 59, then $G(a_o)$ is the desired density function of a_o compatible with the two parameter Weibull distribution of t_o. This compatibility between the initial crack distribution $G(a_o)$ and the distribution of the time to crack initiation $W(t_o)$ is schematically shown in Fig. 30 . An example of such compatible density function is plotted in Fig. 31 where the values of Weibull parameters as

well as those of the parameters involved in the crack propagation law (Eq. 58) used for the plot are indicated. The distribution function associated with this density function is then plotted on the Frechet probability paper in Fig.32 . Since the Fréchet distribution is defined by the density function

$$G(a_o) = \frac{\alpha^*}{\beta^*}\left(\frac{a_o}{\beta^*}\right)^{-\alpha^*-1} \exp\{-(a_o/\beta^*)^{-\alpha^*}\} \qquad a_o \geq 0 \quad (61)$$

and is not limited to the right, the plot in Fig.32 naturally curves upward asymptotically approaching a vertical line at $a_o = a^*$ which in this example is equal to 0.04" and is the upper bound of a_o.

Under the assumptions that the structural component has a pre-existing crack with a density function $G(a_o)$, that the component is subjected to a rigorous inspection at the end of each period of T_o flight hours and that the component is replaced by a new component if a crack is found by the inspection, the probability of failure of an aircraft within the interval $[0, jT_o]$ is given by

$$P(j) = \int_0^\infty G(a_o)P'(j)da_o \qquad (62)$$

where

$$P'(j) = 1 - F[a(T)]\exp\{-H(T) - K_{j-1}\}$$

$$- \sum_{k=2}^{j-1} \prod_{m=1}^{k-1} F^*[a(mT)]F[a(kT)]\exp\{-H(kT) - K_{j-k}\}$$

$$- \prod_{k=1}^{j-1} F^*[a(kT)]\exp\{-H(jT)\} \qquad (63)$$

with

$$K_j = - \ln[1 - P(j)] \qquad (64)$$

It is noted that Eq. 64 involves P(j) but not P'(j). This is because the distribution of initial crack size of the replaced component is assumed to be independent of that of the replacing component.

The comparison between Eqs. 62 - 64 and the corresponding equations in the crack initiation model indicates that the probability of failure can be expressed with considerably less analytical complexities under the assumption of initial crack size distribution, although the integration in Eq. 62 must in general be carried out numerically.

3. Probability of Failure Based on Distribution of Initial Crack Size with Cursory Inspections

Consider the inspection procedure where the rigorous inspection is performed on the aircraft τ times in its service life T at equal interval of T_1 with additional cursory inspections performed ρ times in each rigorous inspection interval

of T_o. Then, $T_1 = (\rho + 1)T_o$, $T = (\tau + 1)T_1$ and $T = (\rho + 1)(\tau + 1)T_o$ (see Fig.33). Under these circumstances, writing P(j) for the probability of failure in the interval $[0, jT_1]$ or $[0, j(\rho + 1)T_o]$, one can show that

$$P(j) = \int_0^\infty P'[(\rho + 1)j]G(a_o)da_o \tag{65}$$

where

$$\begin{aligned} P'(i) = 1 - \{ & \delta[i-(\rho+1)n-1]F[a(T_o)] \\ & + [1-\delta[i-(\rho+1)n-1]]F_c[a(T_o)]\exp[-H(T_o)-K_{i-1}]\} \\ & - \sum_{k=2}^{i-1} \prod_{m=1}^{k-1} \{\delta[i-(\rho+1)n-m]\, F^*[a(mT_o)] \\ & + [1-\delta[i-(\rho+1)n-m]]F_c^*[a(mT_o)]\}\cdot \\ & \{\delta[i-(\rho+1)n-k]F[a(kT_o)] + [1-\delta[i-(\rho+1)n-k]] \\ & \cdot F_c[a(kT_o)]\}\exp\{-H(kT_o) - K_{i-k}\} \\ & - \prod_{k=1}^{i-1} \{\delta[i-(\rho+1)n-k]F^*[a(kT)] \\ & + [1-\delta[i-(\rho+1)n-k]]F_c^*[a(kT_o)]\}\exp\{-H(iT_o)\} \end{aligned} \tag{66}$$

$$K_i = -\ln[1 - P(i)] \tag{67}$$

and

$$\delta[i - (\rho+1)n - k] = \begin{cases} 1 & \text{if there exists a positive integer } n \text{ such that } i-k=(\rho+1)n \\ 0 & \text{otherwise} \end{cases} \quad (68)$$

4. Probability of Failure of Proof Tested Aircraft

To include the effect of the proof load test, define a probability density function $G'(a_o)$ for the initial crack distribution in the following fashion (Refs. 48 and 49)

$$G'(a_o) = \begin{cases} G(a_o) / \int_0^{a_{op}} G(a_o)da_o & 0 \leq a_o \leq a_{op} \\ 0 & a_{op} < a_o \end{cases} \quad (69)$$

where a_{op} is the truncation level on $G(a_o)$ as a result of the proof test. The probability of failure can then be determined by the same procedures as described in 8.2 or 8.3 depending on whether or not the cursory inspections are performed. The necessary modifications consist of replacing $G(a_o)$ by $G'(a_o)$ and the infinite upper bound by a_{op} in the intervals in Eqs. 62 and 65.

It appears difficult at this time to consider the effect of the proof load test within the framework of the crack initiation model described in 8.1. Furthermore, it is pointed out that Eq. 57 also indicates the probability of first failure in a fleet of M aircraft in the interval $[0, jT_o]$ for the cases of 8.2 and

in the interval $[0, j\tau_1]$ in the case of 8.3. In the above, 8.1, 8.2 etc. indicate respectively subsections 1, 2, etc. of this section (Section VIII). The same notation is used for other subsections throughout.

IX. Sensitivity Analysis

1. Model Sensitivity

In the preceding sections, a number of analytical models are introduced with respect to random stress processes, crack propagation laws, rise and fall statistics of the stress process, residual strengths, expected failure rate and inspection procedures for the ultimate purpose of evaluating the probability of aircraft failure. Obviously, the resulting probability of failure depends on these analytical models. Since, however, they are contructed on the basis of the current (and therefore not necessarily perfect) state of the engineering knowledge on the subjects involved with the due consideration for analytical and numerical tractability, it is highly desirable to investigate the sensitivity of the probability of failure to these models. Such sensitivity studies could be performed in terms of numerical examples for those items for which competing or alternative models are proposed. For example, significant difference in the probability of failure may result depending on whether one choses

(a) a single Gaussian or a composite Gaussian for a component process (such as stress process due to clear air turbulence),

(b) a Gaussian process or a non-Gaussian process for maneuver,

(c) counting method I or method II in conjunction with rise and fall statistics (see Fig. 17),

(d) slow crack growth design or fail-safe design,

(e) clumpsize equal to one or any other value,

(f) crack-initiation model or pre-existing crack model,

(g) controlled maneuver or uncontrolled maneuver,

(h) perform inspection or do not perform inspection

(i) perform proof load test or do not perform proof load test.

Although the computer programs are written so that all these items except for item (e) can be dealt with, the sensitivity studies are actually performed only on items (d), (f), (g), (h) and (i) and the results are summarized in terms of graphical comparisons (see Sec. XI). Such results are highly useful in numerically assessing the significance of various models described above.

2. Parameter Sensitivity

After the decision is made to choose a particular model among the alternatives proposed for each of the items indicated above, it is not unusual to face the uncertainties of statistical and other origins under which the values are to be assigned to the parameters of the model. Then, the sensitivity studies are again desirable with respect to these parameters for the purpose of identifying more important parameters in terms of their contributions to the probability of failure.

Writing these parameters as X_1, X_2, ..., X_n, the probability

of failure P can formally be written as a function of X_1, X_2, ..., X_n once the analytical models to be used are decided upon;

$$P = P(X_1, X_2, \ldots\ldots, X_n) \tag{70}$$

In reality, the dependence of P on the parameters is obviously very complex as seen from the analysis developed in the preceding sections.

Treating the uncertainties associated with these parameters as if they were all of statistical origin (or treating X_1, X_2, .., X_n as random variables), the sensitivity of the probability of failure to each of these parameters is evaluated with the first order and second moment approach. Within the framework of this approach, the most reliable value of a parameter X_i is treated as its expected value and written as $\bar{X}_i$, whereas its uncertainty is expressed in terms of coefficient of variation $V_{X_i} = \sigma_{X_i} / \bar{X}_i$ with σ_{X_i} being standard deviation of X_i. The expected value $\bar{P}$ and coefficient of variation V_P of P are then obtained from

$$\bar{P} = P(\bar{X}_1, \bar{X}_2, \ldots\ldots, \bar{X}_n) \tag{71}$$

$$V_P^2 = \sum_{i=1}^{n} \alpha_i^2 V_{X_i}^2 \tag{72}$$

where α_i is referred to as sensitivity index and is given by

$$\alpha_i = \left(\frac{\partial P}{\partial X_i}\right)\left(\frac{\bar{X}_i}{\bar{P}}\right) \qquad (73)$$

where partial derivatives are evaluated at $X_i = \bar{X}_i$ (i = 1, 2,..., n). If $\bar{P}$ and V_P are interpreted as representing the most reliable value of P and its uncertainty respectively, the sensitivity index α_i indicates the contribution of the uncertainty associated with parameter X_i to the uncertainty of $\bar{P}$ through Eq. 72.

Dealing with a transport aircraft, twenty five (25) parameters are investigated for the sensitivity analysis and are listed in Table - 5; Table 3 also shows their most reliable values as expected values and corresponding sensitivity indices squared (α_i^2) for crack initiation model under slow crack growth design, Table 4 for crack initiation model under fail safe design and Table 5 for pre-existing crack model under fail safe design. These results are all obtained under the assumption of five equally spaced rigorous inspections performed during the service life of 15,000 hours. As mentioned earlier, the dependence of P on X_1, X_2, ..., X_n is highly complex and analytical evaluations of partial derivatives in Eq. 73 are in general not possible. Therefore, these derivatives are numerically evaluated in principle as

$$\left(\frac{\partial P}{\partial X_i}\right)_{X_i=\bar{X}_i} = \{P(\bar{X}_1,\bar{X}_2,\ldots,\bar{X}_i+\Delta X_i\ldots,\bar{X}_n) - P(\bar{X}_1,\bar{X}_2,\ldots,\bar{X}_i,\ldots,\bar{X}_n)\}/\Delta X_i$$
$$(i = 1, 2, \ldots, n) \qquad (74)$$

The procedure involved in such numerical evaluation is illustrated in Figure 34 dealing with a_o, the first parameter in Table 2 as an example.

X. Significance of Full-Scale Test

Fatigue testing under loading sequences representative of expected operational conditions obviously provides realistic life estimates. These estimates are, however, usually obtained from full-scale tests involving a single or at most two prototypes, since the cost is prohibitive even for a small number of replications. This subsection therefore attempts to investigate the significance of such full-scale testing from the view point of aircraft reliability estimation. In this respect, the analysis recently developed in Ref. 50 is closely followed where the time to first failure t_1, is related to a reliability figure on the basis of the result of full-scale testing without, however, considering the effect of inspections.

Although the full-scale testing is performed usually only on a single or at most two prototypes as just mentioned, consider for the purpose of theoretical development that n such prototypes are tested with observed lives (times to failure) $t_{o1}, t_{o2}, \ldots, t_{on}$. These observations constitute a sample of size n taken from the density function $W(t_o)$ of the time to failure t_o of individual aircraft (or structural components). Since, as will be seen below, this sample is needed to estimate a measure of location of the distribution of t_o, any density function that provides a reasonable fit to this sample at a central range of distribution may be assumed for $W(t_o)$. For

convenience, however, the two parameter Weibull distribution with the density function given in Eq. 49 is assumed for t_o. The time to first failure t_1 in a fleet of size m is then interpreted as the smallest among the sample of size m taken from the Weibull distribution with the density $W(t_o)$ given in Eq. 49. Hence, the distribution function of t_1 is in general one of the extreme value distributions and in this case it is again a Weibull by virtue of stability of the extreme value distribution. In fact, it can be shown to be

$$W_1(t_1) = \frac{\alpha}{\beta_1}\left(\frac{t_1}{\beta_1}\right)^{\alpha-1} \exp\{-(t_1/\beta_1)^{\alpha}\} \tag{75}$$

where, however, the scale parameter β_1 is given by $\beta_1 = \beta/m^{1/\alpha}$ while the shape parameter remains to be α (α and β are shape and scale parameter of the Weibull density for t_o).

Define now the scatter factor S as

$$S = \hat{\beta}/t_1 \tag{76}$$

where $\hat{\beta}$ is the maximum likelihood point estimator of the scale parameter β from a sample of size n (t_{o1}, t_{o2}, ..., t_{on}).

The point estimator $\hat{\beta}$ for n observations t_{oi} is given by

$$\hat{\beta} = \left[\frac{1}{n}\sum_{i=1}^{n} t_{oi}^{\alpha}\right]^{1/\alpha} \tag{77}$$

provided α is known. The distribution function $f_1(\hat{\beta})$ can then be shown to be

$$f_1(\hat{\beta})d\hat{\beta} = \frac{n^n \alpha}{\Gamma(n)\ \beta}\left(\frac{\hat{\beta}}{\beta}\right)^{\alpha n-1} \exp\left[-n\left(\frac{\hat{\beta}}{\beta}\right)^{\alpha}\right]d\hat{\beta} \tag{78}$$

Using Eqs. 75 and 78, one obtains the density function of the quotient $S = \hat{\beta}/t_1$ as

$$f_2(S) = \int_0^{\infty} f_1(St_1)\cdot W_1(t_1)t_1 dt_1 \tag{79}$$

which after some manipulation becomes

$$f_2(S) = \frac{\alpha m n^{n+1} S^{\alpha n-1}}{(m + nS^{\alpha})^{n+1}} \tag{80}$$

By integration, the distribution function of S is obtained as

$$F_2(S) = \left[1 - \frac{S^{\alpha}}{(m/n) + S^{\alpha}}\right]^n \tag{81a}$$

and this probability is identical to the reliability R that the time to first failure t_1 will be at least equal to the maximum likelihood estimate defined by Eq. 77 divided by a scatter factor S;

$$R = \left[\frac{S^{\alpha}}{(m/n) + S^{\alpha}}\right]^n \tag{81b}$$

The values of α representative for different structural materials and for aircraft of fighter and transport type are summarized in Ref. 50 on the basis of existing data and listed here in Table 6. The values of the scatter factor associated with reliability levels R = 0.5, 0.9 and 0.99 are evaluated from Eq. 81b for more conservative values of α = 2, 3, 4 and 5. The results are shown in Tables 7 - 9 for m = 3, 25, 100, 250 and 1,000 and m = 1 and 3. It is important to observe from Tables 7 - 9 that practically no change materializes by increasing n from 1 to 3. This fact is highly significant, as emphasized in Ref. 50, since it means that the full-scale testing performed on two or three prototypes offers practically no advantage over the testing of a single prototype as far as the reliability estimation with respect to the time to first failure is concerned. It is also important to realize that the values of the scatter factor are within a practical range even at a reliability level of .99 particularly when the fleet size is not too large. If the minimum life T_o^* is introduced in the Weibull distribution as indicated in Eq. 50, it can be shown (Ref. 50) that the values of the scatter factor will be reduced significantly even for T_o^* as small as 0.05β.

The results described above provide the theoretical bases on which a realistic method of reliability demonstration can be established as an enforcable part of the certification and procurement procedure. Even more significant is the potential

of this approach in evaluating the possible amount of reduction in the scatter factor when the aircraft are subjected to the periodic inspection as described in Sec. VII, although the approach must in essence use the crack initiation model because of its mathematical development using the Weibull distribution.

XI. Numerical Examples and Discussion

Numerical examples are carried out for long-life aircraft such as transports and bombers using the crack initiation model under slow crack growth and fail safe design and also using the pre-existing crack model under fail safe design. With the crack initiation model, a two-parameter Weibull density is used for the time to crack initiation while the corresponding (compatible) distribution is used with the pre-existing crack model. Tables 3 - 5 show the parameter values used for the numerical computation in the column under "Mean Value." Some of these values are assigned on the basis of experimental evidence, others are chosen to be consistent with conventional static design practice and still others are on the basis of engineering judgement. For example, the values of material constants are consistent with those of structural aluminum, the parameters associated with the detectable crack size are within the range found in available experiments, and the power b in the crack propagation law is assumed to be 4.0 because of the availability of the experimental data under random loading only for $b = 4$.

The parameters involved in the formulation of stress processes are more difficult to estimate since not much data are available in terms of stress history. The usual load data in terms of g cannot directly be used without specific knowledge of the structural system under consideration. The coefficient A

appearing in the rise and fall statistics is obtained from the result of simulation with b = 4 and counting method II (Fig. 17); $A = A_{14} = A_{24} = 115$ for $S_{gC}(t)$ (CAT) and $S_{gT}(t)$ (thunderstorm) assuming that they have narrow-band characteristics equivalent to those simulated processes with $\beta_c = 0.6 - 0.8$ (see Fig. 14 and 19), while $A = A_{34} = 80$ for $S_m(t)$ (maneuver) from the solid curve in Fig. 25 assuming that symmetric exceedance curves apply to transports (Fig. 2). The number of stress cycles per hour such as N_g and N_m represents the expected rate of zero upcrossing since the second counting method is used in this study. Therefore, the evaluation of these values is obviously possible when the spectral density functions of the underlying stress processes are specified. Because of the fact that the spectral densities of "stress" processes are usually not well specified, N_g and N_m are treated as independent parameters. It is emphasized that this does not invalidate either the interpretation or the result of the simulation to evaluate the coefficient A since one can always adjust the time scale so that a desired value of N_g or N_m is obtained without altering the value of A.

The choice of $p_1 = 0.495$, $p_2 = 0.005$ and $p_3 = 0.5$ is made because such a choice appears to represent one of realistic loading conditions. Also, the values of σ_{C1}, σ_{C2} and σ_{C3} as indicated in the tables are judged to be reasonable.

Under the loading and other conditions corresponding to

these parameter values specified in Table 4, a crack of size 0.04", once initiated, grows under fail safe design as shown in Fig. 35 where the corresponding residual strength $R(t_n)$ and failure rate $h(t_n)$ are also plotted. Note that the crack becomes unstable after 4,000 - 5,000 flight hours.

Figs. 36 - 39 illustrate the effect of some of the model sensitivity mentioned in Sec. IX. The probabilities of failure are all in terms of the probability of first failure in a fleet of size 50 for service life of 15,000 flight hours. Therefore, the probability of failure of any aircraft is in approximation one fiftieth of the value indicated.

Figs. 36 (a) and (c) show the difference between the probability of first failure resulting from the pre-existing model and that resulting from the crack initiation model both under fail safe design. The pre-existing model and the crack initiation model are labeled as $G(a_o)$ method and $W(t_o)$ method for simplicity. Figs. 36 (b) and (d) show the same difference under the slow crack growth model. When no inspection is performed, the pre-existing crack model and the crack initiation model produce practically identical probability of first failure under both fail safe and slow crack growth designs. The reason is as follows; when $G(a_o)$ and $W(t_o)$ are compatible, the reduction in the ultimate strength during the time period t_o in the pre-existing model is negligibly small, at least for the numerical examples considered, compared with the ultimate strength R_o

which remains constant until the end of the same time period under the crack initiation model. Fig. 36 also illustrates the effect of rigorous inspection: In all cases, the probability of first failure decreases as the number N of rigorous inspections increases. However, no further improvement is expected for N larger than 14. So long as $N < 14$, the improvements achieved by the same number of rigorous inspections are more significant for the pre-existing crack model than for the crack initiation model under both fail safe and slow crack growth design. This is due to the fact that, as the pre-existing crack a_o grows, it may be detected possibly at the early stage of growth with a size much smaller than a* (= 0.04" in this example) and the cracked structural component replaced thus providing better chances for containing the crack size less than a* throughout the life, while in the crack initiation model the cracks are found only after they are initiated with the size of a*. Comparison between Figs. 36 (a) and (b) and between (c) and (d) show that the fail safe design produces safer aircraft with both pre-existing crack model and crack initiation model at least for this numerical example. It is important to note that all the curves in Fig. 36, in particular, the curve with no inspection, show faster rates of increases in probability of failure after about 4,000 - 5,000 flight hours and that this is the range at which $a(t_n)$ start to increase significantly as mentioned previously with respect to Fig. 35. The same

trend is observed in Figs. 37 - 41 that will follow. The exceptions are those under the favorable effect of proof load test in Fig. 39.

Figs. 37 and 38 indicate the effect of cursory inspections under the various assumptions of the crack size a_1' that can be detected by them. These results are for the pre-existing crack model under fail safe design. Fig. 37 shows that even when a_1' is as small as 0.1", the improvements on the reliability achieved by the cursory inspections are insignificant as long as the number of cursory inspections is small. Each diagram represents a combination of different numbers of rigorous and cursory inspections. As shown in Fig. 38, however, significant improvements can be achieved by increasing the number of cursory inspections considerably. Even then, however, the detectable size must be as small as 0.1".

The results given in Fig. 39 is significant since they indicate generally favorable effect of proof load tests (under both fail safe and slow crack growth designs with the pre-existing model) particularly when a reasonable number of rigorous inspections are performed; for example, 5 inspections in Figures 39 (b) and (d). It should be noted that there apprears to be a critical truncation value a_{op} such that proof load tests producing a truncation less than such a critical value would significantly improve the reliability. Campare, for example, the probability of first failure for 15,000 flight hours for

a_{op} = 0.030 with that for a_{op} = 0.025 in both Figs. 30 (a) and (c).

The parametric sensitivity studies are performed on all twenty-five parameters listed in Tables 3 - 5 using the method described in subsection 9.2 and following the procedures illustrated in Fig. 34. In fact, Fig. 40 (d) shows how the basic probability values made use of in Fig. 34 for the computation of sensitivity index α_i are obtained. Other diagrams in Fig. 40 show corresponding probability values for the parameters $\overline{(\Delta K^b)}^{1/b}_{TH}$ and g (stress equivalent of one g load) both for Table 5 and a_o for Table 4. The resulting values of α_i^2 are listed under the column α_i^2 in Tables 3 - 5 (all for the case of five rigorous inspections). In all cases, the parameter g is most important, followed by $\overline{(\Delta K^b)}^{1/b}_{TH}$. Other more significant parameters are found to be λ', σ_{C_1}, a_o or a*, $\overline{Z^4}$, etc. For fail safe design, μ_o and ξ are also important.

Fig. 41 indicates the probability of first failure when no threshold is considered for $\overline{(\Delta K^b)}^{1/b}$ with log(da/dn) being related to $\log\overline{(\Delta K^b)}^{1/b}$ through a straight line (CD in Fig. 8).

Figs. 42 and 43 give the overall effect of the number of inspections for the pre-existing crack model and the crack initiation model respectively.

For fighters, numerical examples are given with the crack initiation model. In one case, structural details made of steel are considered under slow crack growth design.

The parameters listed in Table 3 are used for numerical computation except for g = 15.5 ksi, $P_3 = 1.0$, $A_{34} = 12$, $\mu_o = 210$ ksi, $(\overline{\Delta K^b})^{1/b}_{TH} = 7.0$ ksi$\sqrt{\text{in}}$ and $c = 3 \times 10^{-9}$. Also, in this case asymmetric processes constructed from single Gaussian processes as introduced in Eq. 30 are used for the stress processes $S_m(t)$ for maneuver with r = 0.3 (this is why $A_{34} = 12$, see Fig. 25), $\sigma_S = \sigma_p$ = between 1.55 g and 0.5 g. The value $\sigma_p = 1.55$ g is consistent with the exceedance curves given in Fig. 3 and appears to represent the upper bound for σ_p, while the value $\sigma_p = 0.5$ g is judged to represent less strenuous maneuver conditions. The results are shown in Figs. 44 and 45. Fig. 44 shows the effect of the number of rigorous inspections while Fig. 45 the effect of σ_S. Figs. 46 - 48 indicate similar results for structural components made of aluminum. The parameters are identical to those listed in Table 3 and 4, depending on whether slow crack growth design or fail safe design is considered. The exceptions are g = 4.2 ksi, $P_3 = 1.0$ and $A_{34} = 12$. The same asymmetric stress processes are used; r = 0.3 (and therefore $A_{34} = 12$) and $\sigma_S = \sigma_p = 0.5$ g - 1.55 g. Fig. 46 shows the effect of the number of rigorous inspections under fail safe design while Figs. 47 and 48 indicate the effect of σ_S under fail safe design and slow crack growth design respectively. It is pointed out, however, that the results indicated in Figs. 45, 47 and 48 do not really represent the effect of σ_S since the identical Weibull density has been used for the time t_o to crack initiation irrespective of σ_S values while in reality the time t_o obviously depends on σ_S.

XII. Conclusion and Recommendation for Further Study

The probability of aircraft failure P_f may be considered as function of a large number of variables. For example,

$$P_f = P_f(M, F, D, G, S, T, I, P, A)$$

where

M = Material selection

F = Fabrication

D = Design practice

G = Geometric configuration

S = Mission spectra

T = Full scale and other testing

I = Inspection procedures

P = Proof test

A = Analysis methods

In the present study, a major effort has been made to incorporate into the reliability evaluation scheme, the effect of material selection, geometrical configuration (fail safe or slow crack), mission spectra, full scale testing, inspection procedures, and proof load test. The effect of design practice implicitly appears, for example, through the stress equivalent of one g load as the design usually equates the ultimate strength to the limit load in terms of g multiplied by a safety factor. Also, the analysis method, which determines the accuracy of the

(calculated) stress equivalent of one g load as well as of (calclulated) strsss processes, influences the reliability. Although their roles are implicit in the analysis presented here, these are important items from the view point of reliability evaluation since the probability of failure has been found to be extremely sensitive to the parameter g_o.

Although this study has provided, it is hoped, an adequate analytical framework for the current effort toward implementation of the reliability-based design criteria for USAF aircraft, there are a number of other items on which further studies are recommended. They include the establishment of

(1) effect of inspection procedures on the scatter factor

(2) more reliable crack propagation law, particularly values of $(\overline{\Delta K^b})^{1/b}_{TH}$ and λ', under random loading

(3) more reliable probability values for detecting cracks of various size by NDI techniques

(4) more realistic model for residual strength for both slow crack growth and fail safe design

(5) range of the parameter values associated with stress processes from existing data depending on loading conditions and structural details, particularly for fighters under maneuver loading

(6) more explicit dependence of the distribution of time to failure on the mission spectra and the crack size at the time of crack initiation with respect to the crack

initiation model

(7) more reliable distribution functions for initial crack size with respect to the pre-existing crack model

(8) effect of having a large number of critical locations on the reliability value of an aircraft

(9) optimum number of periodic inspections on the basis of cost-effectiveness consideration.

Although all these items are important, the items (1) - (5), when accomplished, will have immediate impact on the implementation of the reliability-based design and procurement procedures.

REFERENCES

1. Freudenthal, A.M., "The Safety of Structures", Transactions, ASCE, Vol. 112, P. 125, 1947.

2. Freudenthal, A.M., Garrelts, J.M., and Shinozuka, M., "Analysis of Structural Safety," Journal of the Structural Division, ASCE, Vol. 92, No. STI, 1966, pp. 276-325.

3. Ellingwood, B.R. and Ang, A. H.-S., "Risk-Based Evaluation of Design Criteria," J. of the Structural Division, ASCE, Vol.100, No. ST9, 1974.

4. Ang, A.H.-S. and Cornell, C.A., "Reliability Bases of Structural Safety and Design," J. of the Structural Divsion, ASCE, Vol. 100, No. ST9, 1974.

5. Freudenthal, A.M. (Editor), Structural Safety and Reliability, Pergamon Press, Oxford-New York 1972.

6. Military Specification MIL-A-008861A (USAF), "Airplane Strength and Rigidity, Flight Loads," March 1971.

7. Houbolt, J.C., "Design Manual for Vertical Gust Based on Power Spectral Techniques," AFFDL-TR-70-106, 1970.

8. Neulieb, R.L., Garrison, J.N. and Golden D.J., "Atmospheric Turbulence Field Parameters Determination," Air Force Flight Dynamic Laboratory, AFFDL-TR-72-51, 1972.

9. McClosky, J.N., et al, "Statistical Analysis of LO-LOCAT Turbulence Data for Use in Development of Revised Gust Data," Air Force Flight Dynamic Laboratory, AFFDL-TR-71-29, 1971.

10. Durkee, E.D., "Flight Loads Data from Cargo Aircraft," AFFDL Technical Memorandum 75-26-FBE, Feb. 1975, Wright-Patterson Air Force Base, Ohio.

11. Banazak, D.L., "Study of Exceedance Curve Spread by Aircraft Tail Number by Mission Type and Base For F-4 and A-37B Flight Data," AFFDL-TM-75-37-FBE, Feb. 1975, Wright-Patterson Air Force Base, Ohio.

12. Mayer, J.P. and Hamer, H.A., "Application of Power Spectral Analysis Methods to Maneuver Loads Obtained on Jet Fighter Airplanes During Service Operations," TN-D-902, NASA, 1957, Langley, Virginia.

13. Van Dijk, G.M., "Statistical Load Data Processing," Advanced Approaches to Fatigue Evaluation, NASA, Sixth ICAF Symposium held at Miami Beach, Florida, May, 1971, pp. 565-598.

14. Hill, M.C. and Dillhoff, K.J., "Development of Flight-by-Flight Fatigue Test Data from Statistical Distributions of Aircraft Stress Data, Volume II, Documentation of the B-58 and F-106 Fatigue Spectra Simulation Programs," AFFDL-TR-75-16, May 1975.

15. Wilkins, D.J., et al, "Realism in Fatigue Testing" The Effect of Flight-by-Flight Thermal and Random Load Histories on Composite Bonded Joints," presented at ASTM Symposium on Fatigue of Composit Materials, Bal Harbour, Florida, December 3-4, 1973; to appear in STP, ASTM.

16. Freudenthal, A.M. and Wang, P.Y., "Ultimate Strength Analysis," Air Force Materials Laboratory, AFML-TR-69-60, 1969.

17. Butler, J.P. and Rees, D.A., "Development of Statistical Fatigue Failure Characteristics of 2024-T3 Aluminum Alloy Material Under Simulated Flight-by-Flight Loading," AFML-TR-74-124, 1974.

18. Eggwertz, S. and Lindsjo, G., "Study of Inspection Inter vals for Fail-Safe Structures," FFA Report 120, Aeronautical Research Institute of Sweden, Stockholm, 1970.

19. Eggwertz, S., "Investigation of Fatigue Life and Residual Strength of Wing Panel for Reliability Purposes," in Probabilistic Aspects of Fatigue, edited by Heller, R.A., ASTM STP-511, 1971, pp. 75-105.

20 Whittaker, I.C. and Saunders, S.C., "Exploratory Development on Application of Reliability Analysis to Aircraft Structures Considering Interaction of Fatigue Cumulative Damage and Ultimate Strength," Air Force Materials Lab., AFML-TR-72-283, 1973.

21. Whittaker, I.C. and Saunders, S.C., "Application of Reliability Analysis to Aircraft Structures Subjected to Fatigue Crack Growth and Periodic Inspection," Air Force Materials Lab., AFML-TM-73-92, 1973.

22. Simpkins, D., Neulieb, R.L., and Golden, D.J., "Fatigue - A Test Integrated Damage Modeling Approach," Journal of Aircraft, Vol. 11, No. 9, Sept. 1974, pp. 563-570.

23. Freudenthal, A.M., "Reliability Analysis Based on Time to First Failure," Conference Paper presented at the Fifth I.C.A.F. Symposium, Australia, 1967.

24. Whittaker, I.C. and Besuner, P.M., The Boeing Co., "A Reliability Analysis Approach to Fatigue Life Variability of Aircraft Structures, AFML-TR-69-65, April 1969.

25. Wood, H.A., "The Use of Fracture Mechanics Principles in the Design and Analysis of Damage Tolerant Aircraft Structures," in Fatigue Life Prediction for Aircraft Structures and Materials, AGARD-LS-62, 1973, pp. 4.1-4.3.

26. Tiffany, C.F., "The Design and Development of Fracture Resistant Structures,"Proceedings of Colloquium on Structural Reliability, Carnegie-Mellon University, 1972, pp. 210-215.

27. Yang, J.-N. and Trapp, W.J., "Reliability Analysis of Aircraft Structures under Random Loading and Periodic Inspection," AIAA Journal, Vol. 12, No. 12, Dec. 1974, pp. 1623-1630.

28. Freudenthal, A.M., "Reliability Assessment of Aircraft Structures Based on Probabilistic Interpretation of the Scatter Factor," AFML-TR-74-198, 1974.

29. Rice, J.R. and Beer, F.P., "On the Distribution of Rises and Falls in a Continuous Random Process," Transactions of the ASME, Journal of Basic Engineering, June 1965, pp. 398-404.

30. Yang, J.-N., "Statistics of Random Loading Relevent to Fatigue," Journal of Engineering Mechanics Division, ASCE, Vol. 100, No. EM3, June, 1974, pp. 469-475.

31. Shinozuka, M. and Jan, C.-M., "Digital Simulation of Random Processes and Its Applications," Journal of Sound and Vibration, Vol. 25, No. 1, 1972, pp. 111-128.

32. Shinozuka, M., "Monte Carlo Solution of Structural Dynamics," invited pater at the National Symposium on Computerized Structural Analysis and Design, George Washington University, Washington, D.C., March 27-29, 1972; International Journal of Computers and Structures, Vol. 2, 1972, pp. 855-874.

33. Shinozuka, M., "Digital Simulation of Random Processes in Engineering Mechanics with the Aid of FFT Technique," in Stochastic Problems in Mechanics," S.T. Ariaratnam and H.H.E. Leipholz, editors, University of Waterloo Press, 1974, pp. 277-286.

34. Lin, Y.K., Probabilistic Theory of Structural Dynamics, McGraw-Hill, 1967.

35. National Material Advisory Board, Application of Fracture Prevention Principles to Aircraft, NMAB-302, Feb. 1973, pp. 39-45.

36. Paris, P.C., "The Fracture Mechanics Approach to Fatigue," Proceedings of the 18th. Sagamore Army Materials Research Conference, Syracuse Univ. Press, Syracus, N.Y., 1964, pp. 107-127.

37. Johnson, H.H. and Paris, P.C., "Subcritical Flaw Growth," Engineering Fracture Mechanics, 1968, Vol. 1, Pergamon Press, pp. 3-45.

38. Kitagawa, H., "Application of Fracture Mechanics to Fatigue Crack," Journal of the Japanese Society of Mechanical Engineers, 1972, Vol. 75, No. 642.

39. Bucci, R.J., Clark Jr. W.G., and Paris, P.C., "Fatigue Crack Propagation Growth Rates under a Wide Variation of ΔK For an ASTM A517 Grade F(T-1)," in "Steel Stress Analysis and Growth of Cracks," ASTM, STP 513, 1971.

40. Hardrath, H.F. and Whaley, R.E., "Fatigue-Crack Propagation and Residual-Static-Strength of Build-Up Structures," NACA, TN-4012, 1957.

41. Snider, H.L., et al., "Residual Strength and Crack Propagation Test on C-130 Airplane Center Wings with Service-Imposed Fatigue Damage," CR-2075, NASA, 1972.

42. Shinozuka, M.,"Probability of Structural Failure Under Random Loadings," Journal of the Engineering Mechanics Division, ASCE, Vol. 90, No. EM5, 1964, pp. 147-155.

43. Yang, J.N. and Shinozuka, M., "On the First Excursion Probability in Stationary Narrow-Band Random Vibration II," Journal of Applied Mechanics, ASME, Vol. 39, 1972, pp. 733-738.

44. Yang, J.N., "First-Excursion Probability in Nonstationary Random Vibration," Journal of Sound and Vibration, Vol. 27, 1973, pp. 165-182.

45. Military Specification. Airplane Durability Design Requirements. Mil-A-008866B (USAF), May, 1960.

46. Freudenthal, A.M. and E.J. Gumbel, Minimum Life in Fatigue, J. Amer. Statistical Assoc.,Vol. 49 (1954), 579-597.

47. Yang, J.-N. and Trapp, W.J., "Joint Aircraft Loading/Structure Response Statistics of Time to Service Crack Initiation," AFML-TR-77-174, 1974, Wright-Patterson Air Force Base, Ohio.

48. Shinozuka, M. and Yang, J.N., "Optimum Structural Design Based on Reliability and Proof Load Test," Annals of Assurance Science, Proc. of Reliability and Maintainability, Vol. 8, 1969, pp. 375-391.

49. Heer, E. and Yang, J.N., "Structural Optimization Based on Fracture Mechanics and Reliability Criteria," AIAA Journal, Vol. 9, No. 5, 1971, pp. 621-628.

50. Freudenthal, A.M., "The Scatter Factor in the Reliability Assessment of Aircraft Structures," to appear in J. of Aircraft.

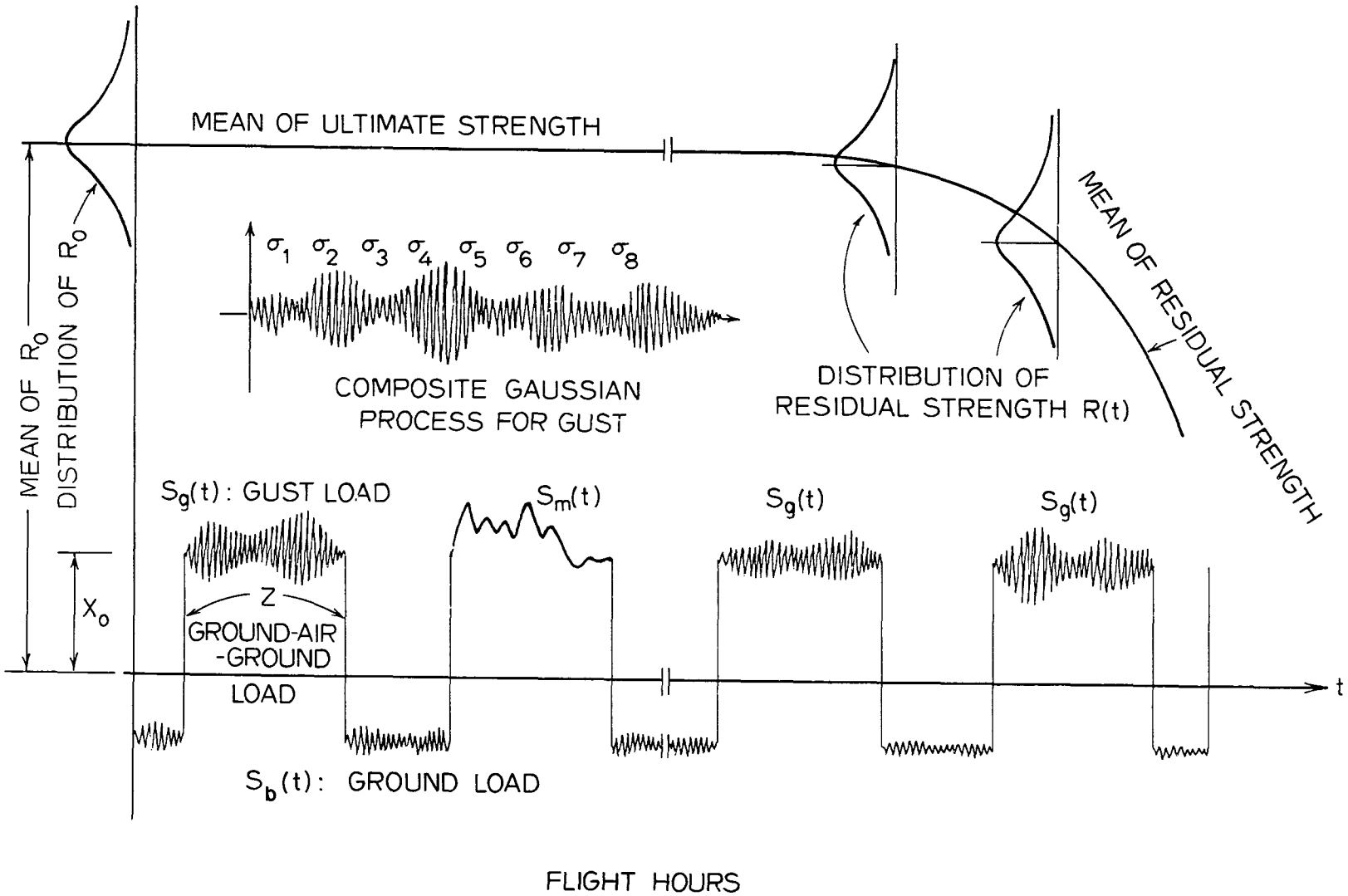

Figure 1. Flight-by-Flight Load Spectrum, Ultimate and Residual Strength

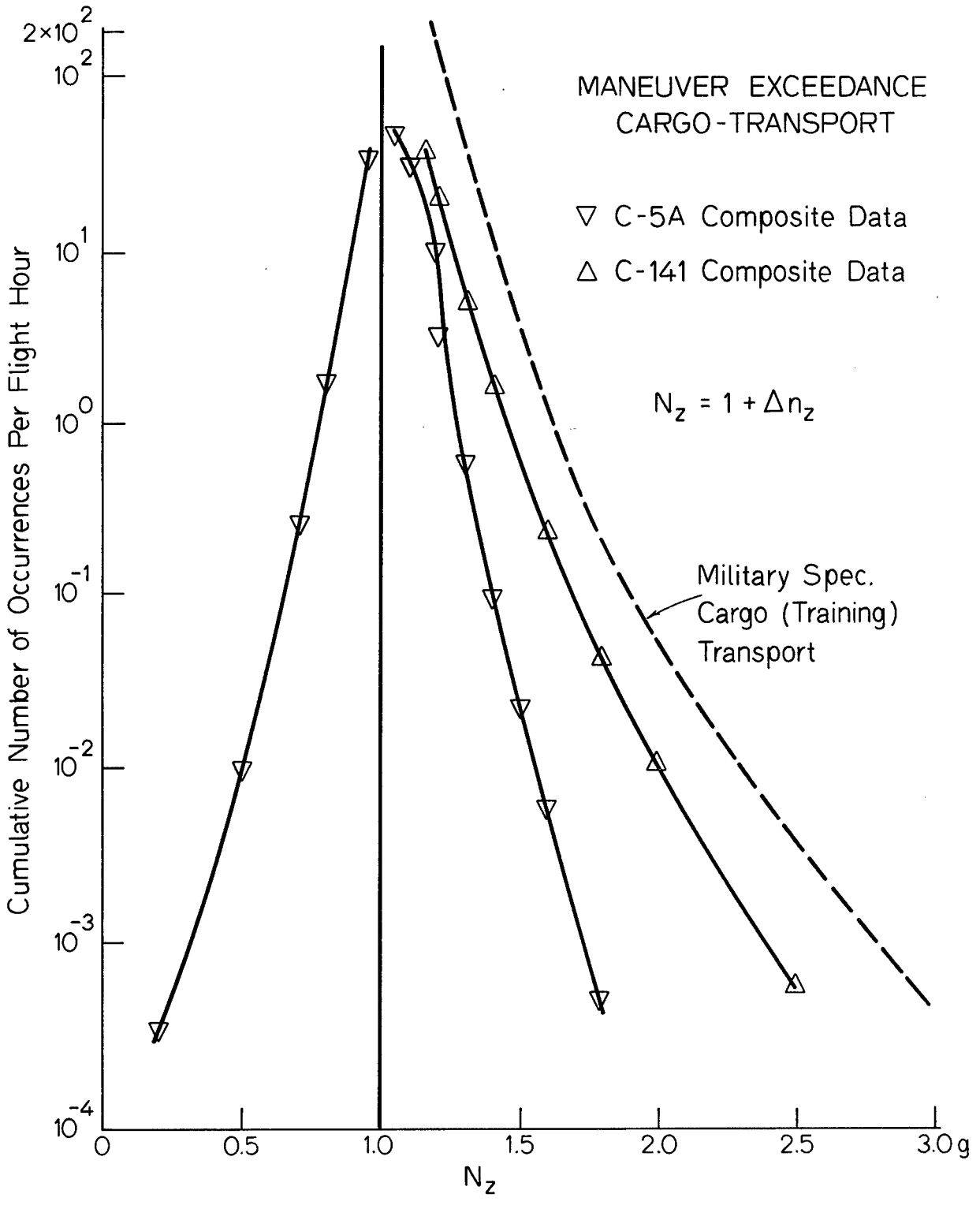

Figure 2. Exceedance Curves for Transports

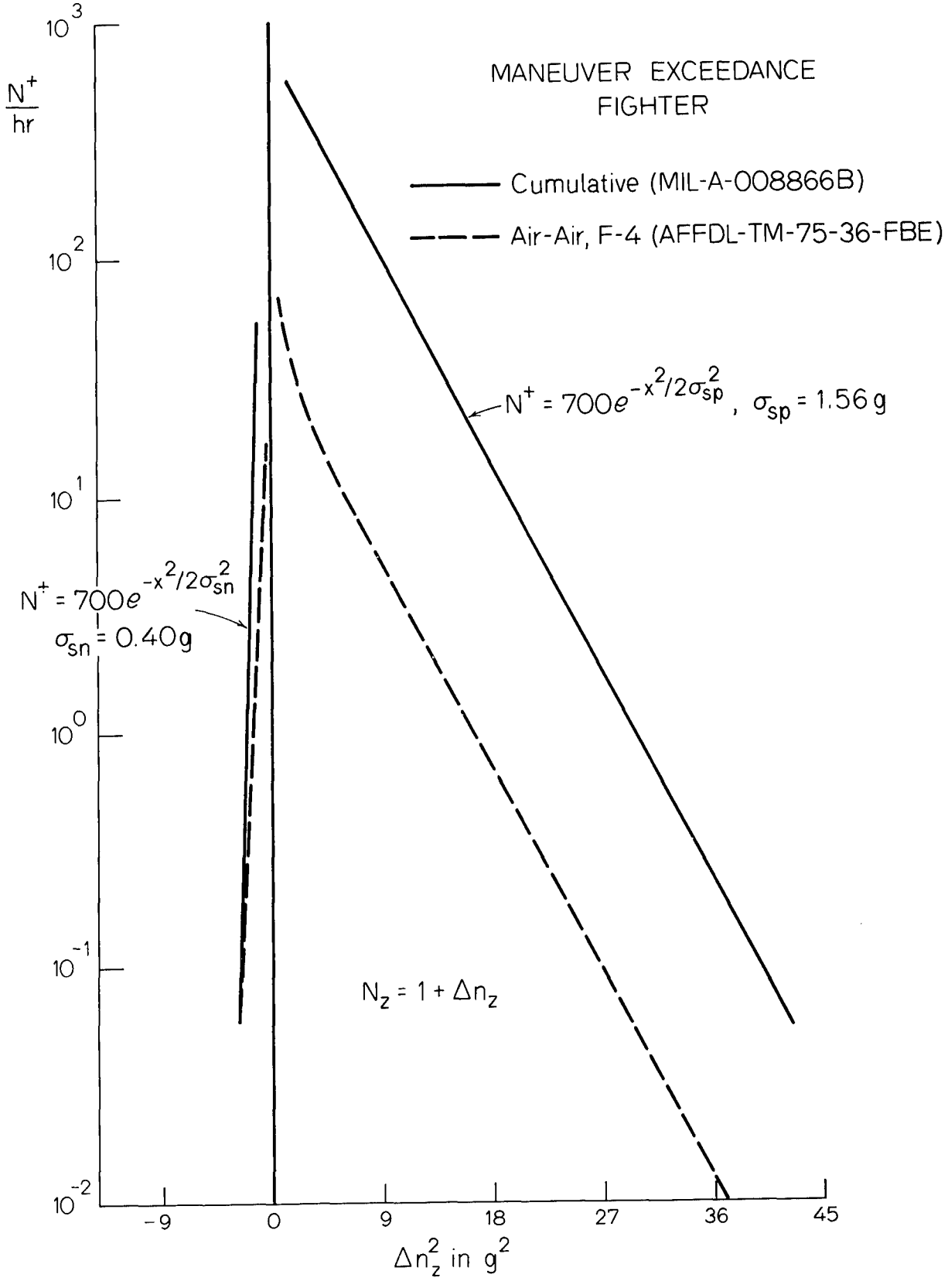

Figure 3. Exceedance Curves for Fighters

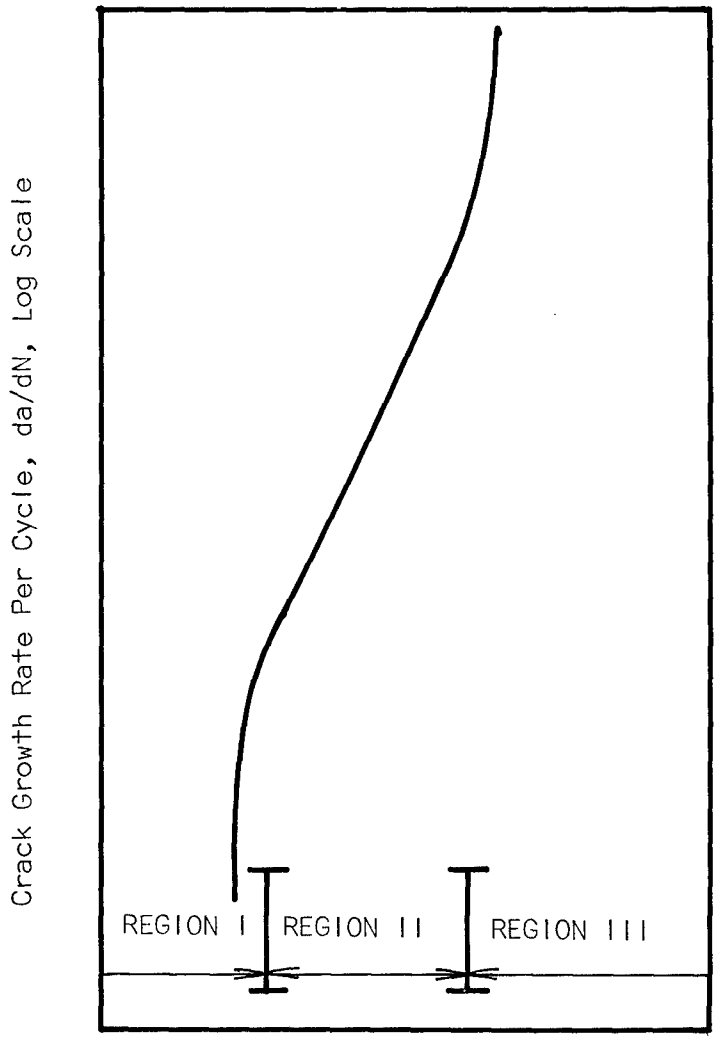

Figure 4. Crack Growth Rate as a Function of Stress-Intensity-Factor Range

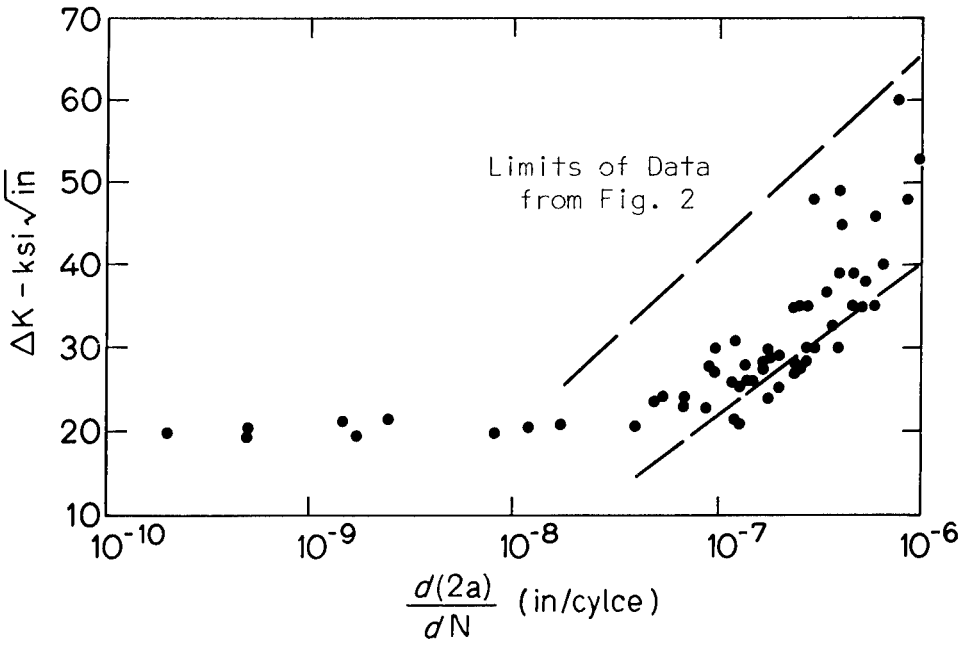

Figure 5. Fatigue Crack Growth Rates at Low Stress Intensities (2024-T3 Aluminum)

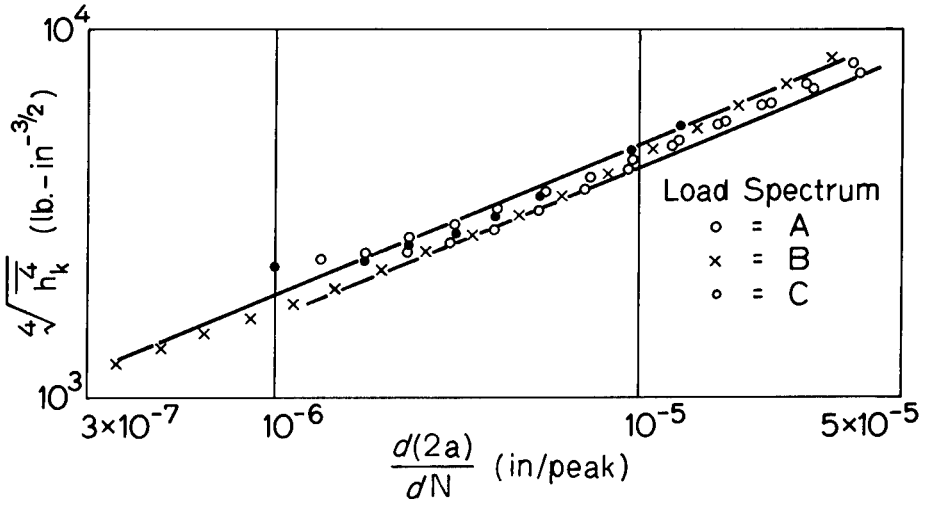

Figure 6. Crack Growth Rates under Random Loading (Ref. 36)

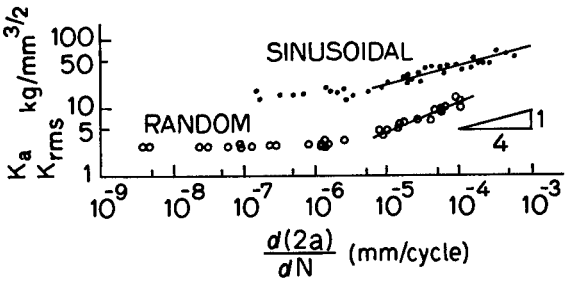

Figure 7. Crack Growth Rates under Sinusoidal and Random Loading (Carbon Steel) (Ref. 38)

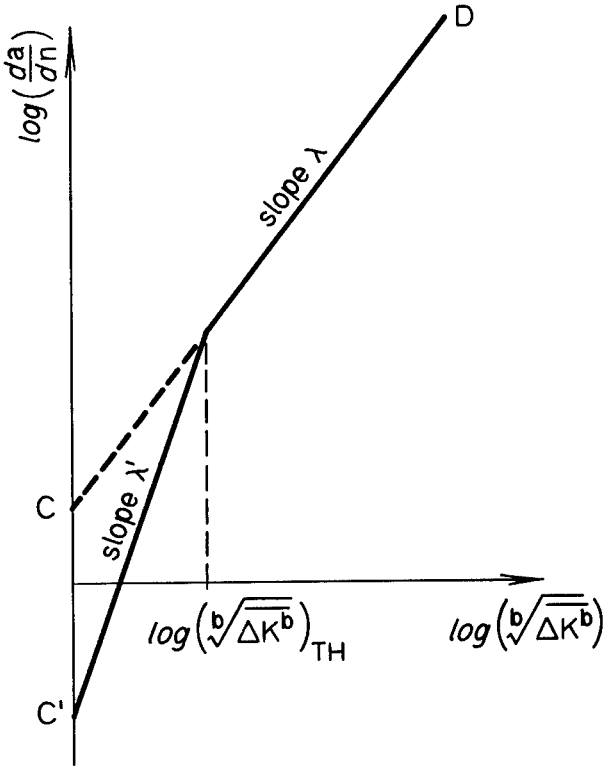

Figure 8. Crack Growth Rate Model Used in Analysis

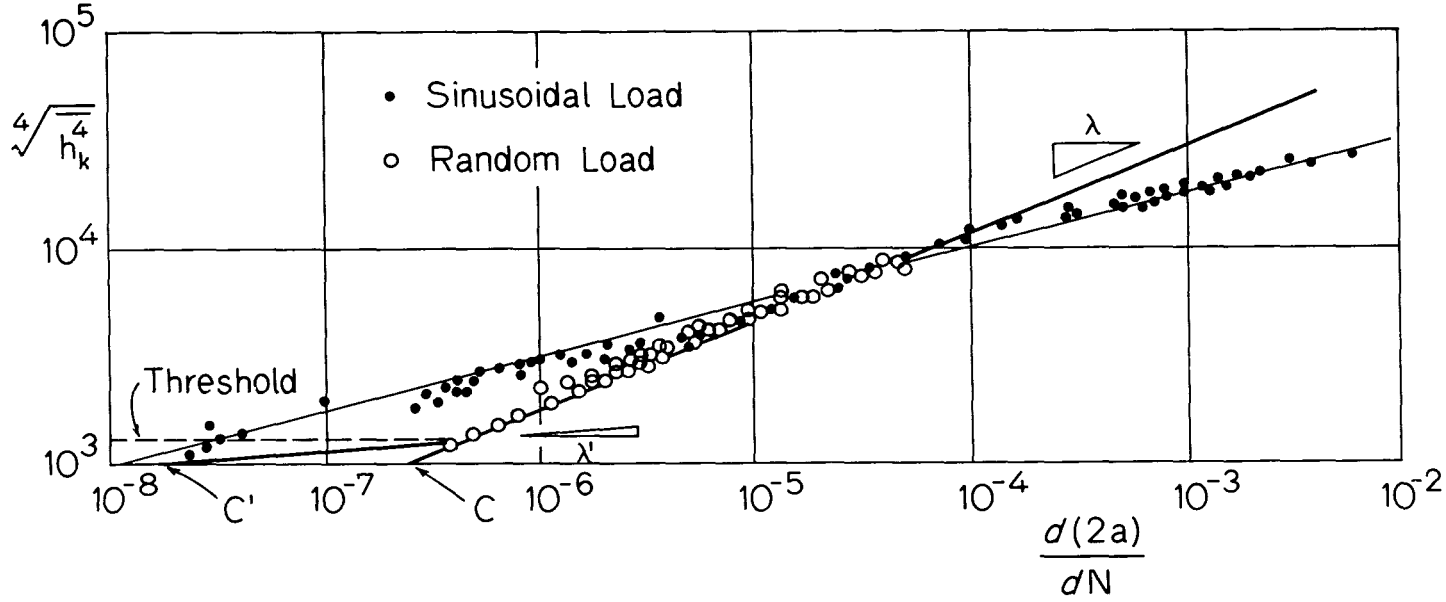

Figure 9. Comparison of Growth Rates under Sinusoidal and Random Loading

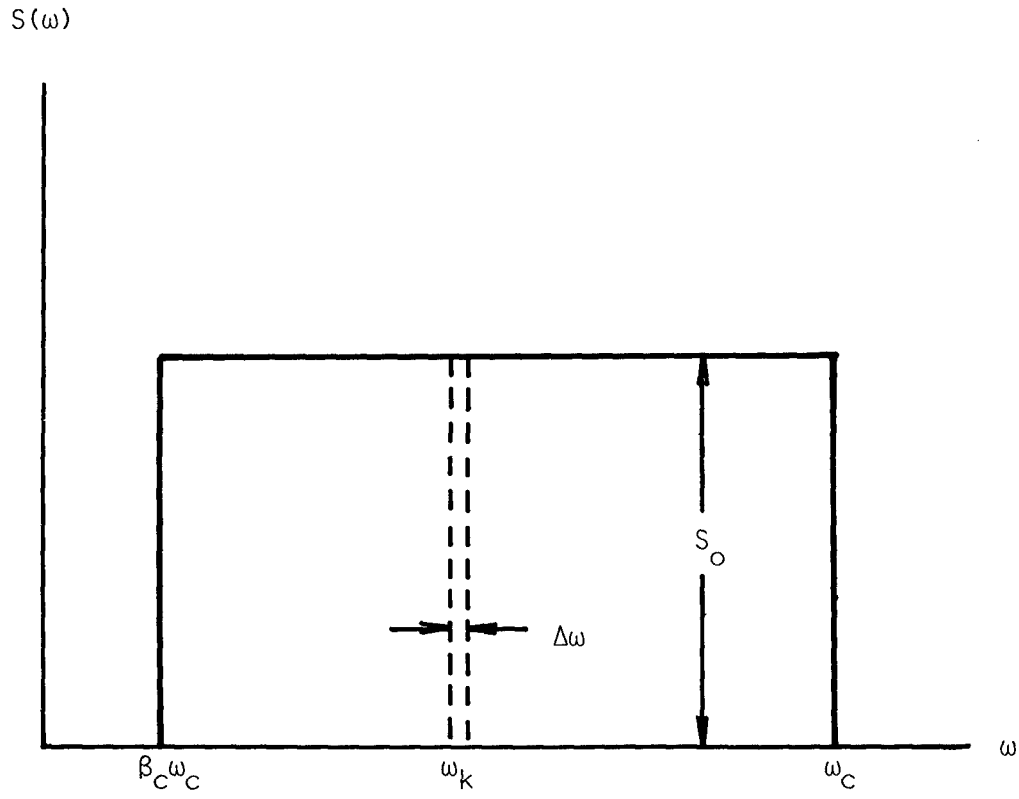

Figure 10. Rectangular Power Spectrum

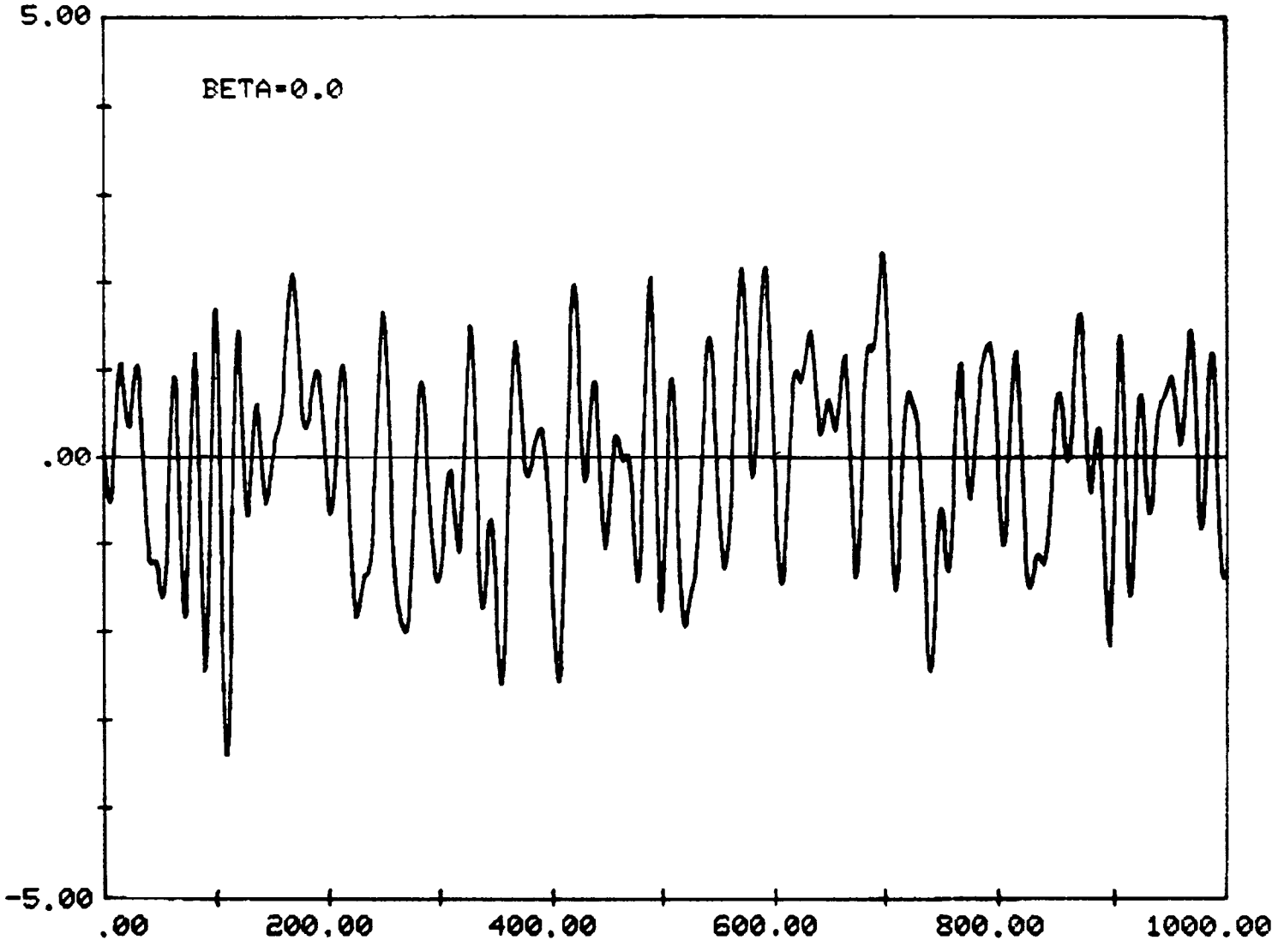

Figure 11. Sample History ($\beta_c = 0$)

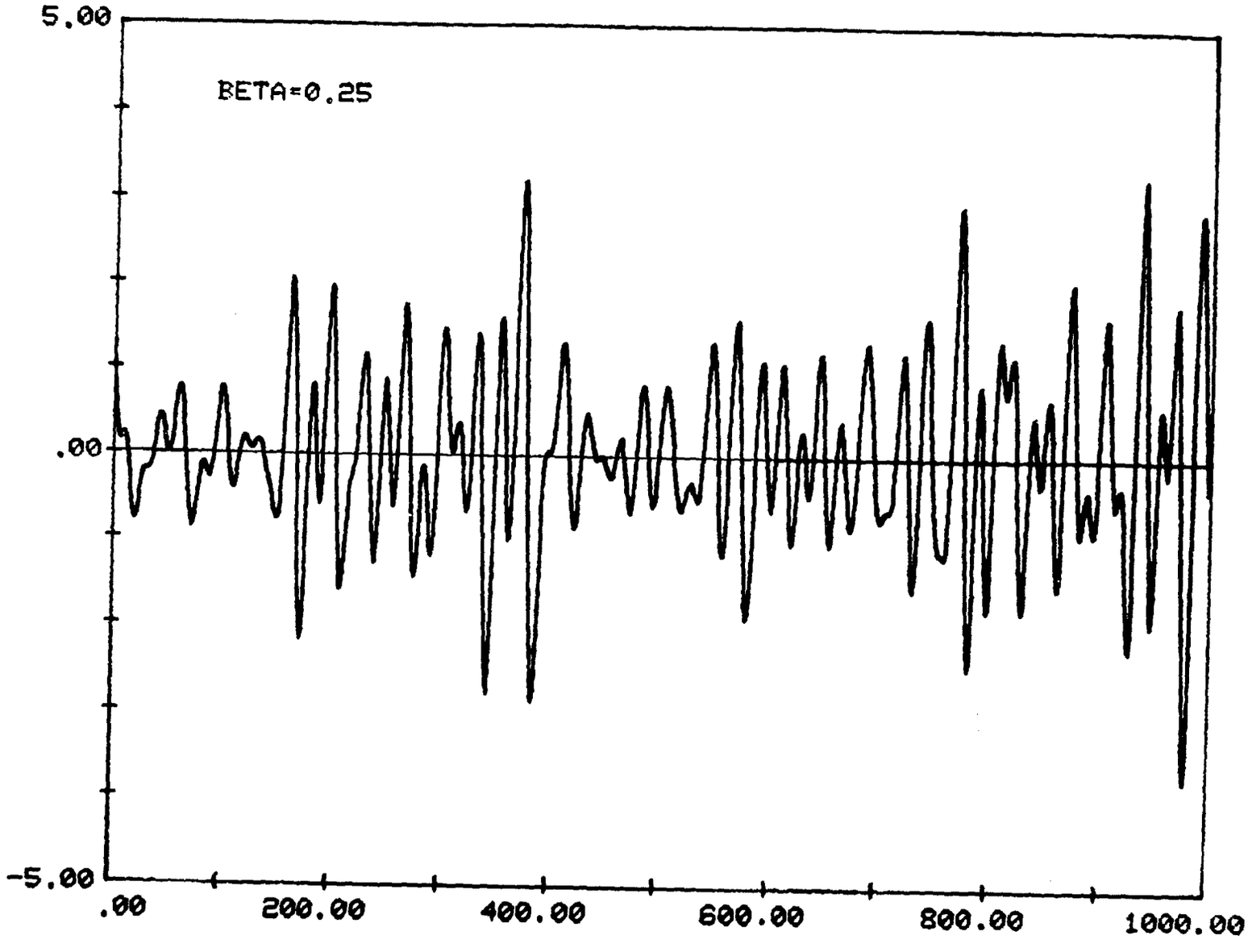

Figure 12. Sample History (β_c= 0.25)

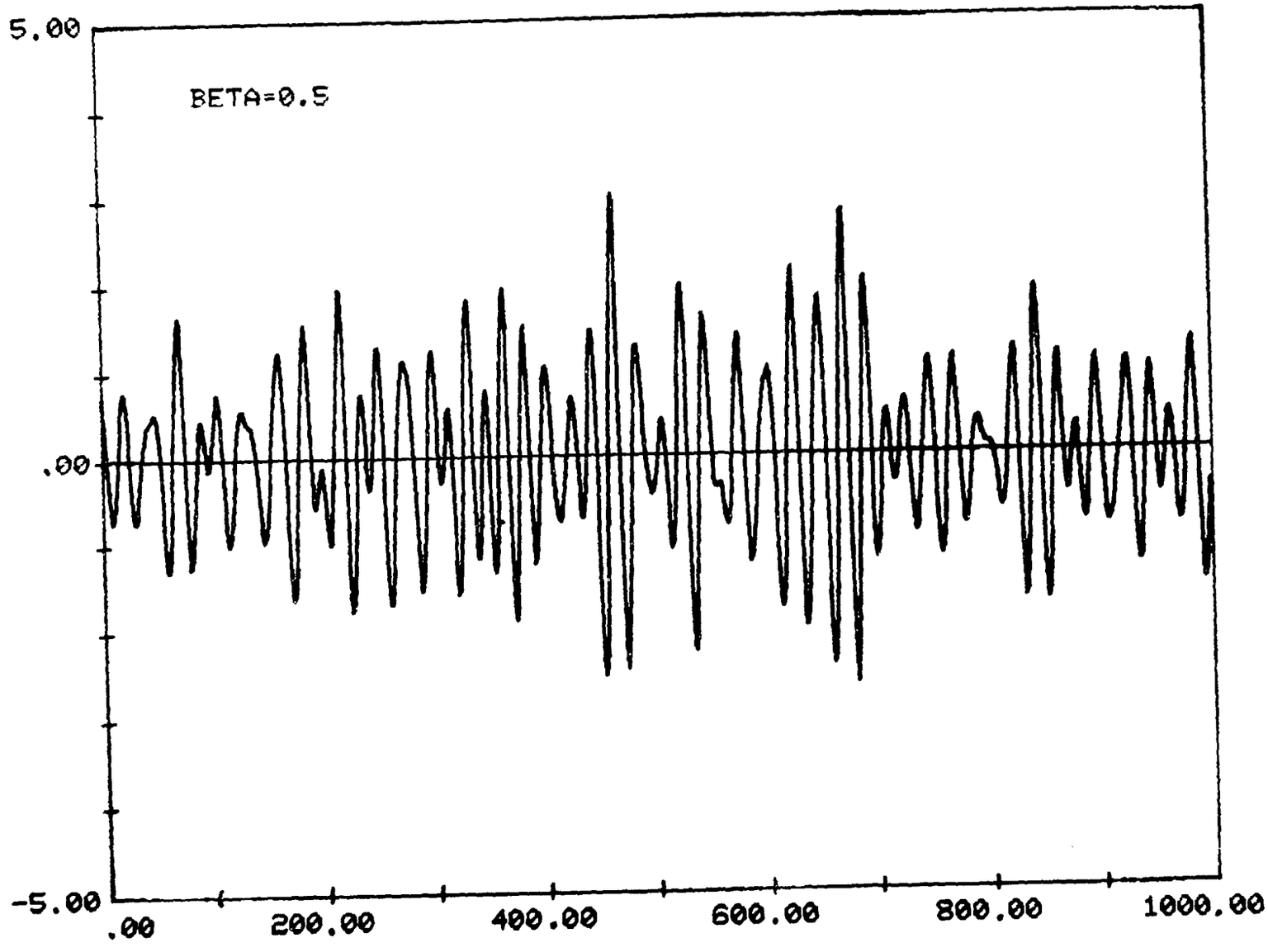

Figure 13. Sample History (β_c= 0.5)

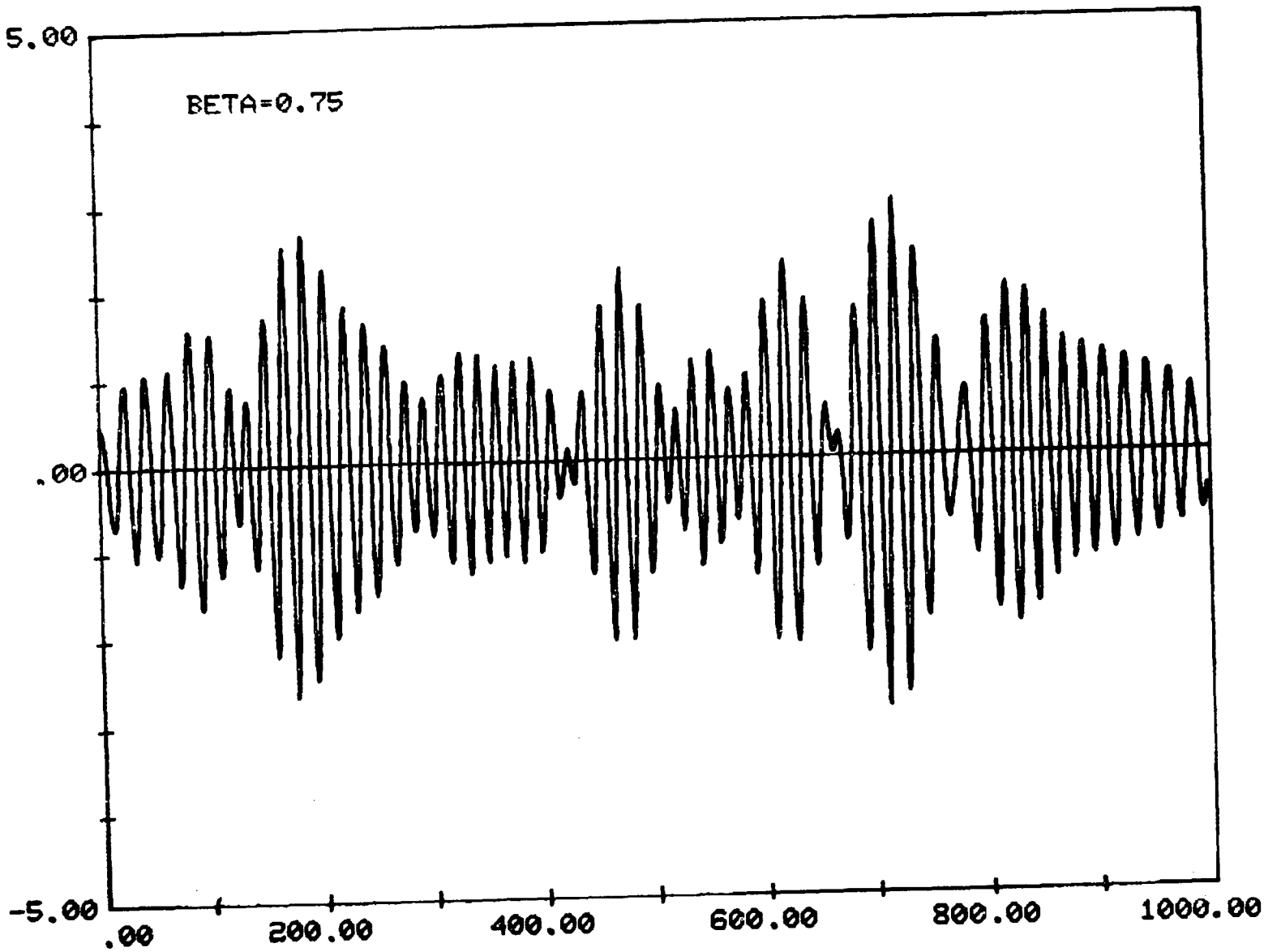

Figure 14. Sample History (β_c= 0.75)

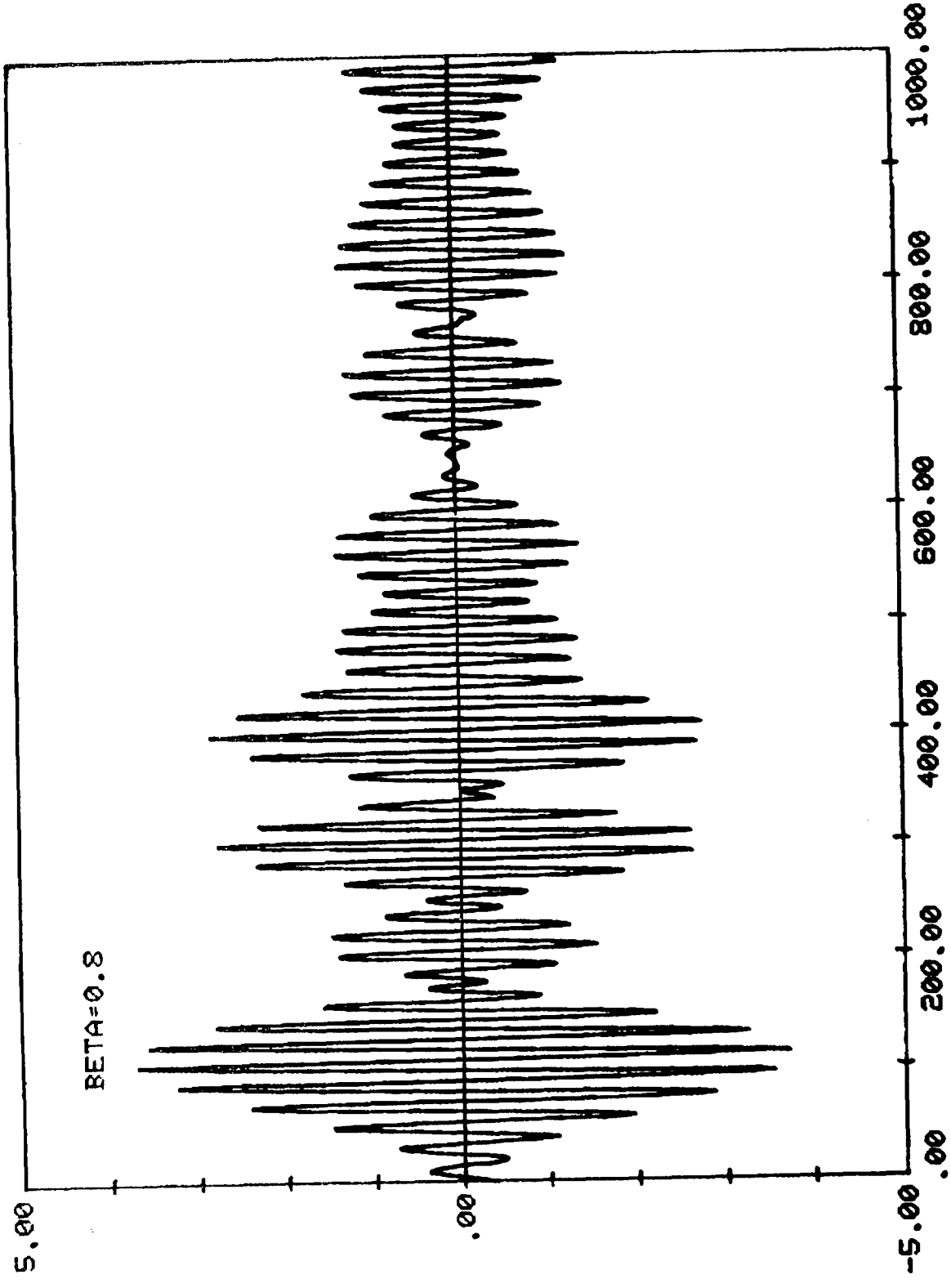

Figure 15. Sample History (β_c = 0.8)

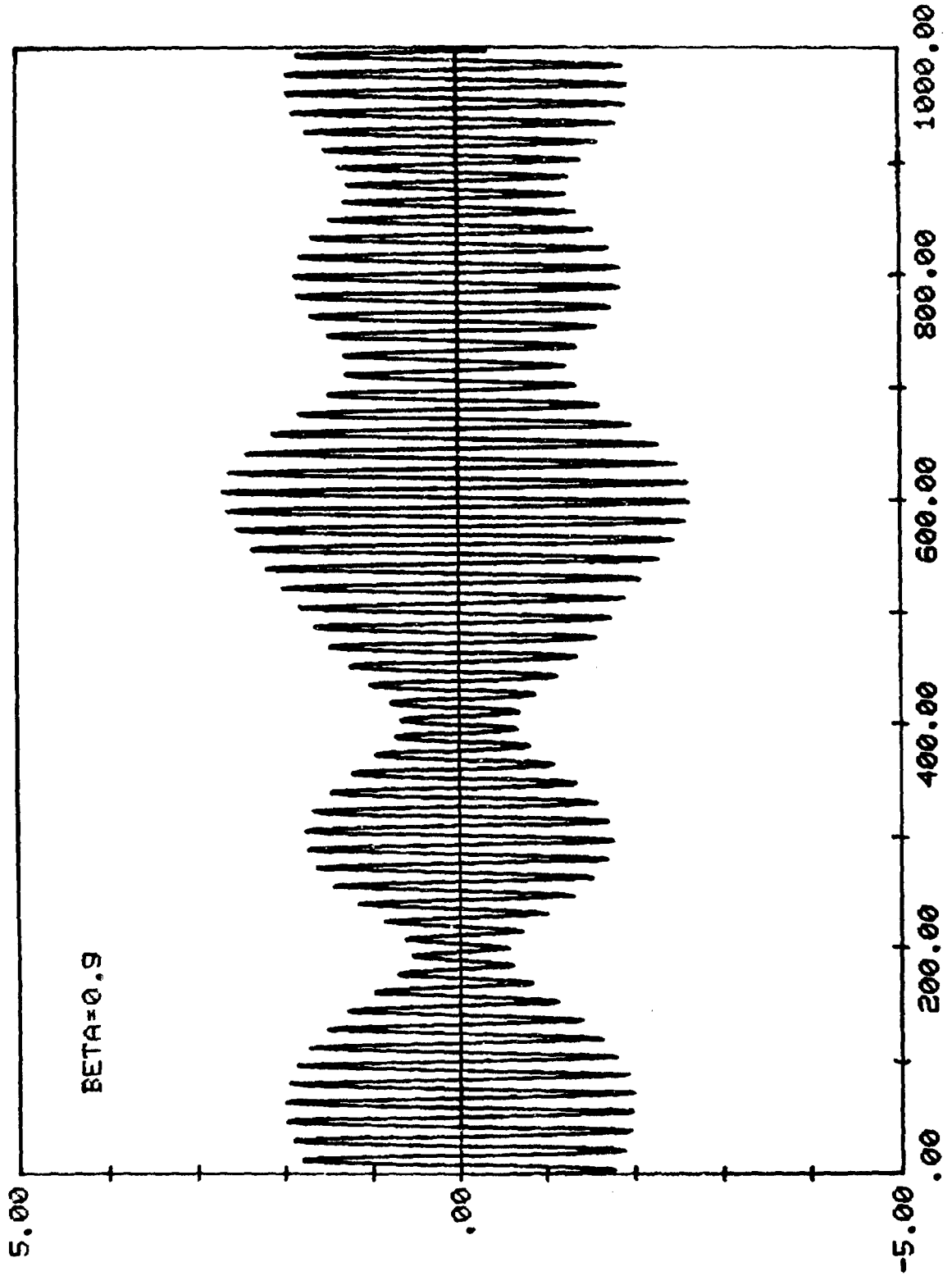

Figure 16. Sample History (β_c= 0.9)

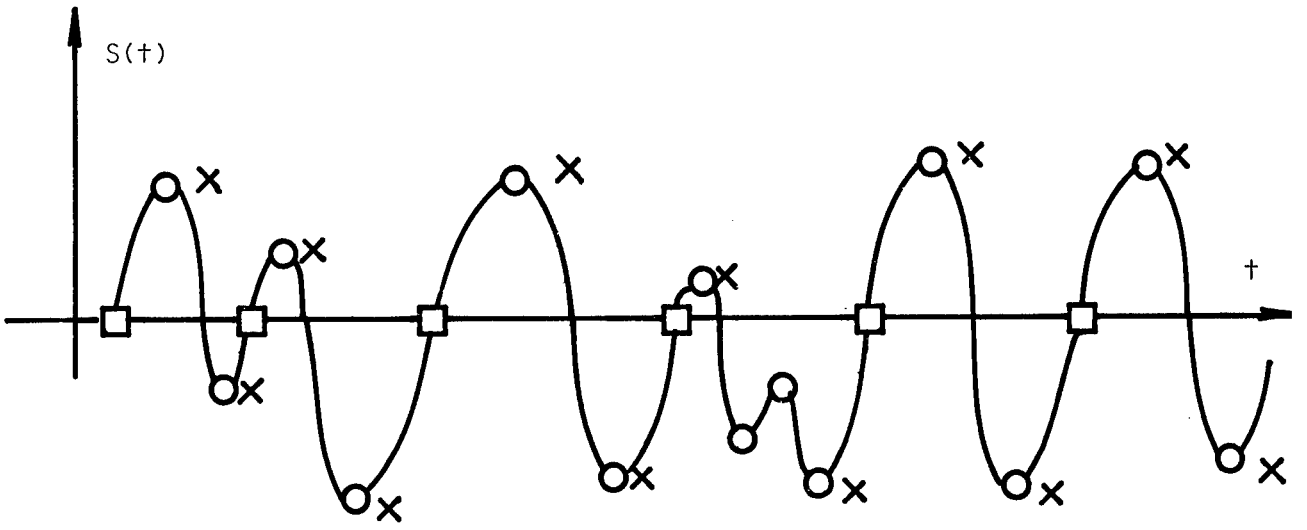

Case I ○ 14 rises and falls

Case II × 12 rises and falls

# of maxima = 7

# of zeros (positive slope) = 6

$$\frac{6}{7} = \frac{12}{14} \longrightarrow \text{irregularity factor}$$

Figure 17. Counting Methods

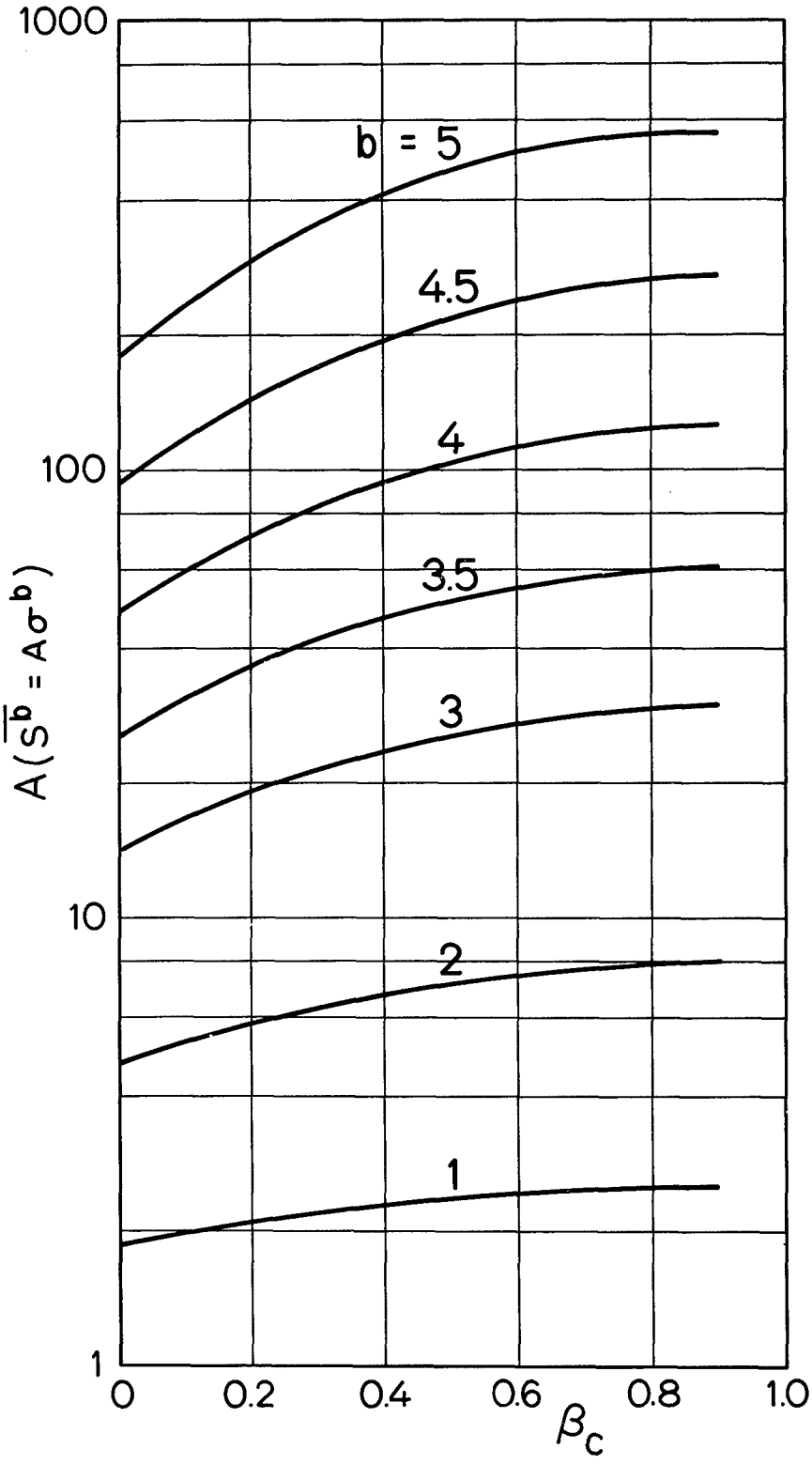

Figure 18. Coefficient A as a Function of Bend-Width Parameter β_c for b = 1, 2, ..., 5 (Case I)

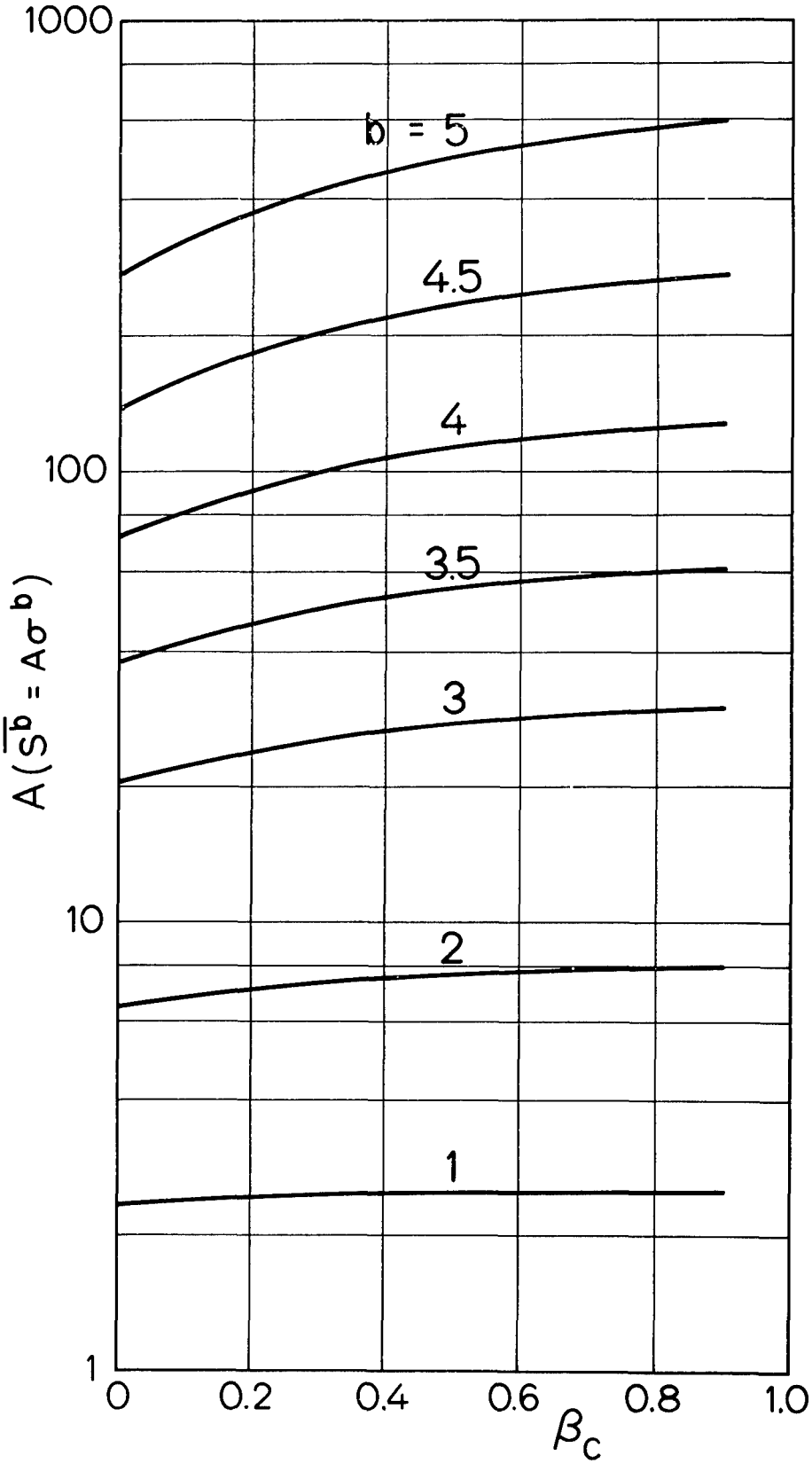

Figure 19. Coefficient A as a Function of Band-Width Parameter β_c for b = 1, 2, ..., 5 (Case II)

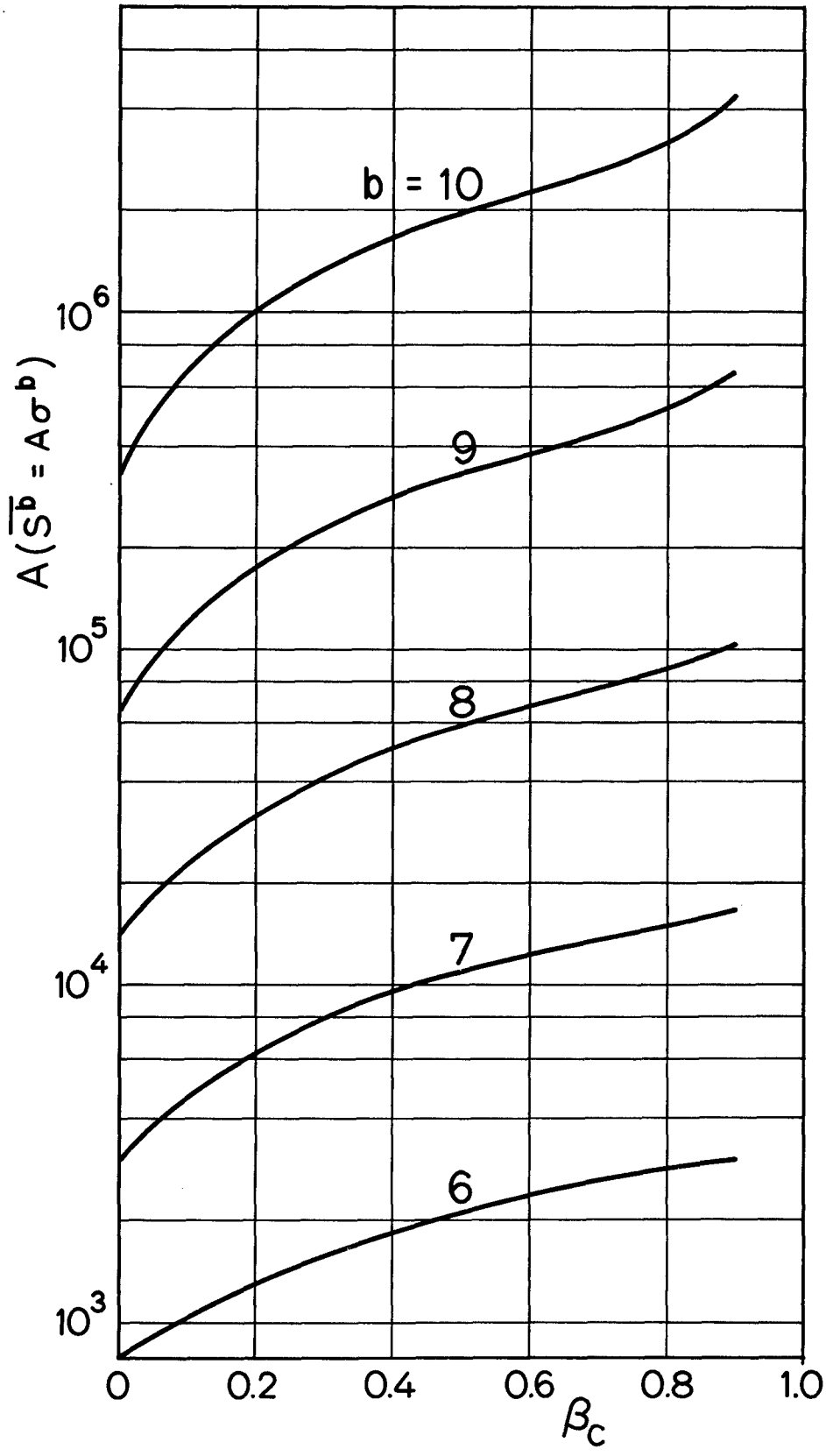

Figure 20. Coefficient A as a Function of Band-Width Parameter β_c for b = 6, 7, ..., 10 (Case I)

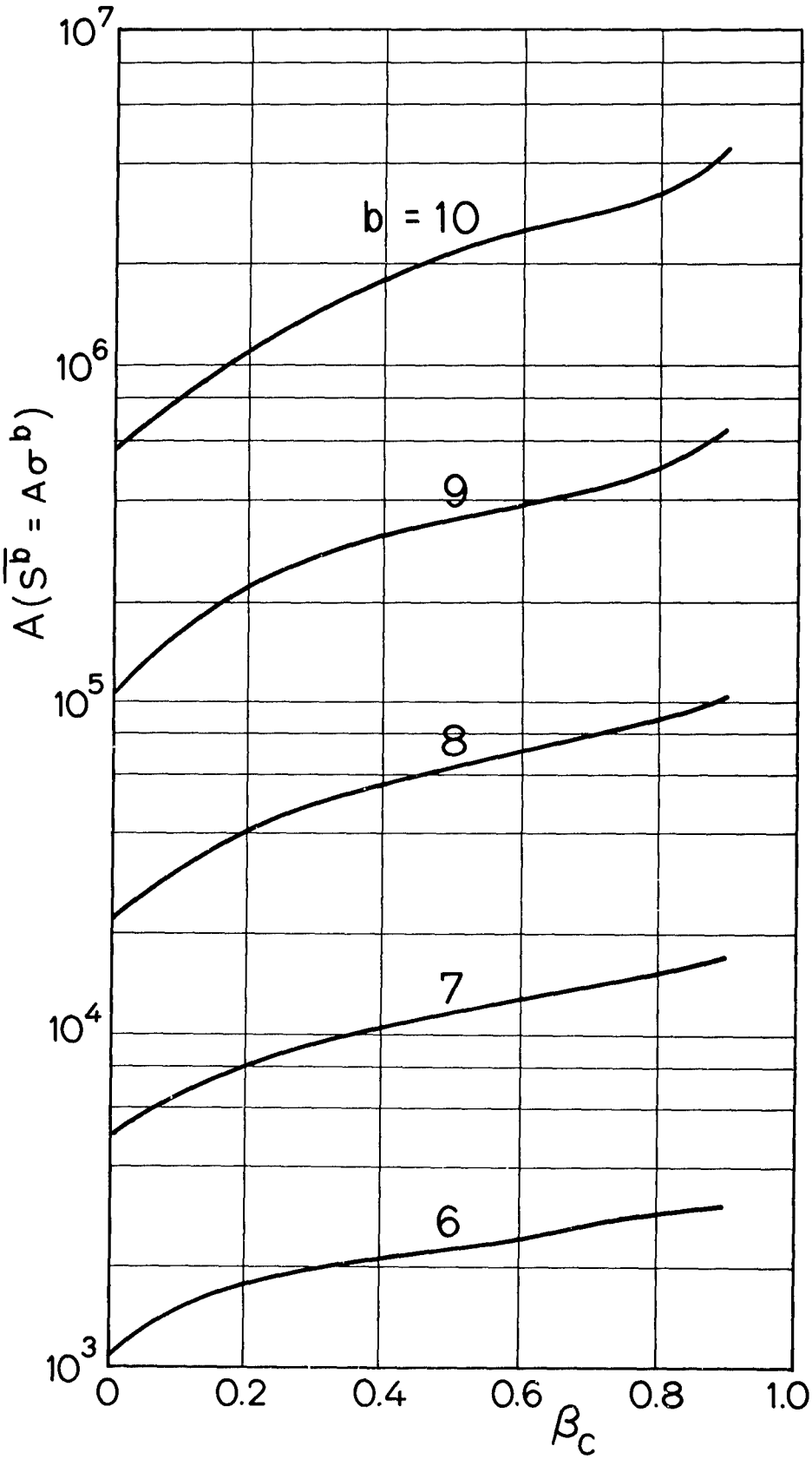

Figure 21. Coefficient A as a Function of Band-Width Parameter β_c for b = 6, 7, ..., 10 (Case II)

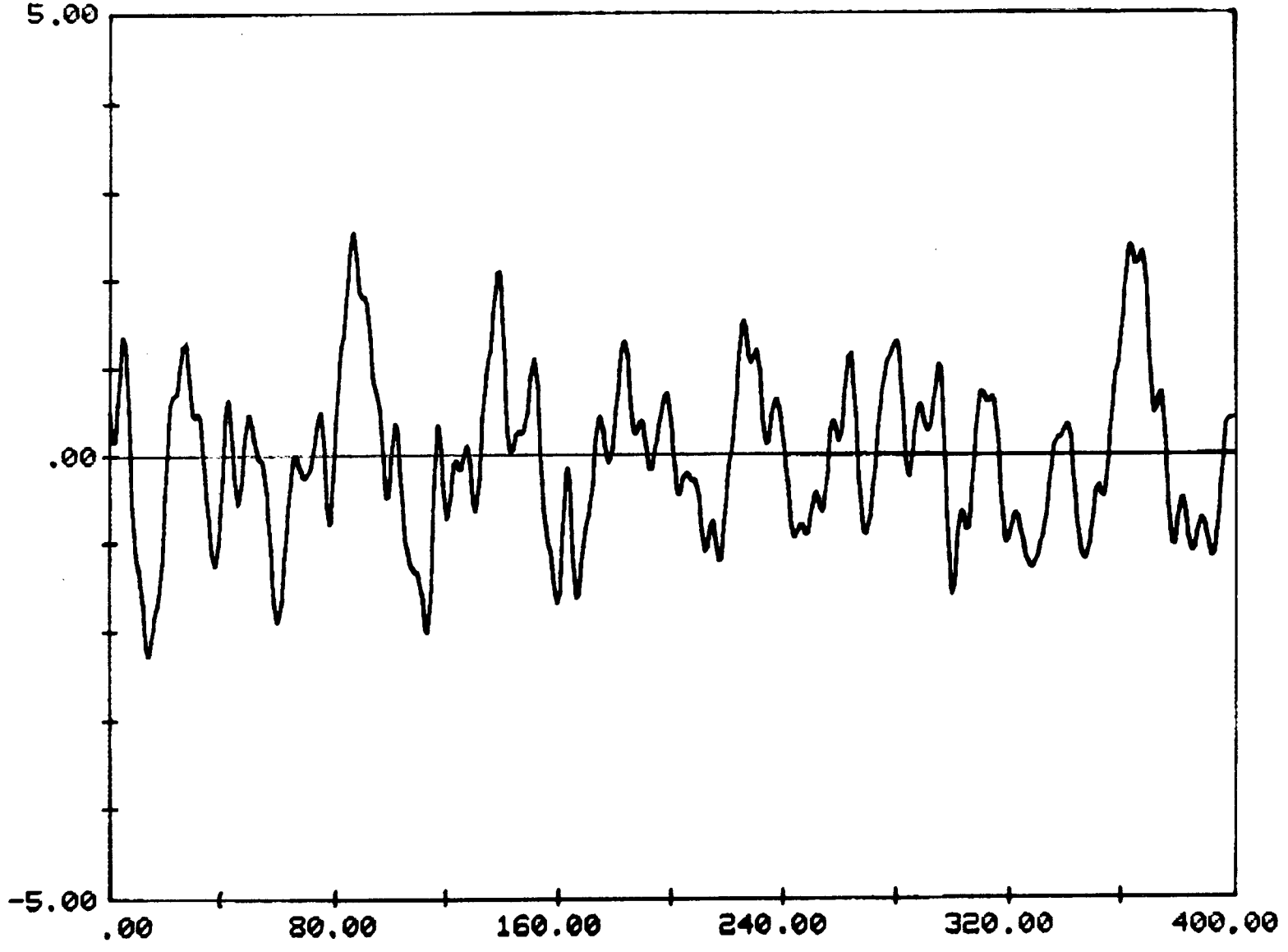

Figure 22. Sample History (Maneuver; Symmetric)

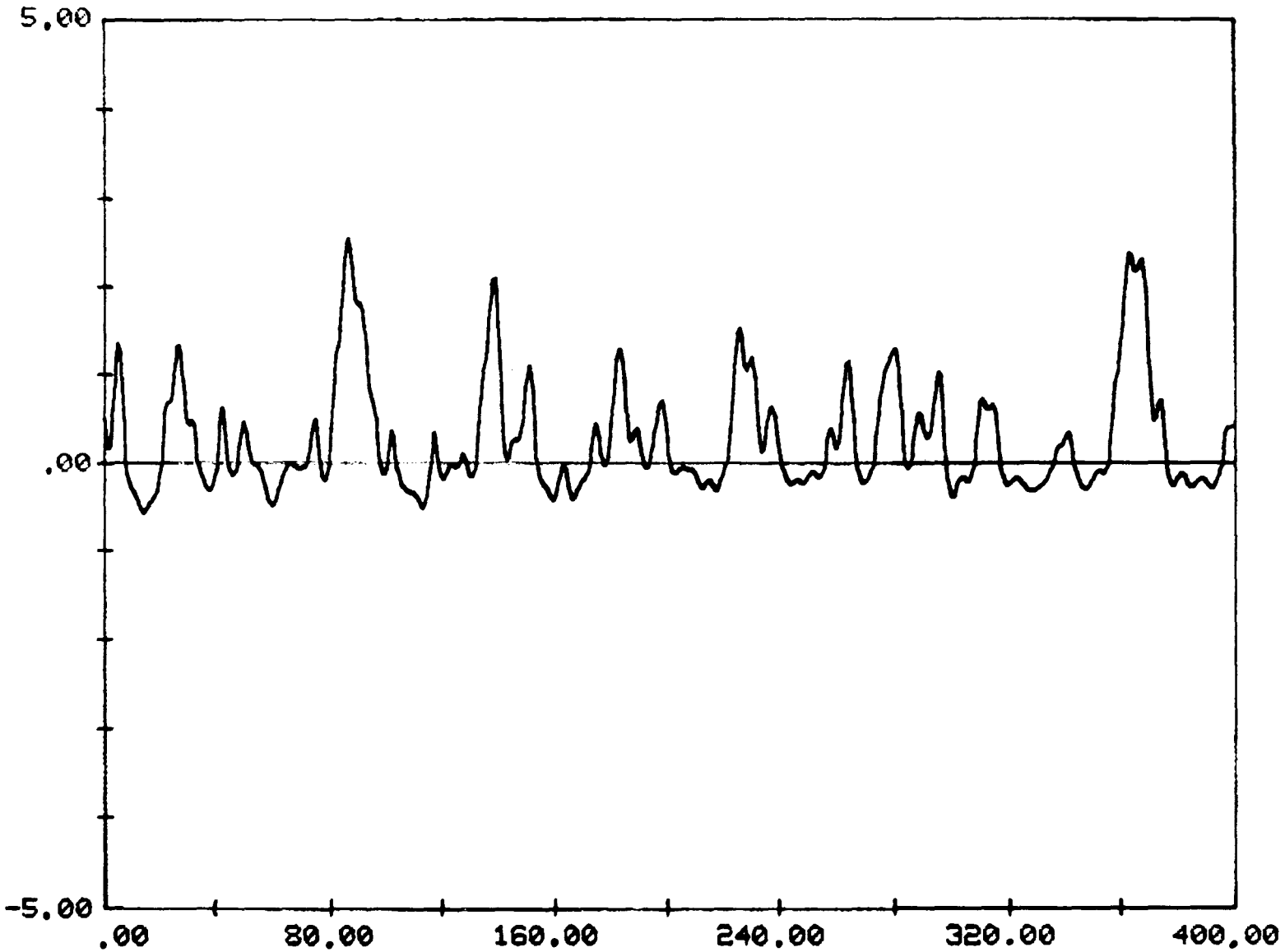

Figure 23. Sample History (Maneuver; Asymmetric)

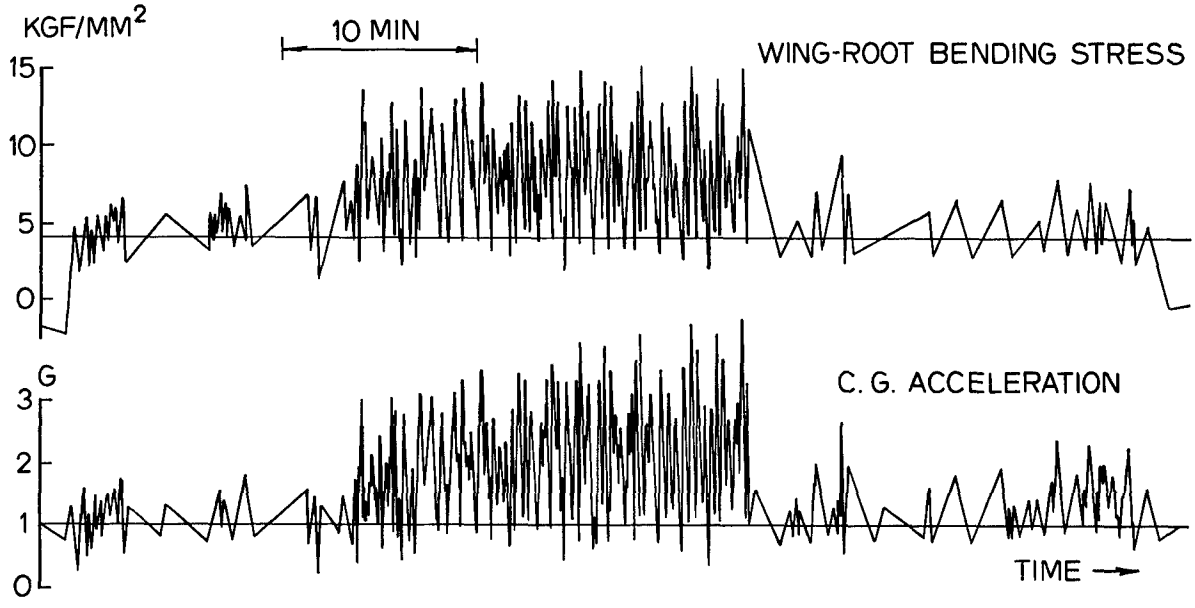

Figure 24. Load-Time History of Typical Fighter Mission

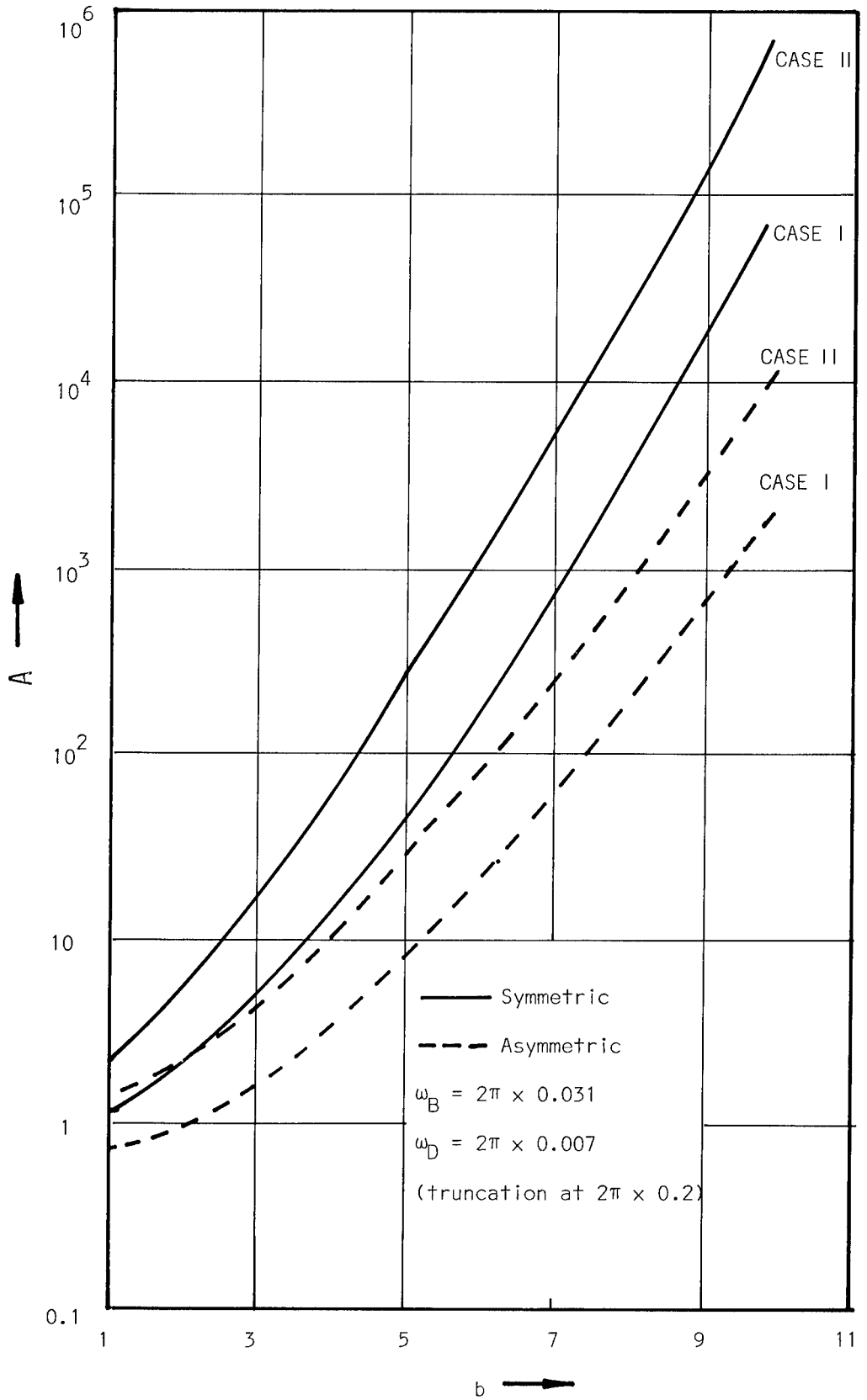

Figure 25. Coefficient A as a Function of Power b (Maneuver)

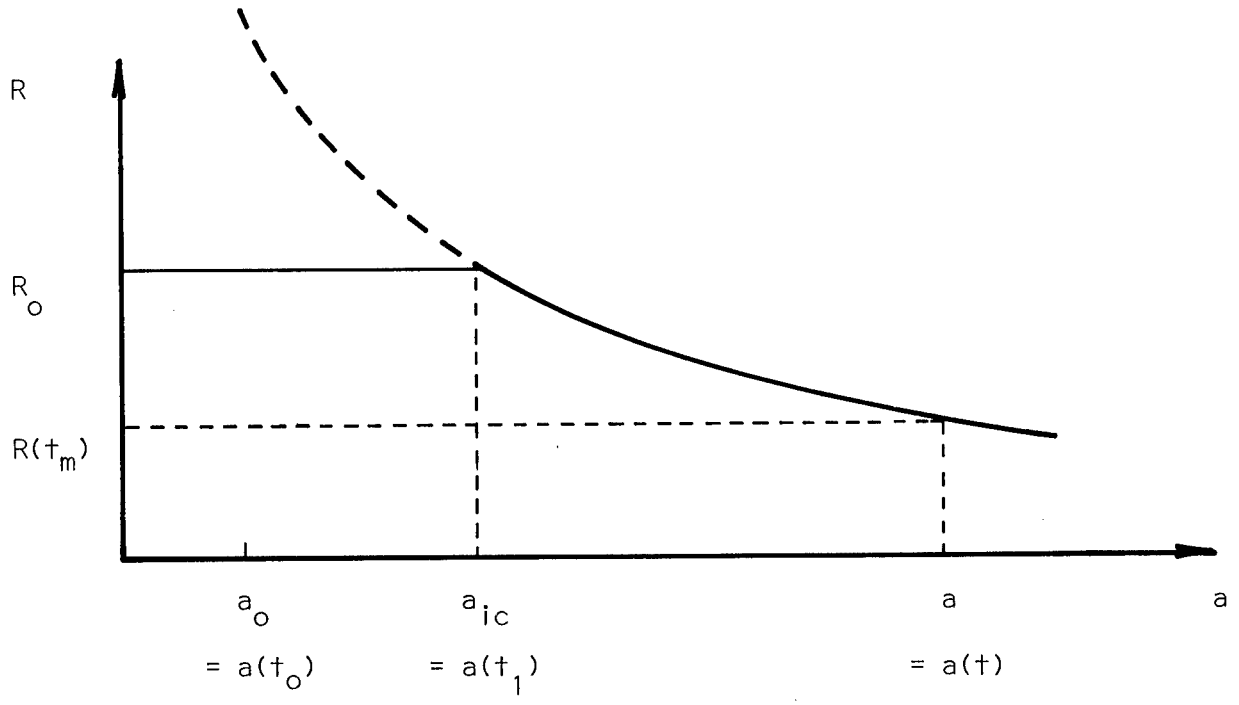

t_{ic} = time to initial critical crack after crack initiation

t_m = time after a_{ic} is reached

Figure 26. Relationships among R_o, $R(t_m)$, a_o, a_{ic} and $a(t)$

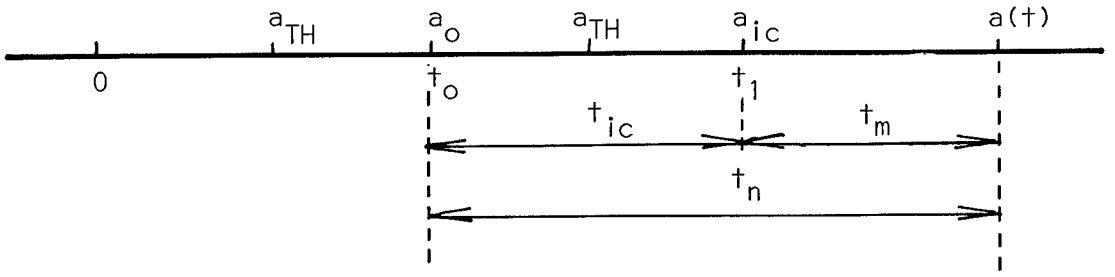

Figure 27. Relationships among t_o, t_1, t_{ic}, t_m and t_n

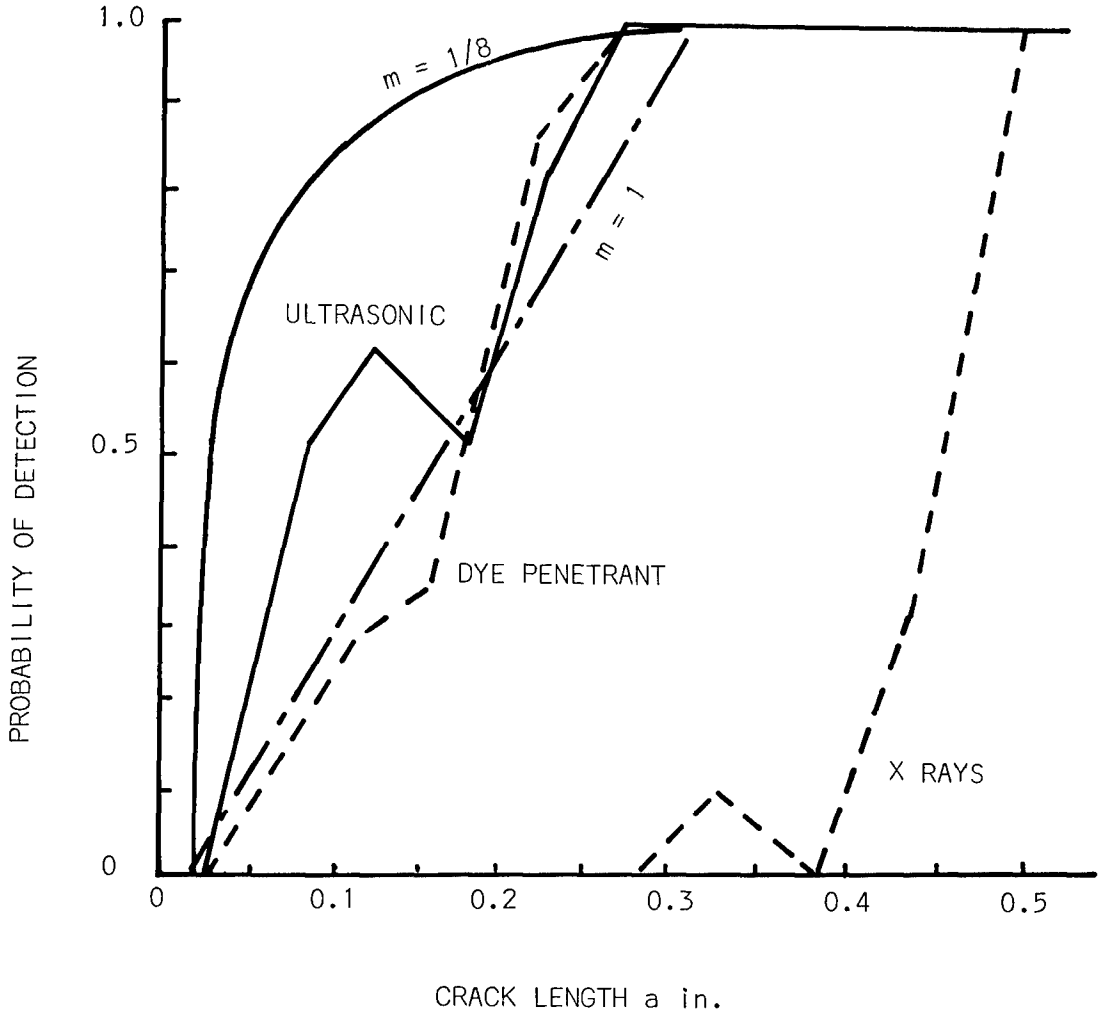

Figure 28. Probability of Detecting a Crack of Size a

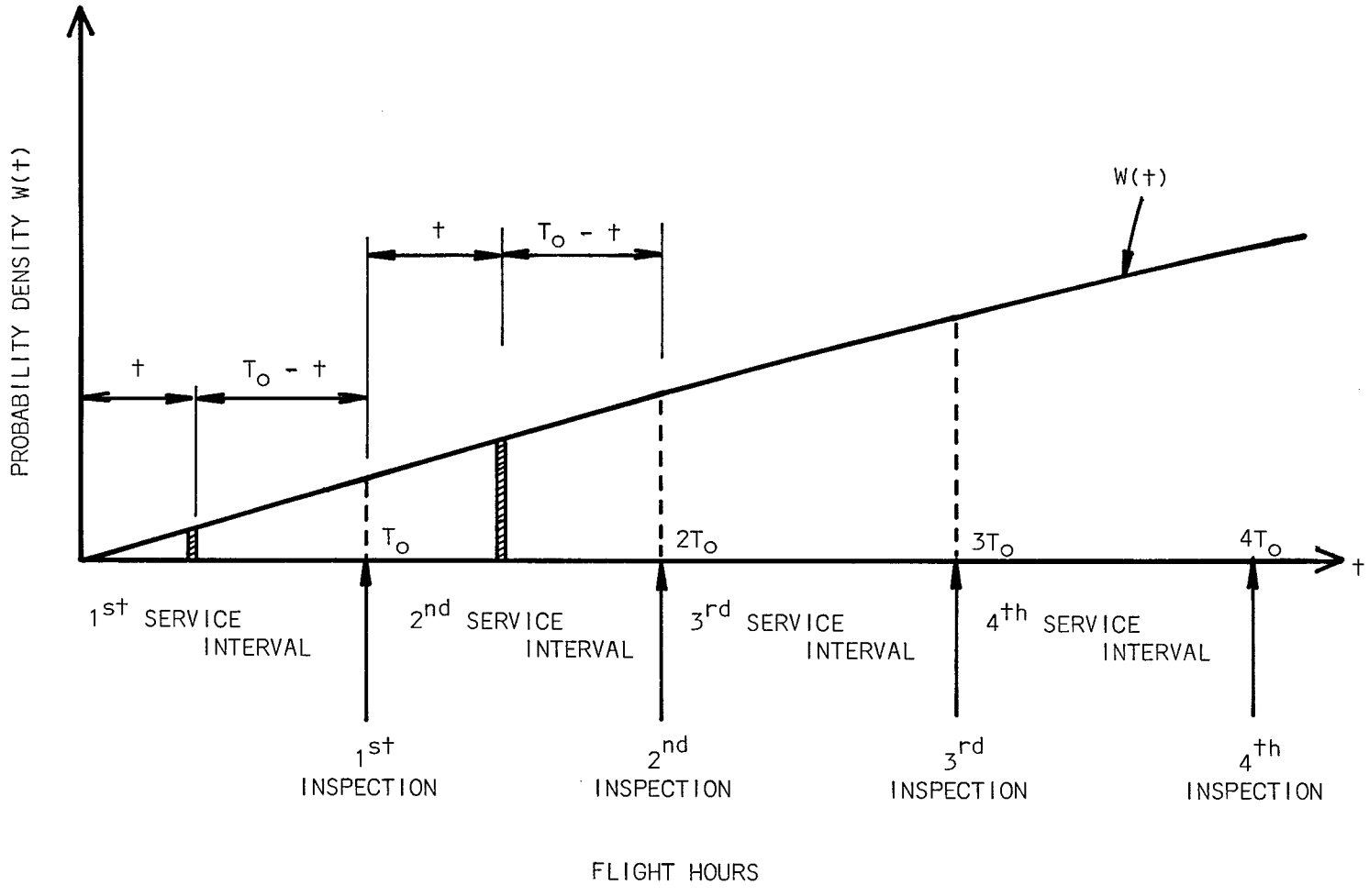

Figure 29. Periodic Rigorous Inspections

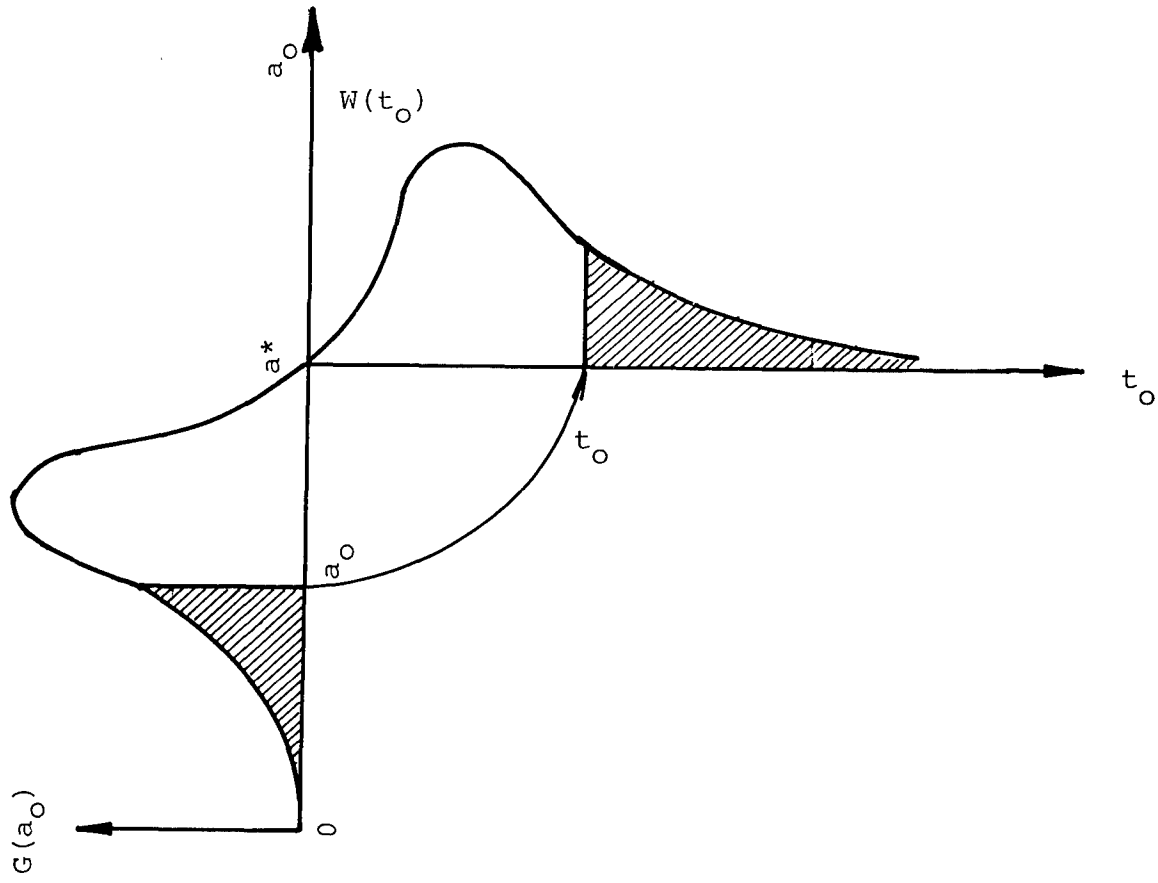

$$G(a_o) = \frac{dt_o}{da_o} W(t_o)$$

$$t_o = \frac{a^{*1-\lambda'/2} - a^{1-\lambda'/2}}{(1 - \lambda'/2)c'(\pi/2)^{\lambda'/2} Q^{\lambda'/b} N_o^{1-\lambda'/b}}$$

Figure 30. Compatibility between $G(a_o)$ and $W(t_o)$

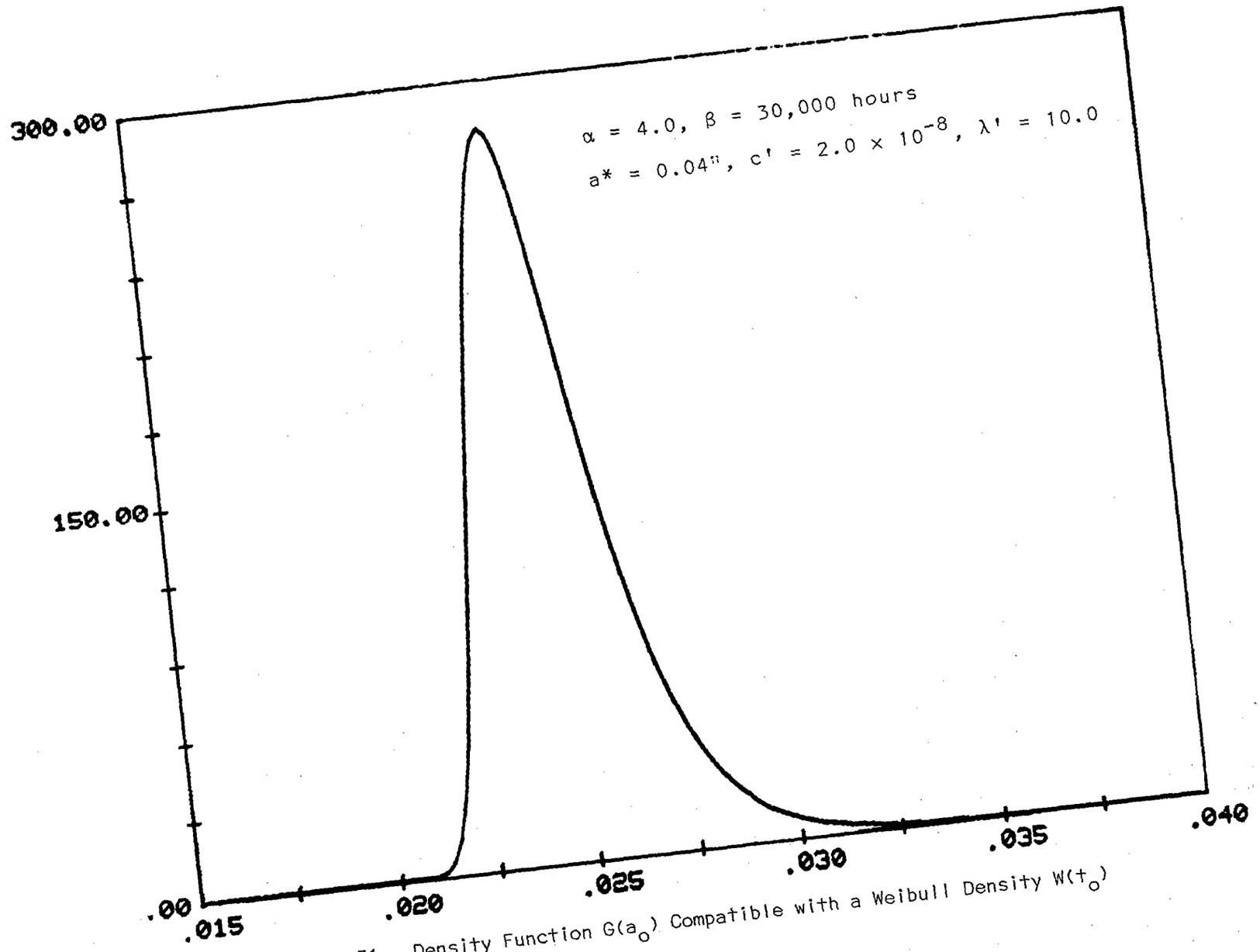

Figure 31. Density Function $G(a_o)$ Compatible with a Weibull Density $W(t_o)$

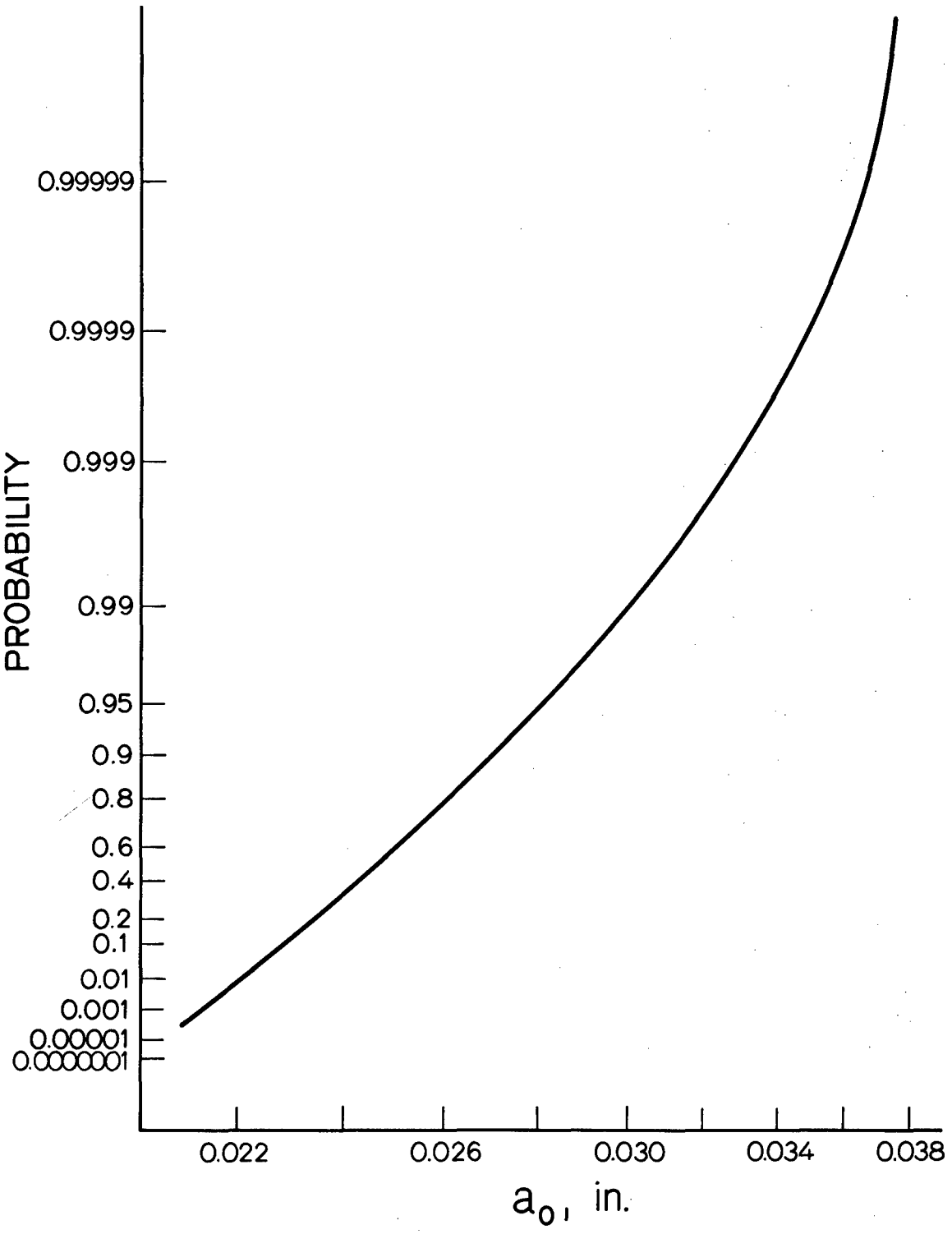

Figure 32. Distribution of Initial Crack Size Plotted on Fréchet Probability Paper

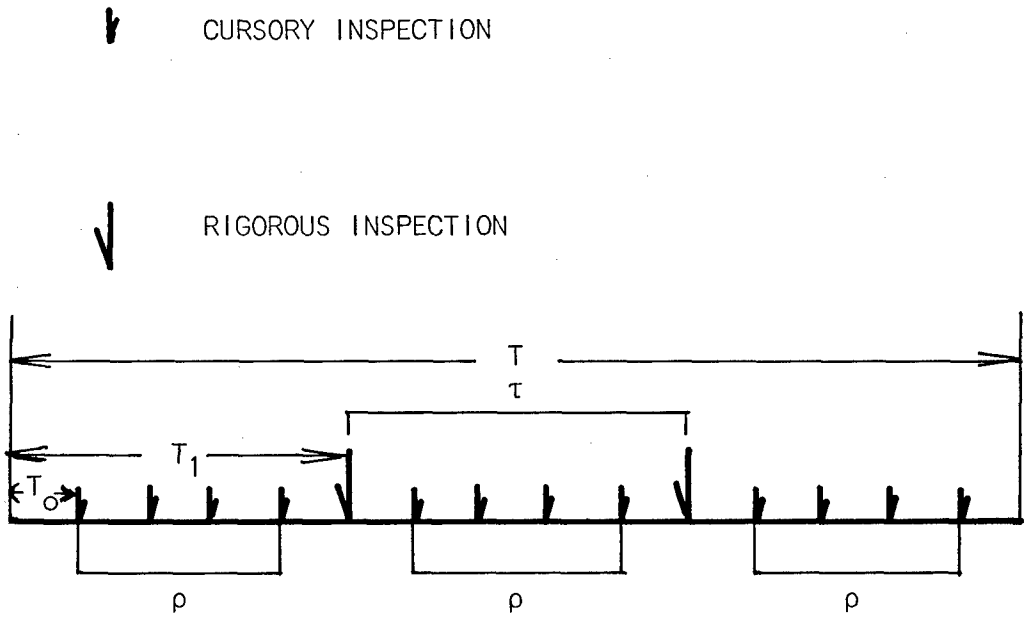

Figure 33. Periodic Rigorous and Cursory Inspections

a_o

X_i	$P_1 (\times 10^{-3})$	$P_{50} (\times 10^{-1})$
0.039	0.410	0.203
0.040	0.493	0.244
0.0405	0.541	0.267
0.041	0.818	0.401
$A=\left(\frac{\partial P}{\partial X_i}\right)_{X_i=\bar{X}_i}$	87.33	42.67
A^2	762.71	1820.44
$B = \frac{\bar{X}_i}{\bar{P}}$	0.0811	0.1639
B^2	0.00658	0.02688
$\alpha_i^2 = A^2 \cdot B^2$	50.21	48.92

P_M: Fleet Size M
Slow Crack Growth

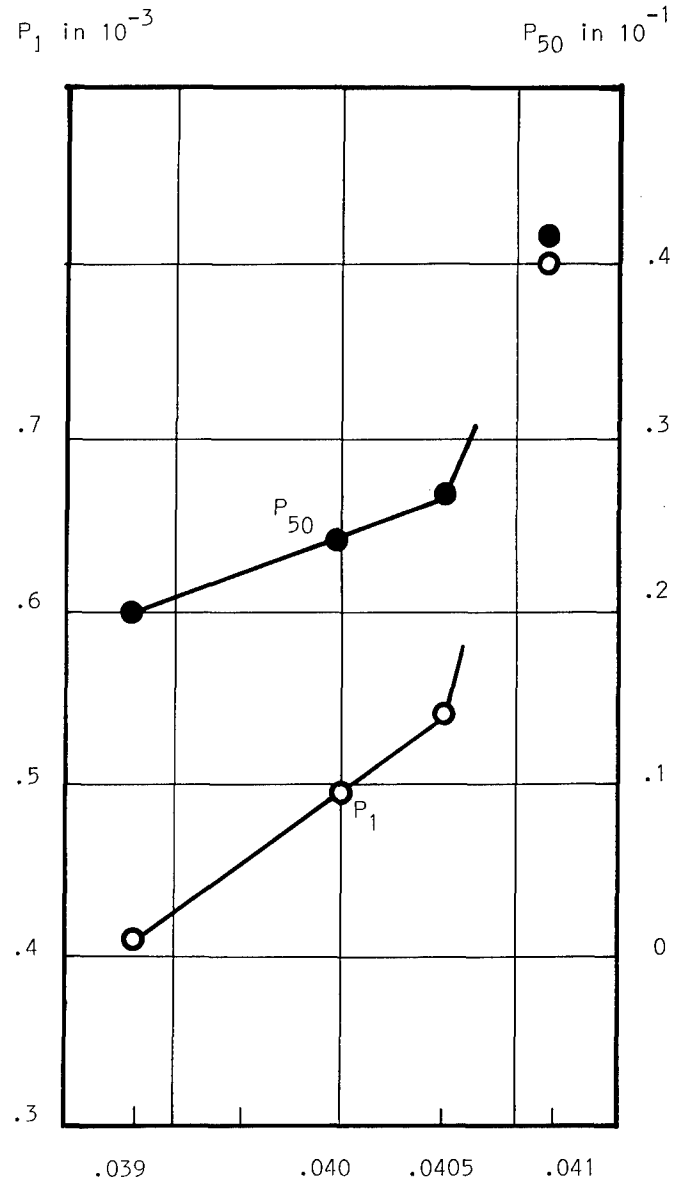

Figure 34. Parametric Sensitivity Analysis Procedure with a_o as an Example

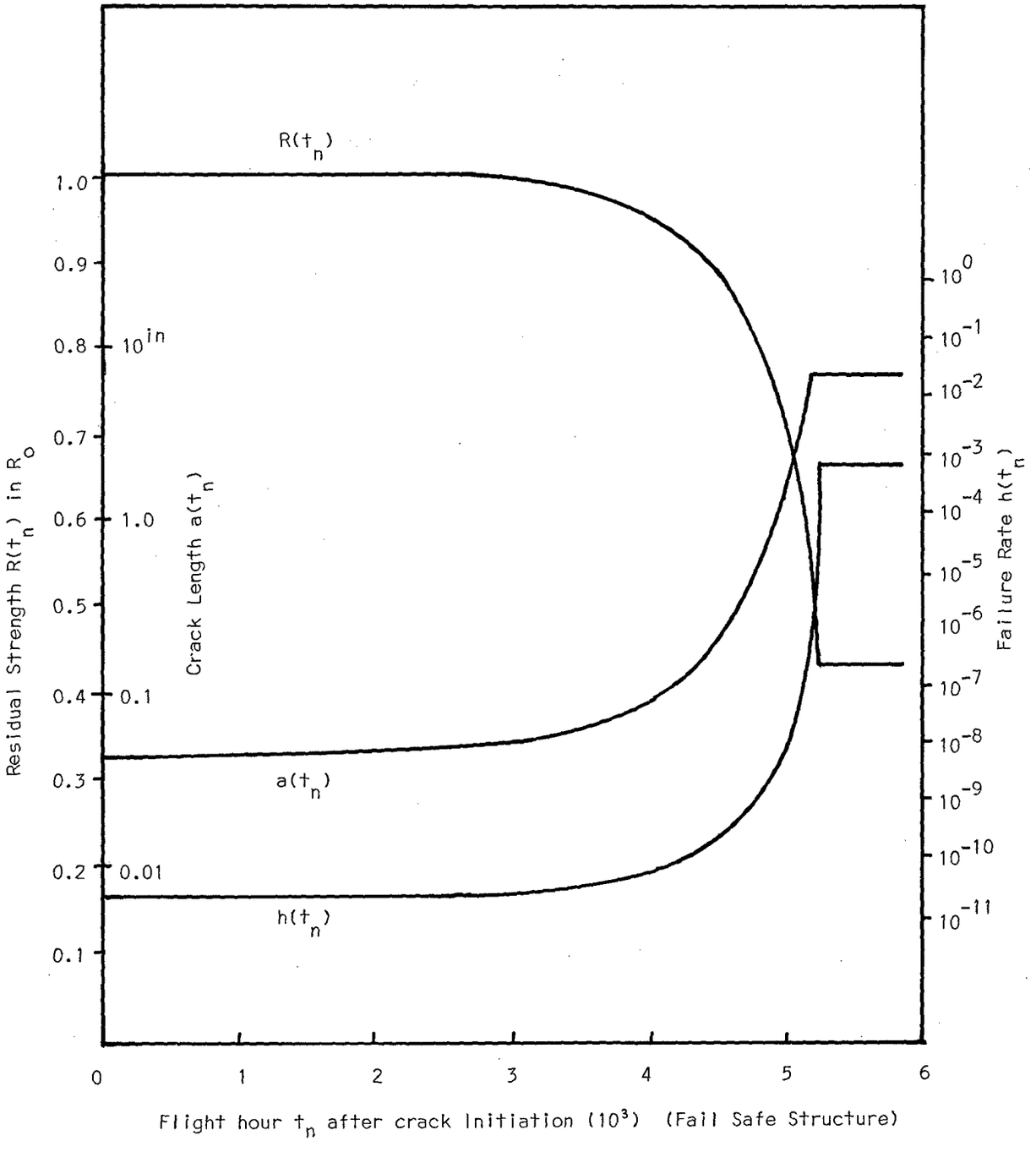

Figure 35. Residual Strength, Crack Size and Failure Rate as Functions of t_n

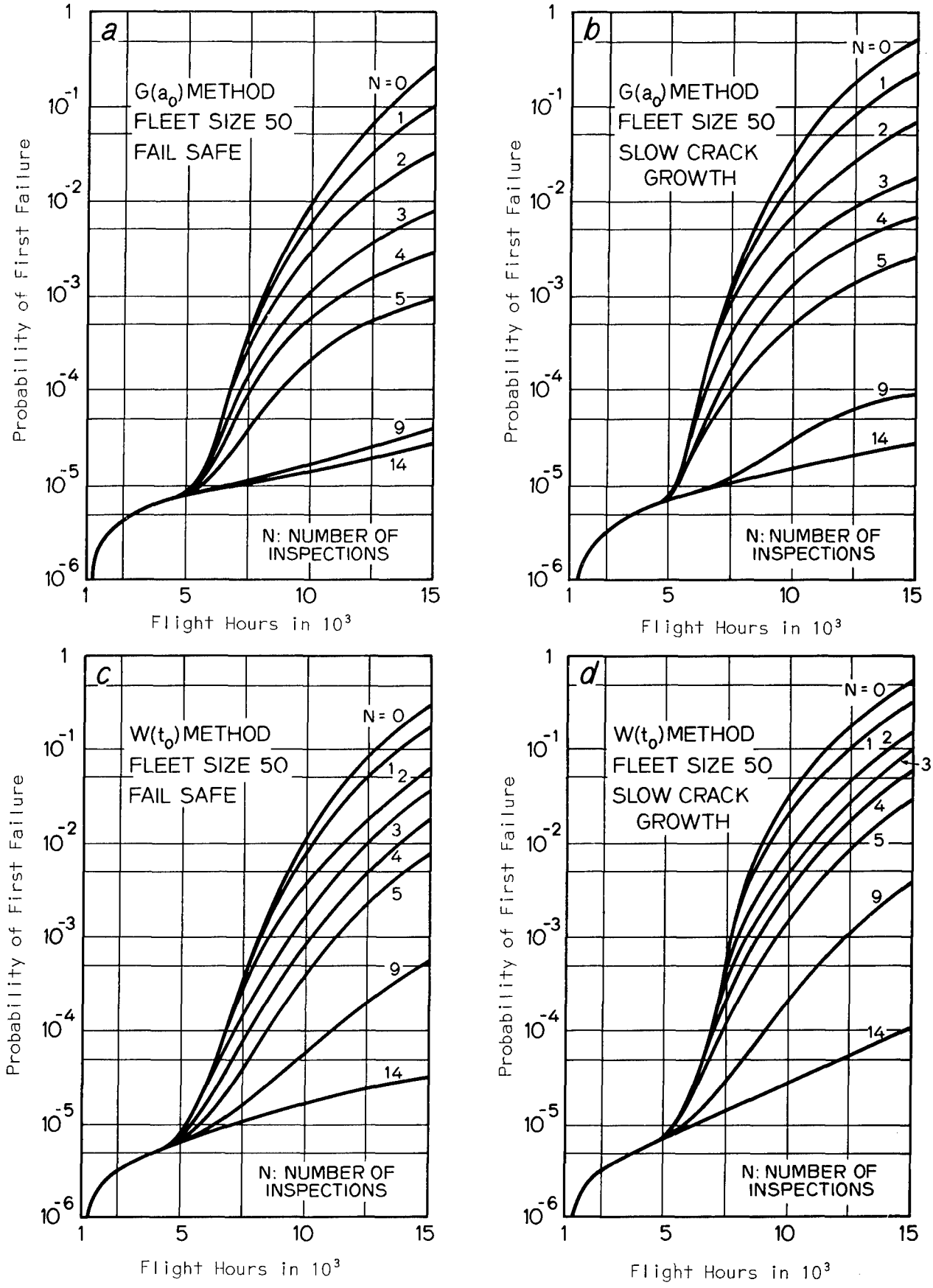

Figure 36. Effect of Rigorous Inspections

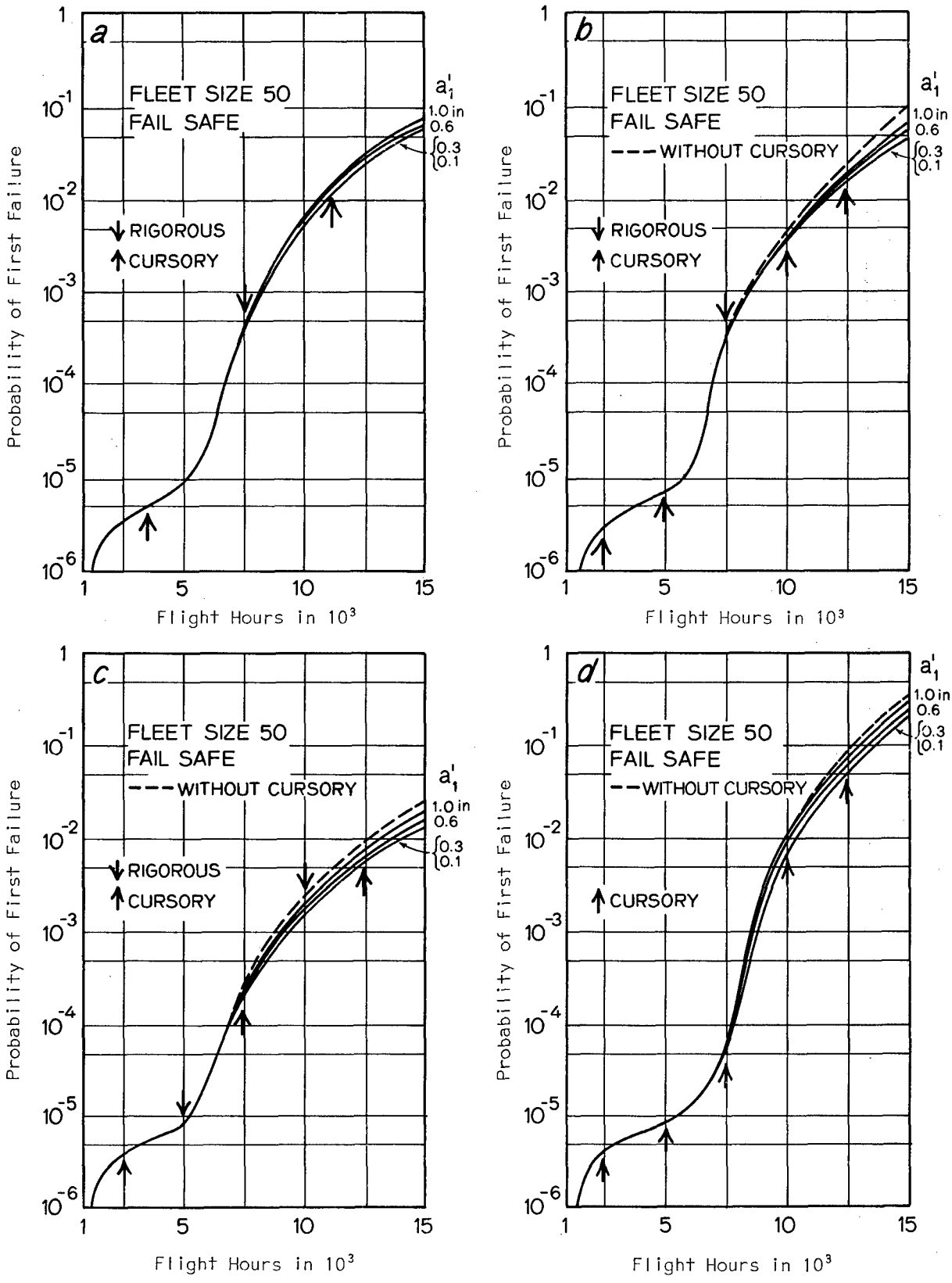

Figure 37. Effect of Cursory Inspections (1)

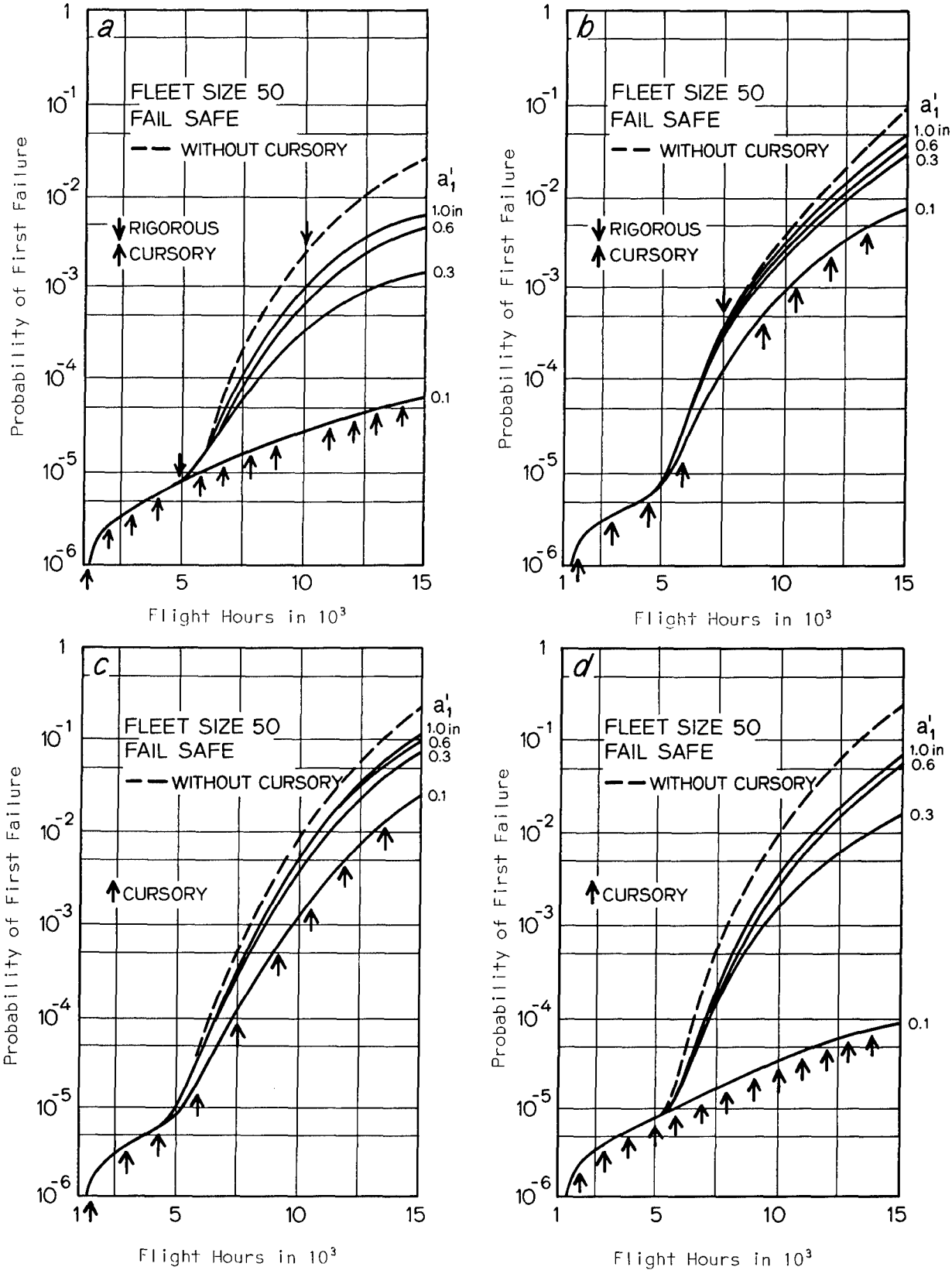

Figure 38. Effect of Cursory Inspections (II)

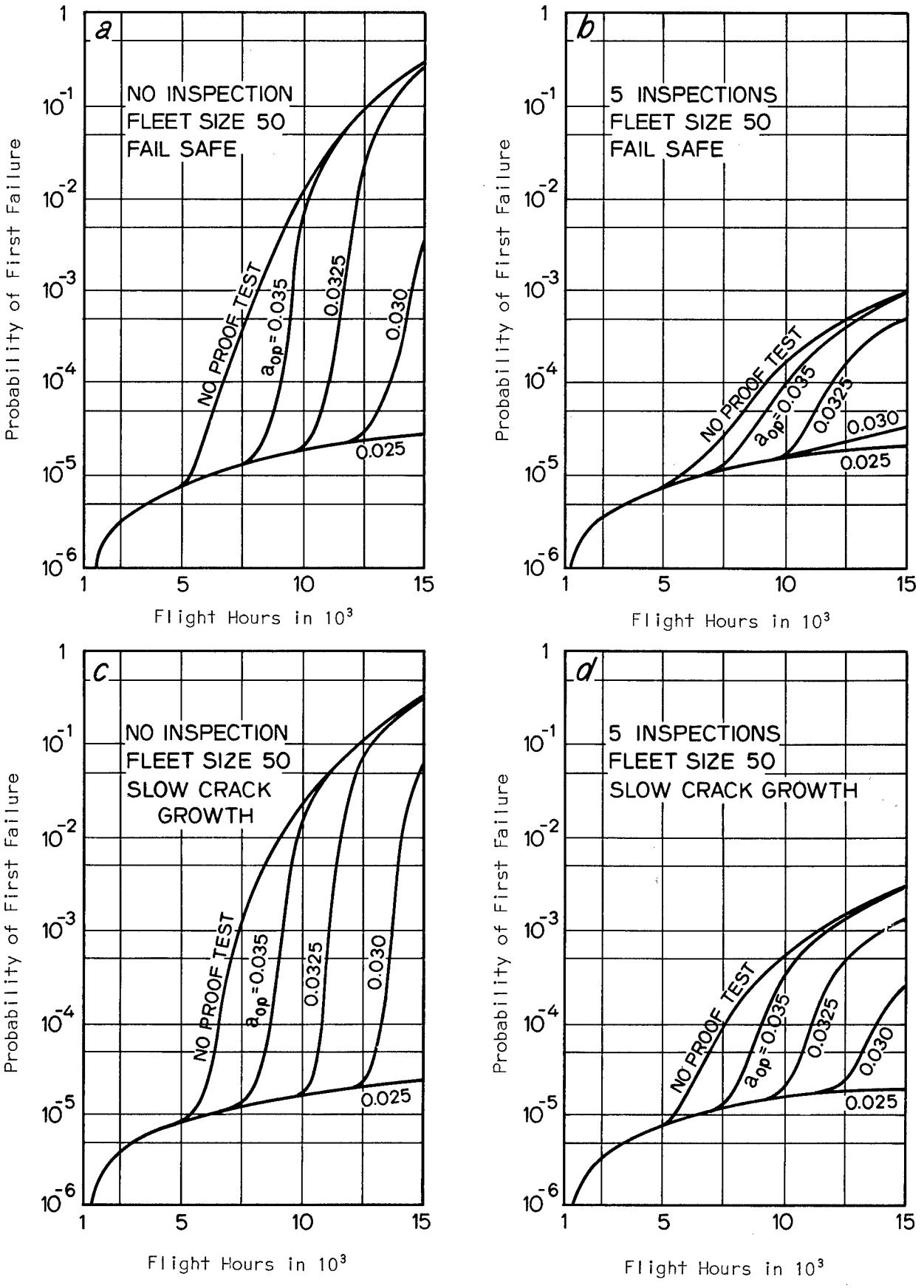

Figure 39. Effect of Proof Load Test

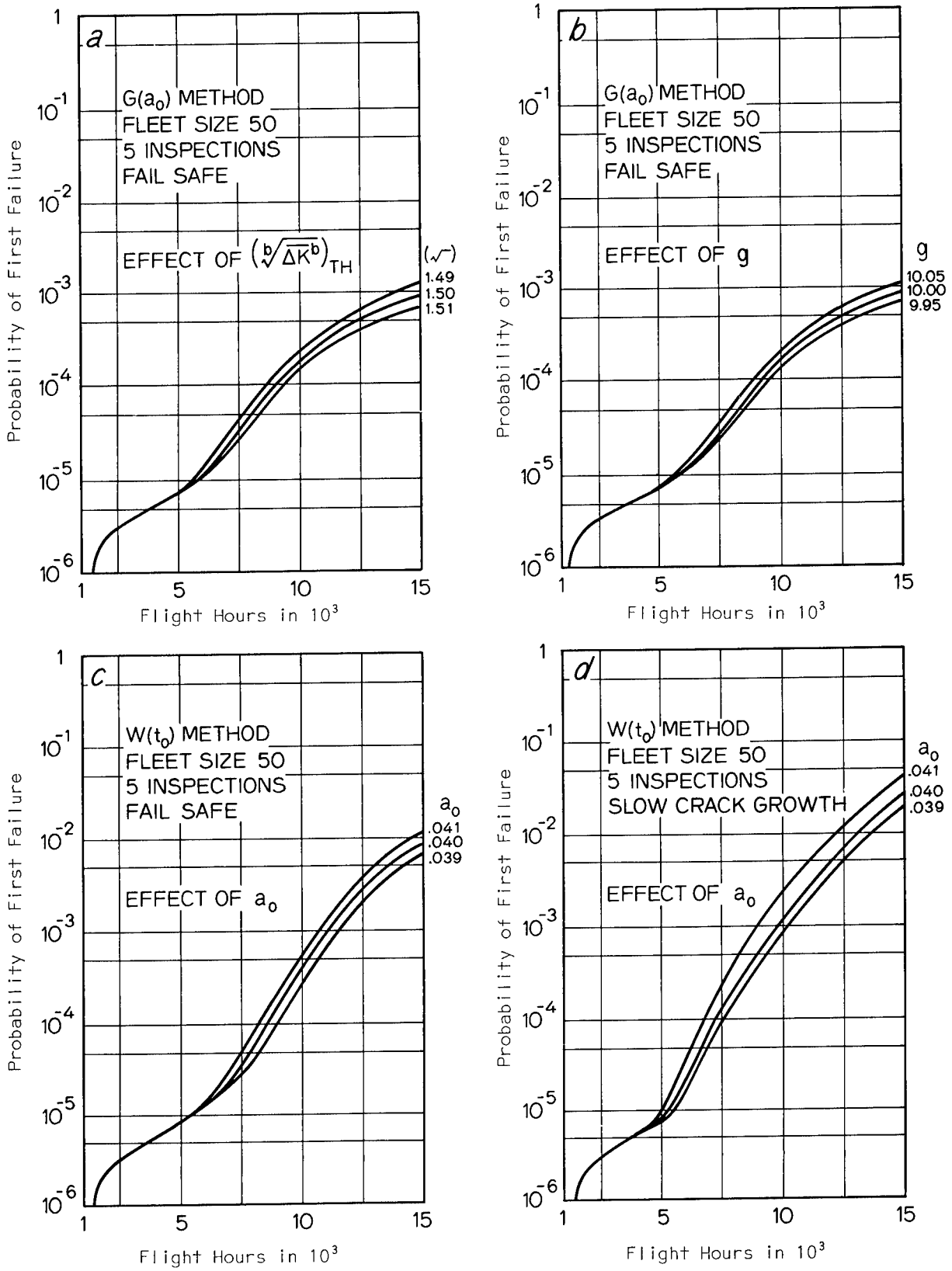

Figure 40. Sensitivity Study (Examples)

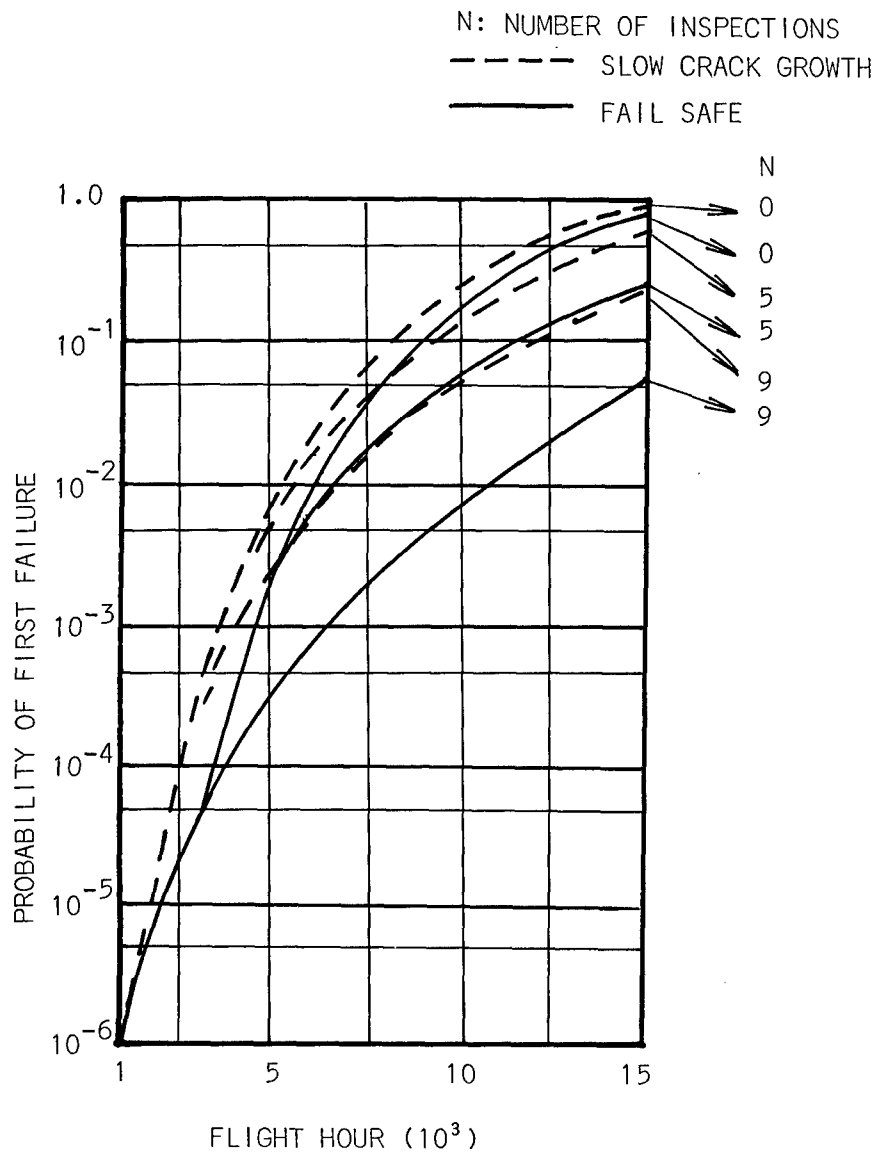

Figure 41. Probability of First Failure When No Threshold is Assumed for $\overline{(\Delta K^b)}^{1/b}$

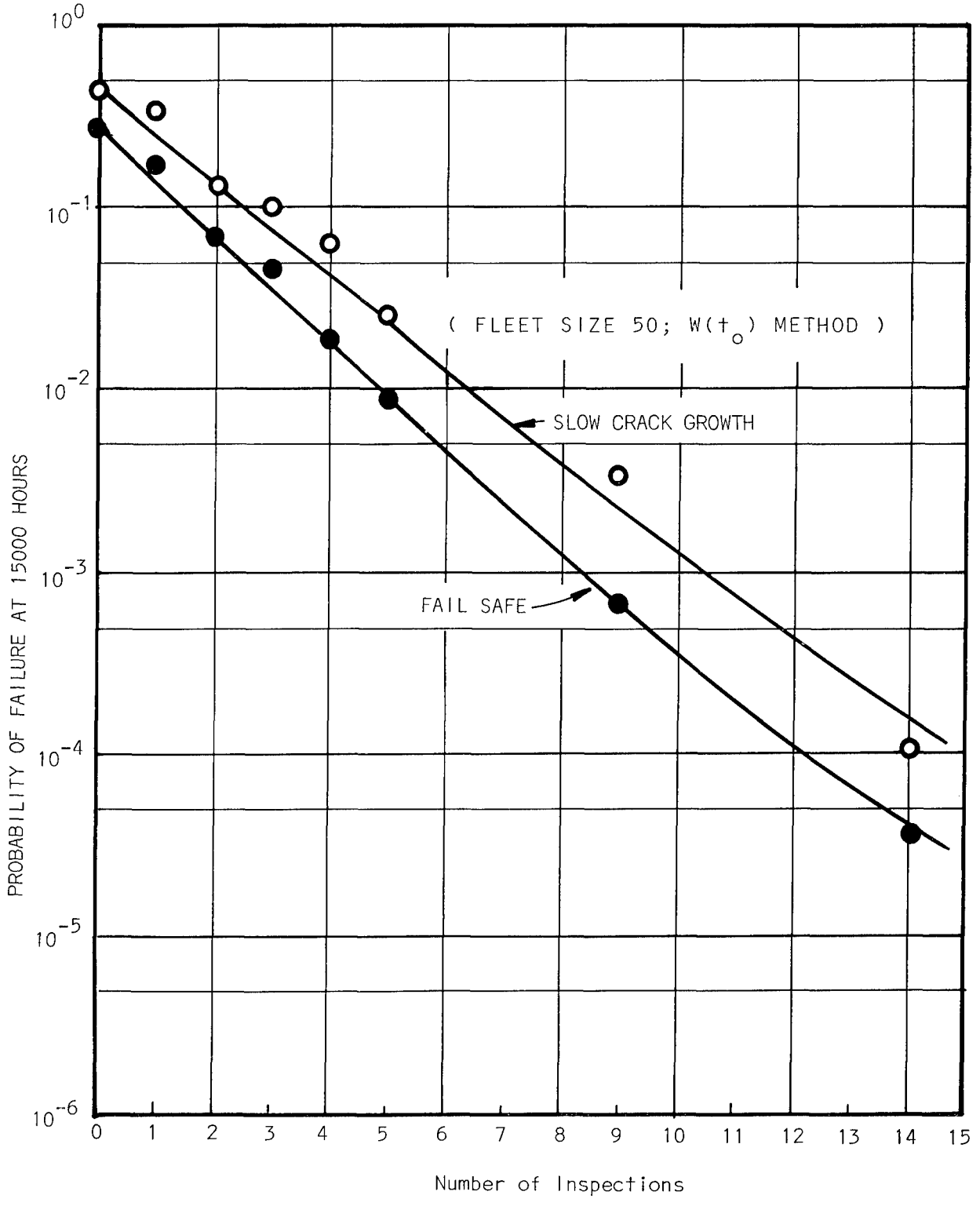

Figure 42. Effect of Number of Inspections (W(t_o) Method)

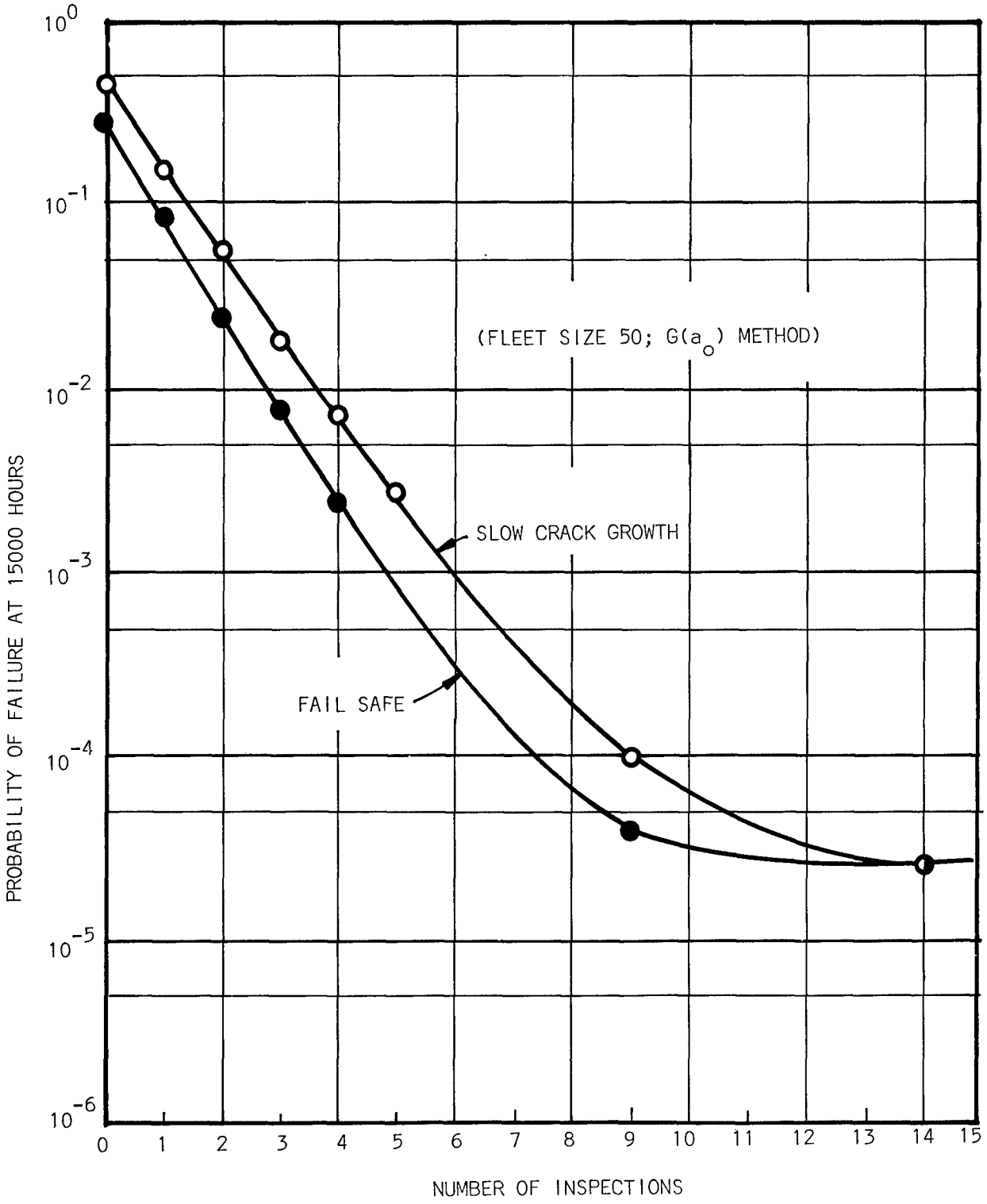

Figure 43. Effect of Number of Inspections (G(a_o) Method)

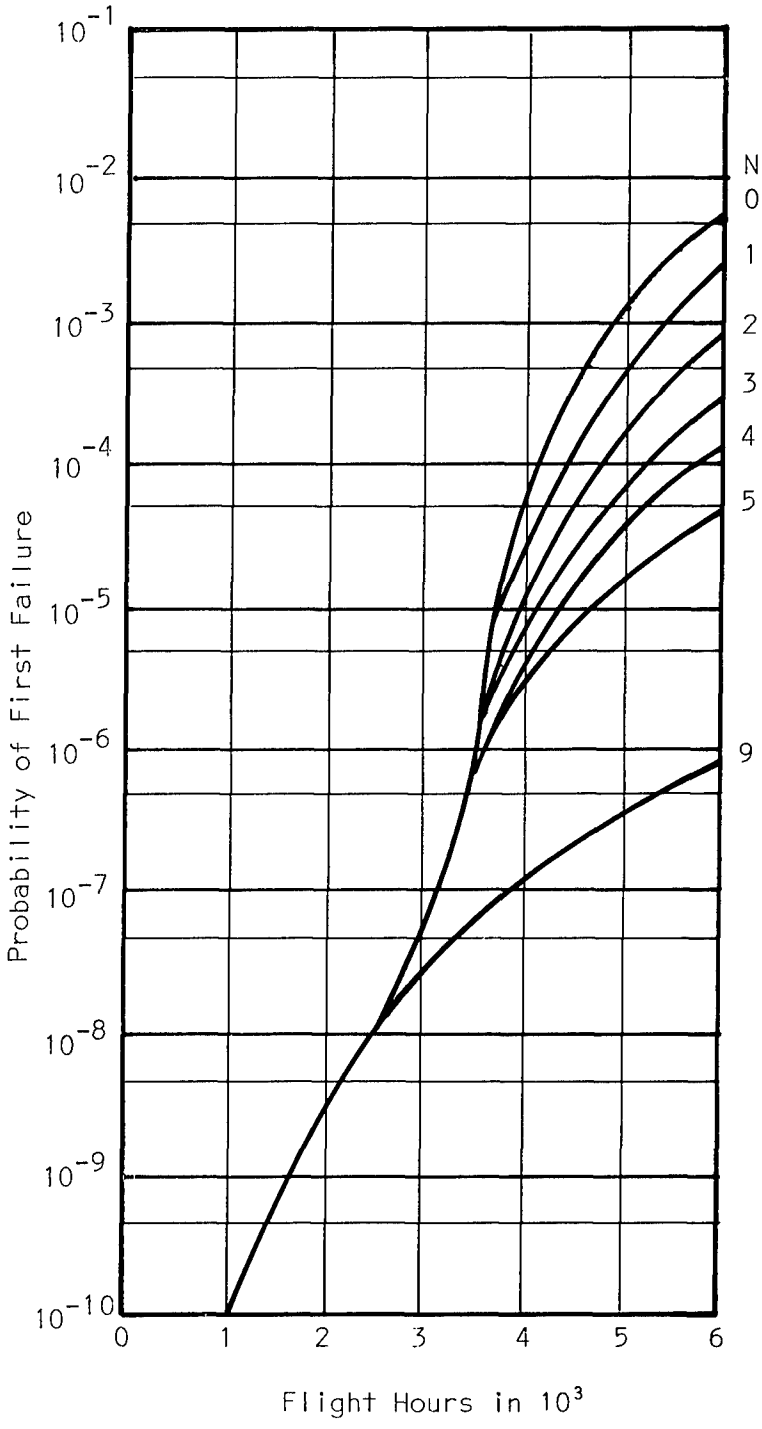

Figure 44. Probability of First Failure of a Fleet of 50 Fighters; Effect of Number of Inspections (Steel)

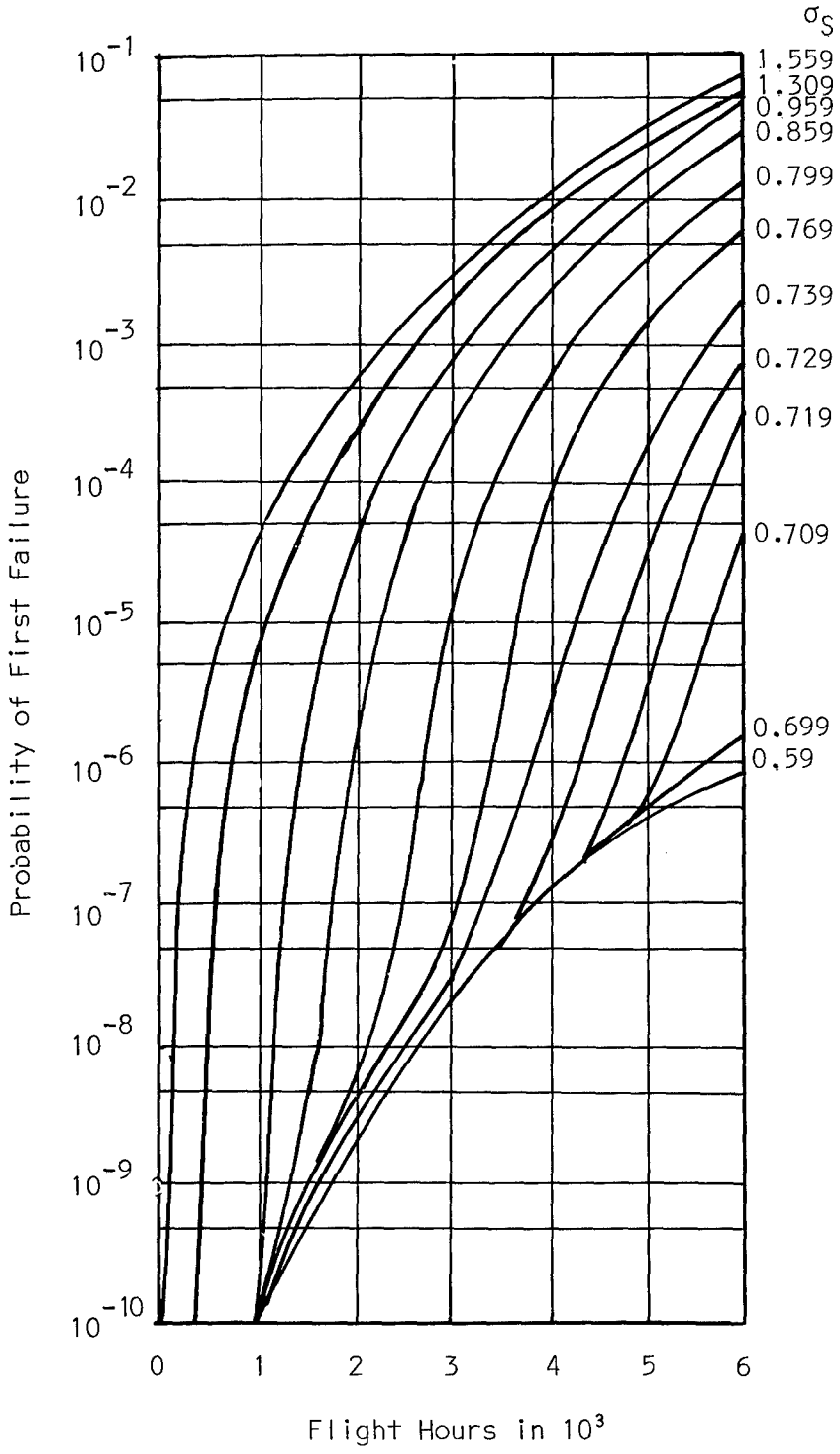

Figure 45. Probability of First Failure of a Fleet of 50 Fighters; Effect of σ_S (Steel)

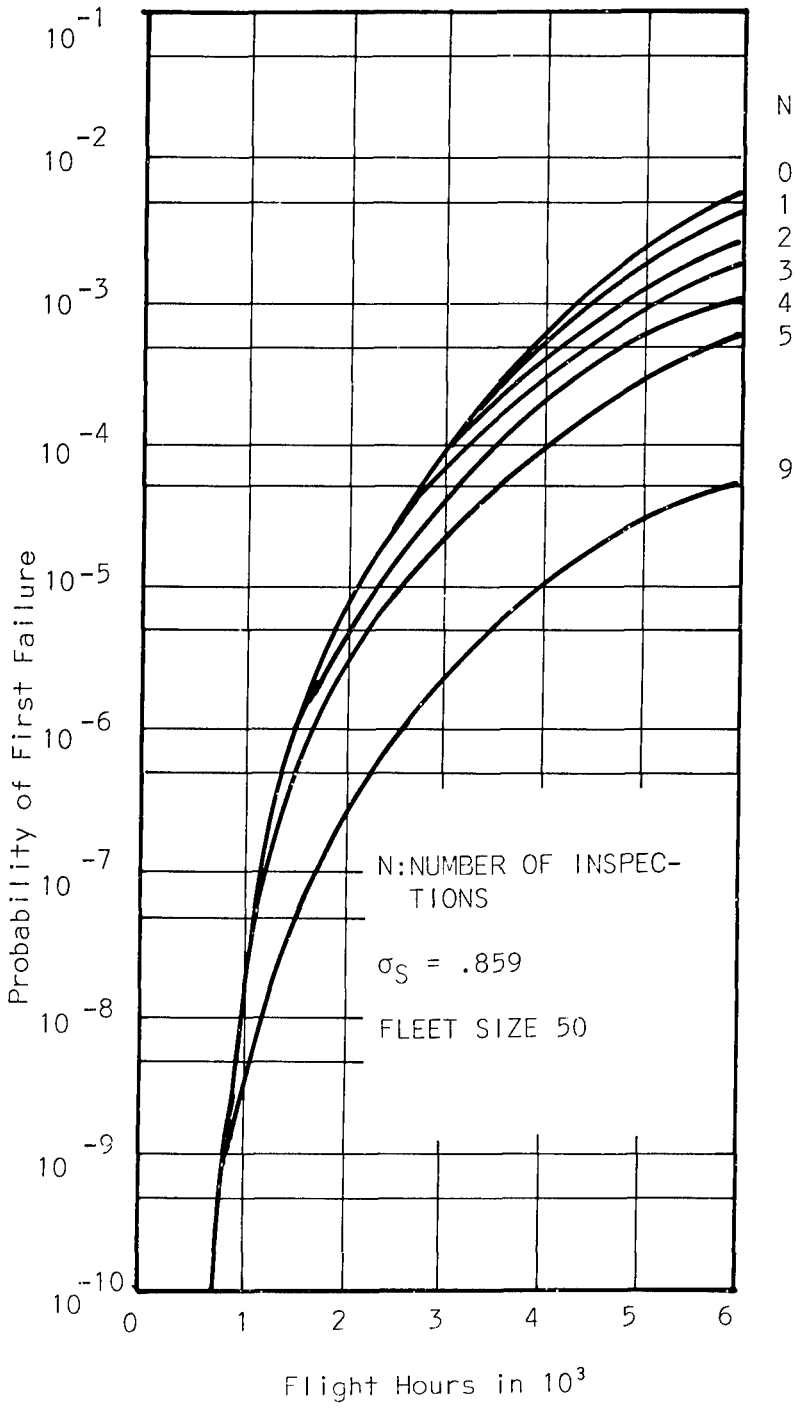

Figure 46. Probability of First Failure of a Fleet of 50 Fighters; the Effect of Number of Inspections (Aluminum)

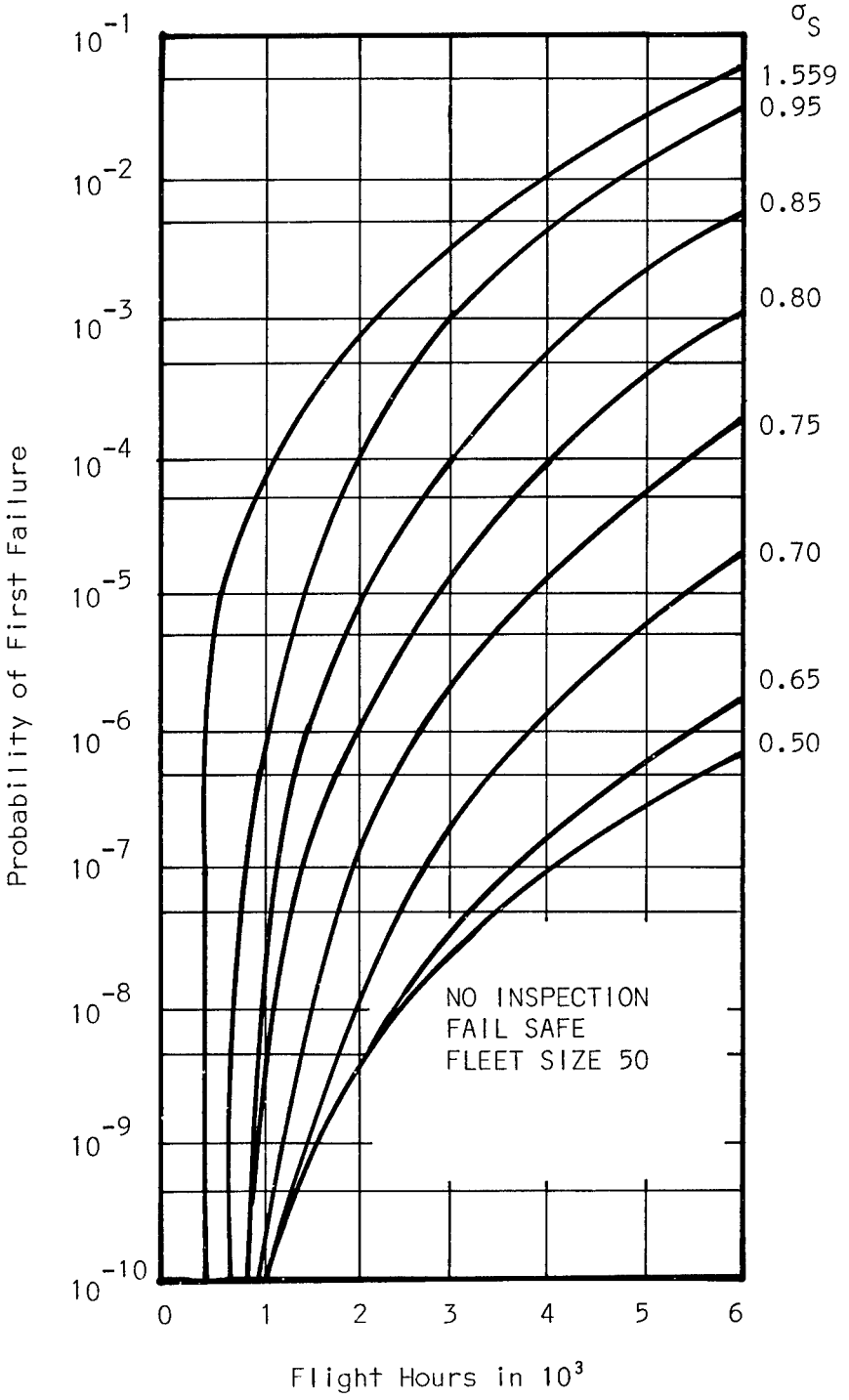

Figure 47. Probability of First Failure of a Fleet of 50 Fighters; the Effect of σ_S (Aluminum; Fail Safe)

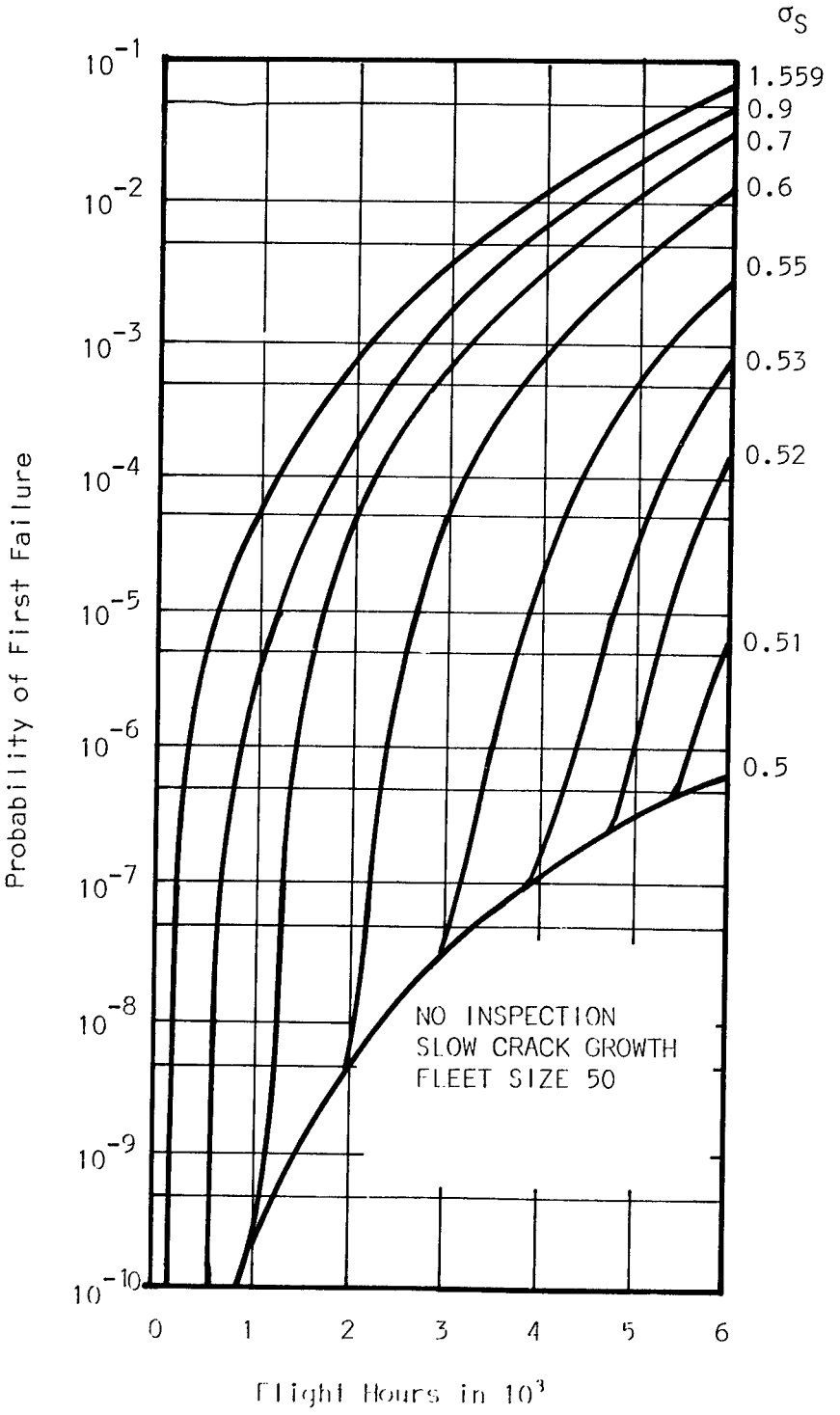

Figure 48. Probability of First Failure of a Fleet of 50 Fighters; the Effect of σ_S (Aluminum; Slow Crack Growth)

TABLE 1. IRREGULARITY RATIO R

$$R = \frac{\sqrt{5}}{3}\,(1-\beta^3)/\sqrt{(1-\beta)\,(1-\beta^5)}$$

β	Theory	Simulation	Error(%)
0	.7454	.7503	.65
.25	.8476	.8485	.10
.50	.9371	.9364	.07
.75	.9868	.9884	.16
.80	.9919	.9898	.21
.90	.9982	.9984	.02

TABLE 2. EXPECTED VALUE OF b-TH POWER OF RISE AND FALL

(a) b = 1

β_c	0	0.25	0.5	0.75	0.8	0.9
Simulation	1.87	2.12	2.35	2.46	2.47	2.50
Ref. 29(Exact)	1.87	2.11	2.35	2.48	-	-
Ref. 30	-	-	-	-	-	-

(b) b = 4

β_c	0	0.25	0.5	0.75	0.8	0.9
Simulation	48.2	77.0	108	121	125	126
Ref. 29	43.6	63.1	81.3	133	-	-
Ref. 30	-	-	-	-	127	128

TABLE 3. SENSITIVITY ANALYSIS (SLOW CRACK GROWTH)

	Parameter	Mean Value	α_i^2 (N=5)
1.	a_o: Crack size initiated at t_o	0.04 in	50.21
2.	c: Material constant	3.0×10^{-7}	22.96
3.	N_g: Number of gust load cycles per hour	600	0.069
4.	N_m: Number of maneuver load cycles per hour	60	0.156
5.	N_z: Number of G-A-G load cycles per hour	0.5	4.866
6.	$A_{14} = A_{24}$	115	8.216
7.	A_{34}	80	1.602
8.	P_3: Fraction of flight hours in maneuver	0.5	0.022
9.	σ_{C1}: Intensity of CAT	0.07g ksi	111.89
10.	σ_{C2}: Intensity of thunderstorm	0.18g ksi	3.887
11.	σ_{C3}: Intensity of maneuver	0.10g ksi	12.75
12.	$\overline{Z^4}$: Average of fourth power of G-A-G cycles Z	$(1.5\ g)^4$	102.35
13.	g: Gravitational acceleration	10 ksi	509.98
14.	K_c: Critical value of stress intensity factor	60 ksi$\sqrt{in}$	0.0750
15.	V_o: COV of ultimate strength	0.056	0.00034
16.	μ_o: Ultimate strength	57 ksi	0.00112
17.	α: Shape parameter	4.0	18.84
18.	β: Scale parameter	30,000 hrs	15.89
19.	U_1: Probability of inspecting cracked details	1.0	60.99
20.	a_1: Maximum undetectable crack size	0.02 in	0.251
21.	a_2: Minimum crack definitely detectable	0.3 in	0.833
22.	m: Parameter appearing in expression for $U_2(a)$	0.125	2.973
23.	$(\overline{\Delta K^b})^{1/b}_{TH}$: Threshold value	1.5 ksi$\sqrt{in}$	240.79
24.	λ': Slope of crack propagation law	10.0	127.88
25.	λ: Slope of crack propagation law	2.5	41.80

TABLE 4. SENSITIVITY ANALYSIS (FAIL SAFE)

	Parameter	Mean Value	α_i^2 (N=5)
1.	a_o: Crack size initiated at t_o	0.04 in	76.69
2.	c: Material constant	3.0×10^{-7}	11.38
3.	N_g: Number of gust load cycles per hour	600	1.291
4.	N_m: Number of maneuver load cycles per hour	60	0.252
5.	N_z: Number of G-A-G load cycles per hour	0.5	5.257
6.	$A_{14} = A_{24}$	115	7.409
7.	A_{34}	80	0.448
8.	P_3: Fraction of flight hours in maneuver	0.5	0.443
9.	σ_{C1}: Intensity of CAT	0.07g ksi	151.84
10.	σ_{C2}: Intensity of thunderstorm	0.18g ksi	49.42
11.	σ_{C3}: Intensity of maneuver	0.10g ksi	10.21
12.	$\overline{Z^4}$: Average of fourth power of G-A-G cycles Z	$(1.5\ g)^4$	86.85
13.	g: Gravitational acceleration	10 ksi	505.58
14.	ξ: Residual strength ratio	0.43	95.96
15.	V_o: COV of ultimate strength	0.056	0.220
16.	μ_o: Ultimate strength	57 ksi	98.97
17.	α: Shape parameter	4.0	19.17
18.	β: Scale parameter	30,000 hrs	15.95
19.	U_1: Probability of inspecting cracked details	1.0	101.18
20.	a_1: Maximum undetectable crack size	0.02 in	0.224
21.	a_2: Mimimum crack size definitely detectable	0.3 in	1.060
22.	m: Parameter appearing in expression for $U_2(a)$	0.125	3.151
23.	$(\overline{\Delta K^b})_{TH}^{1/b}$: Threshold value	1.5 ksi$\sqrt{in}$	227.70
24.	λ': Slope of crack propagation law	10.0	52.54
25.	λ: Slope of crack propagation law	2.5	35.01

TABLE 5. SENSITIVITY ANALYSIS (FAIL SAFE)

	Parameter	Mean Value	α_i^2 (N=5)
1.	a^*: Upper bound of $G(a_o)$	0.04 in	129.13
2.	c: Material constant	3.0×10^{-7}	20.40
3.	N_g: Number of gust load cycles per hour	600	1.208
4.	N_m: Number of maneuver load cycles per hour	60	0.420
5.	N_z: Number of G-A-G load cycles per hour	0.5	15.26
6.	$A_{14} = A_{24}$	115	15.89
7.	A_{34}	80	0.911
8.	P_3: Fraction of flight hours in maneuver	0.5	0.098
9.	σ_{c1}: Intensity of CAT	0.07g ksi	222.45
10.	σ_{c2}: Intensity of thunderstorm	0.18g ksi	81.00
11.	σ_{c3}: Intensity of maneuver	0.10g ksi	21.18
12.	$\overline{Z^4}$: Average of fourth power of G-A-G cycles Z	$(1.5g)^4$	180.22
13.	g: Gravitational acceleration	10 ksi	1322.31
14.	ξ: Residual strength ratio	0.43	93.13
15.	V_o: COV of ultimate strength	0.056	2.340
16.	μ_o: Ultimate strength	57 ksi	114.22
17.	α: Shape parameter	4.0	35.59
18.	β: Scale parameter	30,000 hrs	15.37
19.	U_1: Probability of inspecting cracked details	1.0	129.13
20.	a_1: Maximum undetectable crack size	0.02 in	0.457
21.	a_2: Minimum crack size definitely detectable	0.3 in	2.002
22.	m: Parameter appearing in expression for $U_2(a)$	0.125	8.242
23.	$\overline{(\Delta K^b)}_{TH}^{1/b}$: Threshold value	1.5 ksi $\sqrt{in}$	532.11
24.	λ': Slope of crack propagation law	10.0	152.73
25.	λ: Slope of crack propagation law	2.5	54.56

TABLE 6. REPRESENTATIVE VALUES OF SHAPE PARAMETER α

(a) Between 10 and 20 percentile

Material	Fighter	Transport
Aluminum	4.5	3.5
Titanium	3.0	2.5
Steel (100-200 ksi)	3.5	3.0
Steel (200-300 ksi)	2.5	2.0

(b) In the median range

Material	Fighter	Transport
Aluminum	8.0	6.0
Titanium	6.5	4.0
Steel (100-200 ksi)	7.0	5.0
Steel (200-300 ksi)	5.0	3.5

TABLE 7. SCATTER FACTORS S FOR

RELIABILITY LEVEL R = 0.5

(a) n = 1

m \ α	2	3	4	5
3	1.7	1.4	1.3	1.3
25	5.0	2.9	2.2	1.9
100	10.0	4.6	3.2	2.5
250	15.8	6.3	4.0	3.0
1000	31.6	10.0	5.6	4.0

(b) n = 3

m \ α	2	3	4	5
3	1.9	1.5	1.4	1.3
25	5.6	3.2	2.3	2.0
100	11.3	5.0	3.4	2.6
250	18.0	6.9	4.2	3.2
1000	36.8	10.9	5.9	4.2

TABLE 8. SCATTER FACTORS S FOR

RELIABILITY LEVEL R = 0.5

(a) n = 1

m \ α	2	3	4	5
3	5.2	3.0	2.3	1.9
25	15.0	6.1	3.9	3.0
100	30.0	9.7	5.5	3.9
250	47.4	13.1	6.9	4.7
1000	94.9	20.8	9.7	6.2

(b) n = 3

m \ α	2	3	4	5
3	5.3	3.0	2.3	1.9
25	15.3	6.2	3.9	3.0
100	30.6	9.8	5.6	3.9
250	48.3	13.2	7.0	4.8
1000	97.1	21.0	9.8	6.3

TABLE 9. SCATTER FACTORS S FOR

RELIABILITY LEVEL R = 0.99

(a) n = 1

m \ α	2	3	4	5
3	17.2	6.7	4.2	3.1
25	49.8	13.5	7.1	4.8
100	99.5	21.5	10.0	6.3
250	157	29.1	12.5	7.6
1000	314	46.3	17.7	10.0

(b) n = 3

m \ α	2	3	4	5
3	17.0	6.7	4.2	3.1
25	50.0	13.5	7.1	4.8
100	99.0	21.5	10.0	6.3
250	160	29.1	12.5	7.6
1000	310	46.3	17.7	10.0

☆ U. S. GOVERNMENT PRINTING OFFICE: 1976 — 657-630/1092